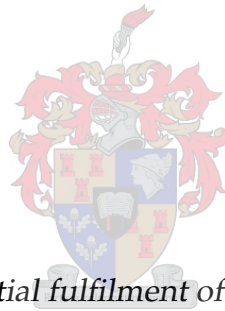


**The control of GAPDH on glycolytic flux in *Lactococcus lactis* and *Plasmodium falciparum***

by

Tagwin Claire Frantz



*Thesis presented in partial fulfilment of the requirements for the degree of Master of Science (Biochemistry) in the Faculty of Science at Stellenbosch University*

Supervisor: Dr. D.D. van Niekerk

Co-supervisor: Prof. J.L. Snoep

April 2022

# Declaration

By submitting this thesis electronically, I declare that the entirety of the work contained therein is my own, original work, that I am the sole author thereof (save to the extent explicitly otherwise stated), that reproduction and publication thereof by Stellenbosch University will not infringe any third party rights and that I have not previously in its entirety or in part submitted it for obtaining any qualification.

Date: ..... 2022/01/01 .....

Copyright © 2022 Stellenbosch University  
All rights reserved.

# Abstract

The parasitic disease, malaria, has the highest prevalence in Africa, and *Plasmodium falciparum*, the parasite responsible for severe malaria, has rapidly become resistant to current treatment options. There is a need for new drug targets, and the glycolytic pathway presents several possibilities since it is a source of energy and carbon for the parasite in certain stages of its life cycle. The malaria parasite utilizes host erythrocyte-derived glucose via glycolysis. The enzyme glyceraldehyde-3-phosphate dehydrogenase (GAPDH) has emerged as a potential drug target in glycolysis, and several studies have associated glycolytic inhibition with organismal death. However, the overall glycolytic inhibition by an irreversible inhibitor, iodoacetic acid (IAA), acting on GAPDH activity has not been investigated in *Plasmodium falciparum*. The lactic acid bacterium, *Lactococcus lactis*, has a glycolytic pathway that is similar in structure to that of *P. falciparum*, and can serve as a model organism in the laboratory environment. It is also of significant industrial importance. Previous studies have, however, found conflicting results for the glycolytic flux control of GAPDH in *L. lactis*.

In this study we investigated GAPDH flux control by using experimental enzyme kinetics, mathematical modeling, and metabolic control analysis to analyze detailed models of glycolysis within *L. lactis* and *P. falciparum*, respectively, and to elucidate the flux control of GAPDH under titrations of IAA.

We show that low flux control is exerted by GAPDH in both species, with the control in *P. falciparum* being marginally larger than in *L. lactis*, but when strongly inhibited, GAPDH obtained full control and was a good target to decrease the glycolytic flux. These results are in excellent agreement with independent simulations of detailed mathematical models that were previously constructed in our group.

# Uittreksel

Die parasitiese siekte, malaria, het die hoogste voorkoms in Afrika, en *Plasmodium falciparum*, die parasiet wat verantwoordelik is vir ernstige malaria, het vinnig weerstandig geword teen huidige behandelingsopsies. Daar is 'n behoefte aan nuwe farmaseutiese teikens, en die glikolitiese pad bied verskeie moontlikhede, aangesien dit 'n bron van energie en koolstof vir die parasiet in sekere stadiums van sy lewensiklus is. Die malariaparasiet gebruik gasheer eritrosiet-afkomstige glukose via glikolise. Die ensiem gliseraldehyd-3-fosfaat dehidrogenase (GAPDH) het na vore gekom as 'n potensiële teiken in glikolise, en verskeie studies het glikolitiese inhibisie met organisme dood geassosieer. Die algehele glikolitiese inhibisie deur 'n onomkeerbare inhibeerder, iodoasynsuur (IAA), wat op GAPDH-aktiwiteit inwerk, is egter nog nie ondersoek in *Plasmodium falciparum* nie. Melksuurbakterieë, *Lactococcus lactis*, het 'n glikolitiese pad wat soortgelyk is aan dié van *P. falciparum*, en kan dien as 'n modelorganisme in die laboratorium omgewing. Dit is ook van groot industriële belang. Vorige studies het egter teenstrydige resultate gevind vir die beheer van GAPDH op die glikolitiese fluksie in *L. lactis*.

In hierdie studie het ons GAPDH-fluksiebeheer ondersoek deur onderskeidelik eksperimentele ensiemkinetika, wiskundige modellering en metaboliese kontrole-analise te gebruik om gedetailleerde modelle van glikolise binne *L. lactis* en *P. falciparum* te analiseer, en om die fluksiebeheer van GAPDH onder titrasies van IAA te belig.

Ons toon aan dat lae fluksiebeheer deur GAPDH in beide spesies uitgeoefen word, met die beheer in *P. falciparum* marginaal groter as in *L. lactis*. Wanneer dit sterk geïnhibeer is, het GAPDH volle beheer verkry en was dit 'n goeie teiken om die glikolitiese fluksie te verminder. Hierdie resultate is in uitstekende ooreenstemming met onafhanklike simulaties van gedetailleerde wiskundige modelle wat voorheen in ons groep gebou is.

# Acknowledgements

I would like to express my sincere gratitude to the following individuals and organisations:

To my supervisor, Dr. D.D. van Niekerk, for all his support, words of encouragement, and guidance he provided me during the project.

To my co-supervisor, Professor Snoep, for all his support and input towards this project is highly acknowledged.

To Klarissa Shaw, for her guidance and contribution made by assisting me with the unfamiliar techniques used.

To my laboratory manager, Mr Arrie Arends, for his devoted support in making the lab environment as safe, secure and comfortable as possible.

To the Western Cape Blood Services (Tygerberg Hospital, Francie van Zyl Street, Parow, Western Cape, South Africa) for the supply of A<sup>+</sup> blood and to Dr. M. de Villiers and her laboratory members (Stellenbosch University) for the provision of malaria strains needed for this study.

The financial assistance of the National Research Foundation (NRF) towards this research is hereby acknowledged. Opinions expressed and conclusions arrived at, are those of the author and are not necessarily to be attributed to the NRF.

To my parents and brother for their words of encouragement, support and motivation during my tertiary education. This thesis would have not been possible without their unflinching love and constant support.

And lastly, to God for giving me the strength and motivation to steadfastly complete my masters degree to the best of my ability under these unprecedented times.

# Dedications

*"The greatest gift God could give someone is not what people perceive as success, but is the love from ones family that helps you to grow from multiple obstacles and become the person you were destined to be" Anonymous*

*This thesis is dedicated to:*

*My parents and brother, without whom I would be nothing. Their support through everything in my life is invaluable. This is a small token of my appreciation.*

# Contents

<b>Declaration</b>	<b>i</b>
<b>Abstract</b>	<b>ii</b>
<b>Uittreksel</b>	<b>iii</b>
<b>Acknowledgements</b>	<b>iv</b>
<b>Dedications</b>	<b>v</b>
<b>Contents</b>	<b>vi</b>
<b>List of Figures</b>	<b>viii</b>
<b>List of Tables</b>	<b>ix</b>
<b>Nomenclature</b>	<b>x</b>
<b>1 Introduction</b>	<b>1</b>
1.1 Background information and research motivation . . . . .	1
1.2 Research Question . . . . .	2
1.3 Aims and thesis outline . . . . .	2
<b>2 Background and literature review</b>	<b>4</b>
2.1 Introduction . . . . .	4
2.2 Energy Demands of <i>P. falciparum</i> and <i>L. lactis</i> : What are the demands and how are they sustained? . . . . .	5
2.3 Glycolysis . . . . .	11
2.4 The role of glyceraldehyde-3-phosphate dehydrogenase . . . . .	11
2.5 Modelling the glycolytic pathway . . . . .	16
2.6 Concluding remarks . . . . .	21

---

<b>3</b>	<b>Materials and Methods</b>	<b>22</b>
3.1	Research Design . . . . .	22
3.2	Raw Materials and Chemicals . . . . .	23
3.3	Preparation of Reagents, Media and Buffers . . . . .	23
3.4	Methodology . . . . .	28
<b>4</b>	<b>Results</b>	<b>40</b>
4.1	Growth of <i>L. lactis</i> . . . . .	40
4.2	Growth of <i>P. falciparum</i> . . . . .	41
4.3	Effect of IAA on Enzyme Activity . . . . .	41
4.4	Effect of IAA on the Glycolytic flux . . . . .	45
4.5	Model Analysis . . . . .	50
4.6	Glycolytic flux control . . . . .	50
<b>5</b>	<b>Discussion and Conclusions</b>	<b>55</b>
5.1	IAA attenuates GAPDH activity in both microorganisms . . . . .	56
5.2	IAA inhibits the glycolytic flux in both microorganisms . . . . .	57
5.3	Low flux control is observed experimentally and within models in both <i>L. lactis</i> and <i>P. falciparum</i> . . . . .	58
5.4	Findings summary . . . . .	62
5.5	Limitations, recommendations and future studies . . . . .	63
5.6	Conclusion . . . . .	65
<b>A</b>	<b>Other glycolytic enzymes as targets</b>	<b>66</b>
A.1	Role of Hexokinase . . . . .	66
A.2	Role of Lactate dehydrogenase . . . . .	67
A.3	Role of Triosephosphate isomerase . . . . .	68
<b>B</b>	<b>Glucose Calibration Curve</b>	<b>70</b>
<b>C</b>	<b>Lactate Calibration Curve</b>	<b>71</b>
<b>D</b>	<b>Enzyme Specificity</b>	<b>72</b>
	<b>Bibliography</b>	<b>73</b>

# List of Figures

2.1	The life cycle of <i>P. falciparum</i> , an interaction between two hosts. . . . .	6
2.2	Central carbon metabolism within the bloodstream form <i>Plasmodium falciparum</i> . . . . .	9
2.3	Metabolism in <i>Lactococcus lactis</i> . . . . .	10
2.4	The glyceraldehyde-3-phosphate dehydrogenase (GAPDH) catalysed reaction. . . . .	12
2.5	Schematic illustration of the kinetics of different enzyme inhibition types. . . . .	14
2.6	The proposed mechanism of <i>Trypanosoma cruzi</i> GAPDH inactivation through IAA. . . . .	15
3.1	Example growth of <i>P. falciparum</i> . . . . .	31
4.1	Growth of <i>P. falciparum</i> 3D7. . . . .	41
4.2	Enzyme specificity of IAA. . . . .	42
4.3	Inhibition of GAPDH activity by IAA in <i>L. lactis</i> and <i>P. falciparum</i> . . . . .	44
4.4	Lactate production curves as a function of time. . . . .	46
4.5	Lactate production flux inhibition by IAA. . . . .	46
4.6	Glucose consumption curves as a function of time. . . . .	47
4.7	Glucose flux as a function of varying iodoacetic acid concentrations. . . . .	48
4.8	Determination of experimental control coefficients. . . . .	52
4.9	Glycolytic flux control of GAPDH. . . . .	53
5.1	Elasticities of the experimental control coefficients as described in Figure 4.8 for both <i>L. lactis</i> and <i>P. falciparum</i> . . . . .	60
B.1	Glucose calibration curve. . . . .	70
C.1	Lactate calibration curve. . . . .	71
D.1	Enzyme specificity of IAA. . . . .	72

# List of Tables

2.1	GAPDH inhibitors as potential therapeutics in <i>P. falciparum</i> . . . . .	17
4.1	Growth of <i>Lactococcus lactis</i> . . . . .	40
4.2	Inhibition parameters of GAPDH. . . . .	43
4.3	Effect of a 30-minute IAA inhibition. . . . .	49
4.4	Flux control coefficients. . . . .	54
A.1	Potential glycolytic enzymes as targets for therapeutic development in <i>P. falciparum</i> . . . . .	69

# Nomenclature

## Enzymes

ALD	Aldolase (EC 4.1.2.13)
ENO	Enolase (EC 4.2.1.11)
EPI	UDP-glucose epimerase
$\beta$ gal	$\beta$ -galactosidase
G3PDH	Glycerol 3-phosphate dehydrogenase (EC 1.1.1.8)
G6PDH	Glucose-6-phosphate dehydrogenase (EC 1.1.1.49)
GALK	Galactokinase
GALPI	Galactose-phosphate isomerase
GAPDH	Glyceraldehyde-3-phosphate dehydrogenase (EC 1.2.1.12)
HK	Hexokinase (EC 2.7.1.1)
LDH	Lactate dehydrogenase (EC 1.1.1.27)
PFK	Phosphofructokinase (EC 2.7.1.11)
$P\beta$ gal	Phospho- $\beta$ -galactosidase
PDH	Pyruvate dehydrogenase
PFL	Pyruvate formate lyase
PGI	Phosphoglucoisomerase (EC 5.3.1.9)
PGK	Phosphoglycerate kinase (EC 2.7.2.3)
PGM	Phosphoglycerate mutase (EC 5.4.2.1)

---

PK	Pyruvate kinase (EC 2.7.1.40)
PMG	Phosphoglucomutase
TBA	Tagatose-bisphosphate aldolase (EC 4.1.2.40)
TPI	Triosephosphate isomerase (EC 5.3.1.1)
TPK	Tagatose-phosphate kinase
TRF	Galactose/uridylyl transferase

### Metabolites

2PGA	2-Phosphoglycerate
3PGA	3-Phosphoglycerate
ACE	Acetate
Acetyl-CoA	Acetyl coenzyme A
B1,3PG	Bis 1,3-phosphoglycerate
DHAP	Dihydroxy acetone phosphate
EtOH	Ethanol
G1P	Glucose-1-phosphate
G6P	Glucose-6-phosphate
GAL	Galactose
GAL1P	Galactose-1-phosphate
GAL6P	Galactose-6-phosphate
GAP	Glyceraldehyde 3-phosphate
GLC	Glucose
F1,6BP	Fructose 1,6-bisphosphate

---

F6P	Fructose-6-phosphate
LAC	Lactate
PEP	Phosphoenolpyruvate
PYR	Pyruvate
Tag6P	Tagatose-6- phosphate
TDP	Tagatose-1,6-diphosphate

### Enzyme Kinetics

$IC_{50}$	Concentration of inhibitor that lowers enzyme velocity by 50%
$K_{eq}$	Equilibrium constant
$K_i$	Inhibition constant
$V_{max}$	Maximal enzyme velocity
$v_i$	Initial rate of an enzyme-catalysed reaction
$K_m$	Substrate concentration at half maximal reaction velocity
$k_{cat}$	Turnover number

### Metabolic Control Analysis

$C_{v_i}^J$	Flux control coefficient
$\epsilon_p^v$	Elasticity coefficient
$R_p^J$	Response coefficient
$J_{v_i}$	Steady-state flux of an enzyme

### General

ADP	Adenosine diphosphate
-----	-----------------------

---

ANOVA	Analysis of variances
ATP	Adenosine triphosphate
3-BP	3-Bromopyruvate
BSA	Bovine serum albumin
CM	Culture media
CO <sub>2</sub>	Carbon dioxide
2-DG	2-deoxy-D-glucose
EMP	Embden-Meyerhof-Parnas pathway or glycolysis
EPM	Erythrocyte plasma membrane
HEPES	4-(2-hydroxyethyl)-1-piperazineethanesulfonic acid
HT	Hexose transporter
IAA	Iodoacetic acid
IDC	Intraerythrocytic developmental cycle
Inh	Inhibitor
iRBCs	Infected red blood cells
kDa	Kilodalton
LND	Lonidamine
MES	2-(N-morpholino)ethanesulfonic acid
MRS broth	de Man, Rogosa and Sharpe broth
NAD <sup>+</sup>	Nicotinamide adenine dinucleotide (oxidized)
NADH	Nicotinamide adenine dinucleotide (reduced)
NADP <sup>+</sup>	Nicotinamide adenine dinucleotide phosphate (oxidized)
ORN	Ornidazole

OXA	Oxalate
O <sub>2</sub>	Oxygen
PBS	Phosphate buffered saline
PPM	Parasite plasma membrane
PVM	Parasitophorous vacuole membrane
pRBCs	Parasitised red blood cells
RBCs	Red blood cells or erythrocytes
RPMI media	Roswell park memorial institute media
SO	Sodium oxamate
Tween 80	Polysorbate 80
%v/v	Volume per volume (millilitre solute per 100mL volume solution)
% m/v	Mass per volume (grams solute per 100mL volume solution)
% w/w	Weight per weight (grams solute per 100 grams solution)
WHO	World health organisation

# Chapter 1

## Introduction

### 1.1 Background information and research motivation

Despite the recent advancements in the eradication strategies of malaria, parasite resistance to drugs and the mortality rate amongst infected individuals remain relatively high. In 2019, the world health organisation (WHO) reported an estimated prevalence of 229 million sufferers and 409000 deaths worldwide, with 94% of all sufferers residing on the African continent, and 67% of all deaths being children [1]. The parasitic protozoan, *Plasmodium falciparum*, causes the most severe form of malaria and undergoes a complex life cycle between two hosts: mosquito vector and human host. The parasite life cycle consumes large amounts of glucose from its host erythrocyte to ensure its survival, growth and multiplication [2].

Similarly, the industrial lactic acid bacterium (LAB), *Lactococcus lactis*, known for its role in the fermentation processes used in the cheese and dairy industries, are also dependent on glycolysis for its free energy production and consumes large amounts of glucose. Increasingly, more countries are becoming food insecure and strategies are needed to enhance the quality of food products and prevent them from spoiling as quickly to sustain food security worldwide, but specifically in Africa where 66% of the population experiences food scarcity [3].

In both microorganisms the glycolytic pathway converts glucose to lactate in the presence of various enzymes and cofactors. Although lactate production may be desirable in the case of *L. lactis*, increased lactate produced by *P. falciparum*, enhanced anaerobic glycolysis in tissues and hypoxic cells, and activated immune cells (via aerobic glycolysis) hastens the onset of lactic acidosis and hypoglycemia in severe malaria patients [4, 5]. An

improved understanding of regulation of glycolysis via enzymes such as glyceraldehyde-3-phosphate dehydrogenase (GAPDH), may inform metabolic engineering strategies for industrial bacteria such as *L. lactis*, and facilitate the search for potential drug targets for controlling the energy supply and lactate flux in the malaria parasite.

Mathematical models can assist in gaining a better understanding of regulation of metabolic pathways. Mathematical modeling based upon fundamental principles and experimental parametrization allows us to describe and predict the behaviour of metabolism and identify control points. In the case of *P. falciparum*, mathematical models assist us in finding potential new drug targets or treatment regimens as current treatments are becoming less lethal to the most resistant forms of the parasite.

Metabolic control analysis (MCA) allows us to assess the flux control distribution over the enzymes within the glycolytic pathway to identify enzymes that would contribute a large effect on the overall flux if they were to be inhibited [6]. The flux control of an enzyme can be quantified experimentally if an enzyme-specific inhibitor is available. If a mathematical model of the pathway exists, control analysis can also be performed *in silico*. If data and model results are similar this can serve as a form of confirmation and model validation.

## 1.2 Research Question

To what extent does GAPDH control the glycolytic flux in the malaria parasite, *P. falciparum*, and in the lactic acid bacterium, *Lactococcus lactis*?

## 1.3 Aims and thesis outline

To answer the research question, we used the specific inhibitor, iodoacetic acid (IAA), to affect the flux through inhibition of GAPDH, and compared the experimental results to the effect modeled in the Penkler model of the parasite [4] and the Hoefnagel model of the bacterium [7]. The project was therefore divided into two main aims:

1. **Determine the flux control of GAPDH in *L. lactis*.** The approach to achieve this aim was: **1)** characterize the effect of IAA titrations on the glycolytic flux, **2)** measure

the GAPDH enzyme activity of *L. lactis* cell lysates at varying IAA concentrations, and 3) analyze the effect IAA has on the Hoefnagel model [7] to elucidate what is seen in experimentally determined data.

2. **Determine the flux control of GAPDH in *P. falciparum*.** The approach to achieve this aim was: 1) characterize the effect of iodoacetic acid (IAA) titrations on the glycolytic flux, 2) measure the GAPDH enzyme activity of *P. falciparum* cell lysates at varying IAA concentrations, and 3) analyze the effect IAA has on the Penkler model [4] to elucidate what is seen in experimentally determined data.

This thesis is divided into five chapters. **Chapter 1** provides a general introduction to the topic covered in this thesis, including the research question, aims and thesis outline. **Chapter 2** provides a review of the important concepts. It includes broad overviews of the *P. falciparum* parasite life cycle and biology in relation to its energy demands, as well as glucose metabolism in *L. lactis*. This is followed by a review of inhibition studies of GAPDH in conjunction with the other glycolytic enzymes. The chapter ends with an introduction to systems biology, metabolic control analysis (MCA), and kinetic modeling. **Chapter 3** provides a detailed description of all the materials and methods that were used to meet the objectives of the study. The experimental results are discussed in the context of the Penkler and Hoefnagel models in **Chapter 4**. **Chapter 5** presents a discussion of the research findings, including the recommendations that are needed to overcome the limitations of the models as well as future research prospects.

## Chapter 2

# Background and literature review

This chapter presents a comparative review of two microorganisms, *Lactococcus lactis*, and *Plasmodium falciparum*. Emphasis is placed on how the energy demands of both organisms manifest and the role of the enzymes of the Embden-Meyerhof-Parnas (EMP) pathway as potential drug targets. I then looked at possible inhibitors of glycolysis and how these may play a role in lowering the enzymatic activity of glycolytic enzymes. In the context of the malaria parasite, this would impede glycolysis, parasite growth and facilitate parasite killing. *Lactococcus lactis* can serve as a model organism for identifying drug targets within the EMP pathway, which has a close resemblance to that of *P. falciparum*. The chapter is concluded with an elaboration of how systems biology and metabolic control analysis (MCA) may play a pivotal role in uncovering potential control points and drug targets within glycolysis by describing the control distribution of the enzymes on metabolite concentration and flux.

### 2.1 Introduction

The Embden-Meyerhof-Parnas (EMP) pathway (glycolysis) is utilized by many organisms to obtain energy, in the form of ATP, for survival. Organisms such as *Lactococcus lactis* [8], *Plasmodium falciparum* [6], *Trypanosoma brucei* [9], *Saccharomyces cerevisiae* [10] and *Escherichia coli* [11], as well as mammalian muscle cells [12], rely to a certain extent on the catabolism of glucose to products such as lactate or ethanol (in yeast) for this process of energy generation. Whereas lactate production is an effective method of food production and preservation, which contributes to the texture, flavor, organoleptic quality, and pathogen growth reduction [13] of *L. lactis* fermented foods [14, 15], in mammalian cells, elevated lactate production above basal levels has been associated with disease as is the case for *P. falciparum* malaria [5], leading to secondary disease modalities namely,

## 2.2. Energy Demands of *P. falciparum* and *L. lactis*: What are the demands and how are they sustained?

hypoglycemia (blood glucose concentration < 2.2mmol/L), lactic acidosis (blood lactate concentration > 5mmol/L), anemia, brain disorders, and fever [4, 16].

*P. falciparum* is of interest as it causes the most lethal form of malaria that is endemic to Asia, South America and Africa [17]. In 2019 alone, the world health organisation (WHO) recorded 229 million malaria-related infections and 409 000 deaths with Africa having the highest prevalence of infections, constituting 94% of all cases, and deaths [1]. Additionally, children under the age of five accounted for 67% of all malaria-related deaths in Africa [1, 17]. To date, the primary causative agent of severe malaria, *P. falciparum*, has rapidly gained global resistance to well-known treatment regimens, such as artemisinin and chloroquine, that are currently in use [18, 19]. This global resistance occurs due to the extensive use of antimalarial drugs [20], the discontinuation of medication prior to infection resolution [21] and the adaptability of the parasite to various environments [21]. Since no novel drugs have become known as prospective alternatives to the current treatments, children, pregnant women, and immunocompromised individuals are still at risk.

On the other hand, *L. lactis* is of interest as it shares similar glycolytic properties with *P. falciparum* and since there has been controversy related to the flux control of GAPDH in literature, it is necessary to redetermine the flux control and regulation of GAPDH in *L. lactis*. In addition *L. lactis* can be easily cultivated in the laboratory setting, and can be used to optimise an inhibition protocol for the glycolytic enzymes that could be adapted for malaria parasite. In the dairy industry, *L. lactis* plays a pivotal role in food production and preservation by converting 90% of all sugars to lactic acid [14, 22–24]. A role for *L. lactis* has also emerged as a delivery organism for antigens, therapeutics, and immune proteins [25, 26] to treat disease. Metabolic manipulation of *L. lactis* could therefore lead to improved food quality, shelf-life, availability of food, and human health.

## 2.2 Energy Demands of *P. falciparum* and *L. lactis*: What are the demands and how are they sustained?

The metabolism of glucose through anaerobic glycolysis is indispensable to the survival of the bloodstream form (BSF) parasite in mammalian infection as glycolysis contributes

## 2.2. Energy Demands of *P. falciparum* and *L. lactis*: What are the demands and how are they sustained?

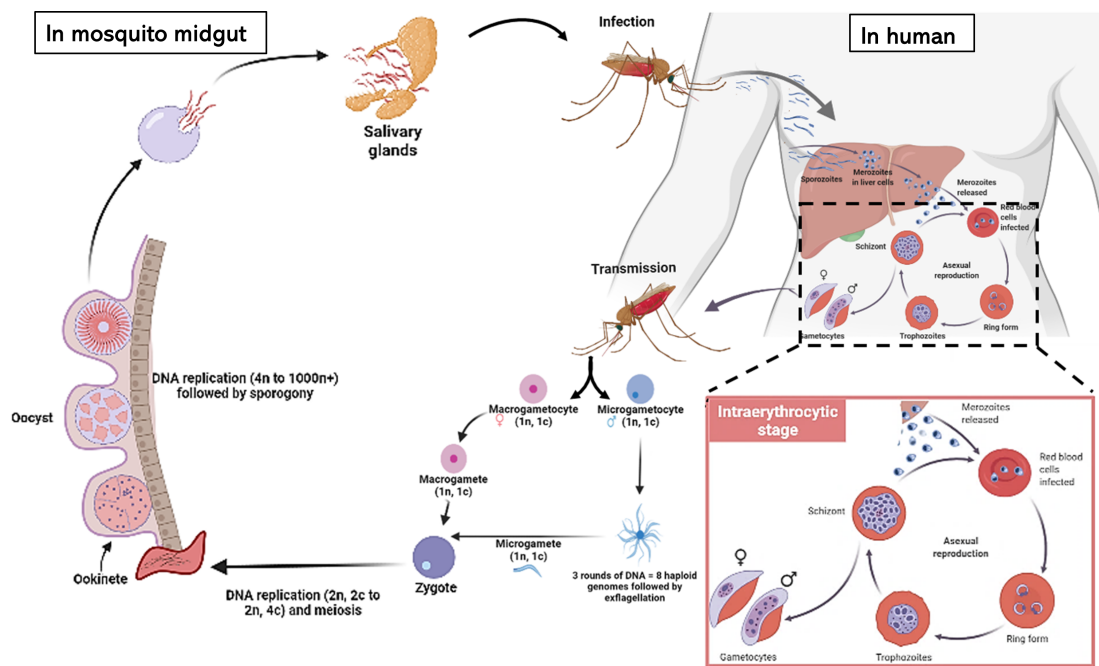


**Figure 2.1: The life cycle of *P. falciparum*, an interaction between two hosts.** This figure illustrates the *Plasmodium* life cycle transmission between two hosts. In malarial infections, *Plasmodium* parasites are transmitted from female anopheles mosquito hosts (left) to human hosts (right). An initial liver stage propels the parasite into its asexual intraerythrocytic cycle, from which sexual forms develop in a mosquito. In the mosquito, the internalized parasite undergoes meiotic and mitotic replication to produce sporozoites, which can infect more human hosts. Figure adapted from: Lee, A.H., Symington, L.S. and Fidock, D.A.: DNA repair mechanisms and their biological roles in the malaria parasite *Plasmodium falciparum*. *Microbiology and Molecular Biology Reviews*, vol. 78, no. 3, pp.469-486, 2014. [27]

the only source of energy, in the form of ATP production, to the blood-stage infection life cycle [28]. This stage is initiated when a blood meal is taken from a human host by a female *Anopheles* mosquito. During this blood meal, threadlike sporozoites are injected into the bloodstream of the host (Figure 2.1). These sporozoites transport themselves to the liver hepatocytes, where they multiply via mitotic nuclear divisions in a process called schizogony [29], to form merozoites. When these merozoites are released upon hepatocyte rupture, they travel to peripheral circulation and invade erythrocytes (red blood cells (RBCs)) [16, 27, 29]. Merozoites are tiny cells that invade host RBCs by firstly attaching to the surface of the erythrocytic membrane through an apex that releases rhoptries. Secondly, the merozoites invade erythrocytes and releases dense granules, while accumulating a vacuole that contains invaginated pieces of the erythrocytic membrane. These invaginations become internalised forming both the parasite plasma membrane (PPM) and parasitophorous vacuole membrane (PVM) that surrounds the parasite [30] (Figure 2.2). This erythrocytic invasion by merozoites initiates the asexual (i.e. intraerythrocytic)

## 2.2. Energy Demands of *P. falciparum* and *L. lactis*: What are the demands and how are they sustained?

---

stage. Parasites within these invaded erythrocytes mature and multiply over a 48-hour intraerythrocytic developmental cycle (IDC) to produce rings, trophozoites, and finally schizonts [29]. Rings are identified by their distinct ring morphology under a light microscope and mature into trophozoites, which are larger in size and the most metabolically active form of the parasite [31]. Schizonts, on the other hand, are multi-nucleated versions of the parasite. The infected erythrocytes containing schizonts rupture and release up to 32 merozoites that ultimately reinvade uninfected erythrocytes [16]. This is when the symptoms of malaria are manifested. This whole process is repeated in the next 48-hour cycle. Figure 2.1 shows an enlarged intraerythrocytic stage indicating different BSFs of the parasite namely, merozoites, rings, trophozoites and schizonts. The synchronization of these BSFs of the parasite and rupturing of RBCs are associated with the clinical symptoms and pathology of the disease with periodic fever-chill cycles [29].

Glycogen is not stored during this intraerythrocytic cycle. Therefore, simple sugars such as glucose and/or fructose are essential for the continual growth and reproduction of the parasite [29]. Neither parasite nor erythrocyte contains the pyruvate dehydrogenase (PDH) complex required to promote the tricarboxylic acid cycle (TCA) during the intraerythrocytic stage. Thus, all ATP that is produced comes directly from glycolysis [32, 33] and the redox balance is maintained by the production of lactate.

Unlike the asexual blood-stage, the gametocyte stage relies on both glycolysis and the tricarboxylic acid cycle (TCA) for energy production [5]. The gametocyte stage begins when intraerythrocytic parasites form male or female gametocytes and become infectious over a two-week period. Once ingested by a mosquito, they generate gametes which, when paired, form zygotes. A zygote becomes an ookinete after meiosis, which exits the blood meal confines and crosses over the midgut epithelium before settling under the basal lamina to form an oocyst. The sporozoites generated by sporogony within an oocyst undergo multiple replication cycles in order to produce thousands of haploid varieties, which migrate to the mosquito salivary glands for the next blood meal [27]. The dependence on the TCA cycle within the mosquito vector is much greater than in the human host [34, 35]. Pyruvate obtained from glycolysis can enter the TCA cycle via the PDH enzyme complex to produce acetyl-CoA.

In the uninfected red blood cells (uRBCs) glucose consumption rates are relatively low

## 2.2. Energy Demands of *P. falciparum* and *L. lactis*: What are the demands and how are they sustained?

and in the region of  $5\mu\text{mol}$  per 24 hours per  $10^9$  RBCs [36]. However, upon parasite invasion, the glucose consumption rate in the parasite-infected erythrocytes (iRBC) increases by up to 100 times [17, 37–40]. During the intraerythrocytic development cycle (IDC), 60–70% of the glucose that is consumed by *P. falciparum* is used for lactate production [36], with the remaining glucose used for anabolic processes such as the export of cytoadherence surface proteins, hemoglobin digestion, nuclei segmentation, DNA replication, and the formation of blood stage forms (merozoites, rings, trophozoites, and schizonts). [41]. Glucose is transported over several plasma membranes to reach the parasite. First, it is transported into the erythrocyte by way of a facilitative glucose transporter, GLUT 1, located on the erythrocyte plasma membrane (EPM). Glucose then crosses over the PVM [21] and eventually crosses the PPM via the *P. falciparum* hexose transporter (*PfHT*) (Figure 2.2). The end-product of glycolysis, lactate, is exported out of the parasite cytosol by means of a lactate-proton co-transporter, which simultaneously discharges protons. These lactate and protons are further transported out of the erythrocyte membrane.

Unlike *P. falciparum*, *L. lactis* consumes 90% of all sugars (galactose, lactose and/or glucose) to produce lactate, acetate, ethanol, and formate/ $\text{CO}_2$  anaerobically and transports them either via the phosphoenolpyruvate phosphotransferase system (PTS) or the permease system (PERM) (Figure 2.3). Galactose via the PERM enters the cytosol and is phosphorylated by the Leloir pathway (highlighted in light blue, Figure 2.3) before it enters glycolysis as glucose-6-phosphate. The PTS has the ability to phosphorylate sugars upon sugar transport across the membrane [42]. Both galactose and lactose that enter via the PTS and PERM feed into the glycolytic pathway at specific metabolites within the pathway, which increases the yield of lactate produced by *L. lactis* during glycolysis. When glucose is absent and galactose and lactose is present, the bacterium is still able to survive but with a reduced growth rate compared to what it would have in the presence of glucose [43].

2.2. Energy Demands of *P. falciparum* and *L. lactis*: What are the demands and how are they sustained?

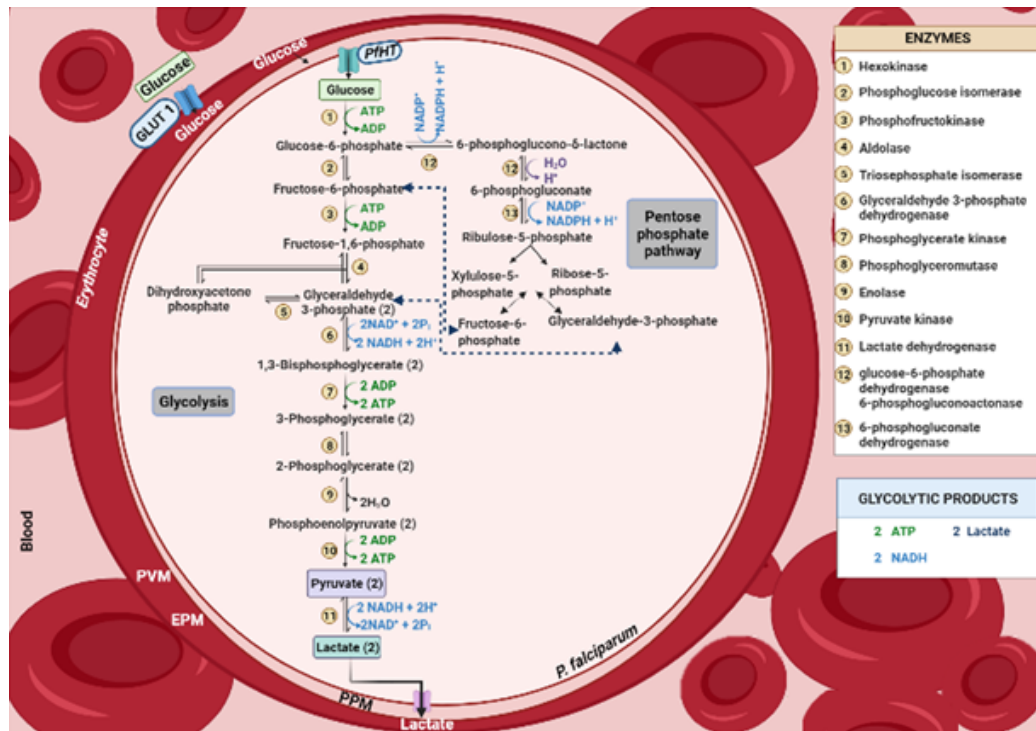


**Figure 2.2: Central carbon metabolism within the bloodstream form *Plasmodium falciparum*.** A diagram illustrating glucose metabolism including the pentose phosphate pathway within a *P. falciparum* infected erythrocyte. The salvage pathway, glycerol branch, and carbon dioxide fixation are not shown on the scheme as it is used minimally. Note that although only one erythrocyte is seen, many erythrocytes are infected within a malaria patient simultaneously. Abbreviations: ALD: aldolase; DHAP: dihydroxyacetone phosphate; 1,3BPG: 1,3-bisphosphoglycerate; ENO: enolase; F6P: fructose-6-phosphate; EPM: erythrocyte plasma membrane; FBP: fructose 1,6-bisphosphate; GAP: glyceraldehyde 3-phosphate; G-6-P: glucose-6-phosphate; GAPDH: glyceraldehyde-3-phosphate dehydrogenase; GLC: glucose; Gly-3-P: glycerol-3-phosphate; GLUT1: glucose transporter; G3PDH: glycerol 3-phosphate dehydrogenase; HT: hexose transporter; Mito: mitochondrial enzymes; PEP: phosphoenolpyruvate; 2-PGA: 2-phosphoglycerate; 3-PGA: 3-phosphoglycerate; PGI: glucose-6-phosphate isomerase; PGM: phosphoglycerate mutase; PFK: phosphofructokinase; PGK: phosphoglycerate kinase; PK: pyruvate kinase; PPM: parasite plasma membrane; PVM: parasitophorous vacuole membrane; PYR: pyruvate; PfHK: *P. falciparum* hexokinase; TPI: triose-phosphate isomerase; TAL: transaldolase; TKT: transketolase. Figure adapted from: Preuss, J., Jortzik, E. and Becker, K.: Glucose-6-phosphate metabolism in *Plasmodium falciparum*. *IUBMB life*, 64(7), pp.603-611, 2012.

## 2.2. Energy Demands of *P. falciparum* and *L. lactis*: What are the demands and how are they sustained?

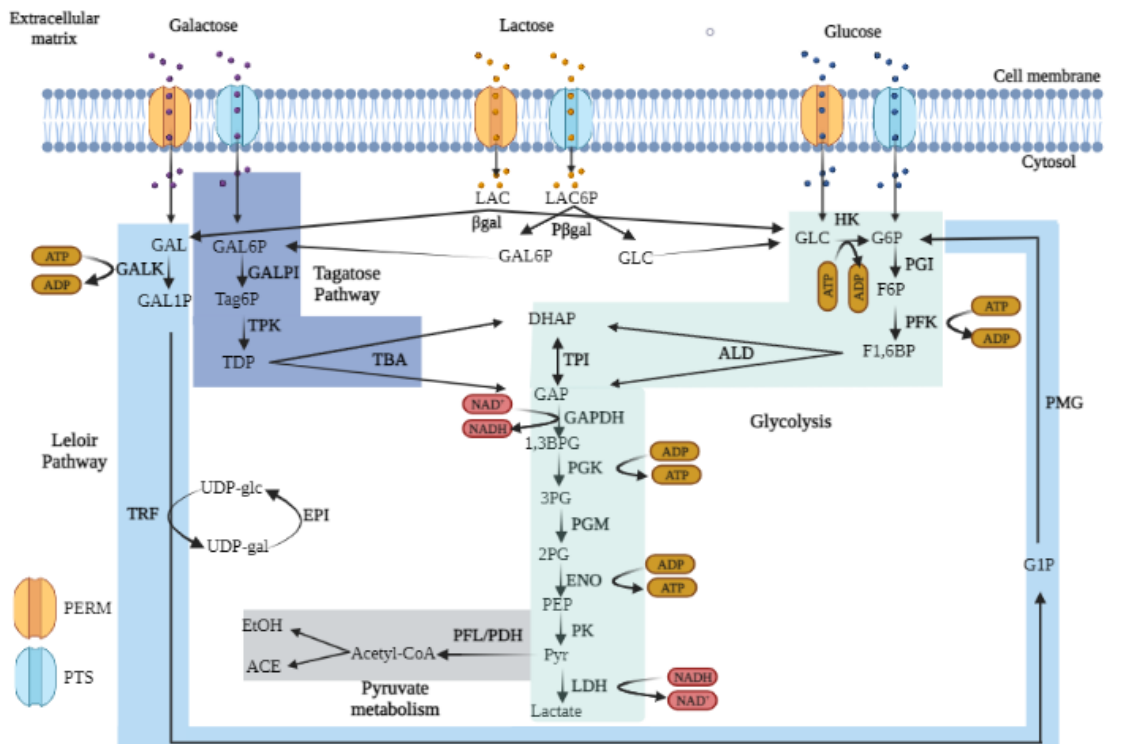


**Figure 2.3: Metabolism in *Lactococcus lactis cremoris* MG1363.** A diagram illustrating galactose, glucose, and lactose metabolism including sugar uptake by the permease systems (PERM) and phosphoenolpyruvate (PEP)-dependent phosphotransferase systems (PTS) into the cytosol of *L. lactis*. Abbreviations: ALD: aldolase; DHAP: dihydroxyacetone phosphate; 1,3BPG: 1,3-bisphosphoglycerate; ENO: enolase; F6P: fructose-6-phosphate; F1,6BP: fructose 1,6-bisphosphate; G1P: glucose-1-phosphate; G6P: glucose-6-phosphate;  $\beta$ gal:  $\beta$  galactosidase; GAL: galactose; GAL1P: galactose-1-phosphate; GAL6P: galactose-6-phosphate; GALK: galactokinase; GAP: glyceraldehyde 3-phosphate; GAPDH: glyceraldehyde-3-phosphate dehydrogenase; GLC: glucose; HK: hexokinase; PEP: phosphoenolpyruvate; 2-PGA: 2-phosphoglycerate; 3-PGA: 3-phosphoglycerate; P $\beta$ gal: phospho- $\beta$ -galactosidase; PDH: pyruvate dehydrogenase; PFK: phosphofructokinase; PFI: phosphoglucose isomerase; PGK: phosphoglycerate kinase; PGM: phosphoglycerate mutase; PK: pyruvate kinase; PMG: phosphoglucomutase; PYR: pyruvate; TPI: triose-phosphate isomerase; Tag6P: tagatose-6-phosphate; TBA: tagatose-bisphosphate aldolase; TDP: tagatose-1,6-diphosphate; TPK: tagatose-phosphate kinase; TRF: galactose/uridylyl transferase; EPI: UDP-glucose epimerase. Figure adapted from: Coccagn-Bousquet, M., Even, S., Lindley, N.D. and Loubière, P.: Anaerobic sugar catabolism in *Lactococcus lactis*: Genetic regulation and enzyme control over pathway flux. *Applied Microbiology and Biotechnology*, 60(1-2), pp.24-32, 2002.

## 2.3 Glycolysis

Metabolism is a complex network that connects chemical processes, such as glycolysis (Embden-Meyerhof-Parnas), the tricarboxylic acid cycle (TCA), and the pentose phosphate pathway (PPP) to each other within a cell [44]. However, glycolysis is the only process that occurs in almost all organisms regardless of the presence (aerobic) or absence (anaerobic) of oxygen, and results in conversion of glucose to pyruvate aerobically and lactate anaerobically [33]. Glycolysis begins with the uptake of glucose from external sources to the interior of the cell. Within the cell, glycolysis is divided into two phases namely, upper glycolysis (comprising hexokinase (HK), phosphoglucose isomerase (PGI), phosphofructokinase (PFK), aldolase (ALD), and triose-phosphate isomerase (TPI)), and lower glycolysis (consisting of the enzymes glyceraldehyde-3-phosphate dehydrogenase (GAPDH), phosphoglycerate kinase (PGK), phosphoglycerate mutase (PGM), enolase (ENO), and pyruvate kinase (PK)). Two phosphorylation steps by HK and PFK consume ATP for the phosphorylation of glucose and fructose-6-phosphate (F6P) during upper glycolysis, while lower glycolysis produces ATP during 3-phosphoglycerate (3PG) and pyruvate formation by PGK and PK, respectively. This entire process results in the net production of 2 molecules of lactate, ATP, and H<sub>2</sub>O (equation 2.3.1, Figures 2.2 and 2.3).



In both *P. falciparum* and *L. lactis* metabolites from the branched pathways (tagatose and Leloir pathway in *L. lactis*, and the pentose phosphate pathway in *P. falciparum*) are recycled back into glycolysis. However, in the absence of glucose, *L. lactis* is able to compensate for energy production from other sources (galactose and lactose) much better than *P. falciparum* that can only use fructose as an alternative source.

## 2.4 The role of glyceraldehyde-3-phosphate dehydrogenase

In *P. falciparum* and *L. lactis* glyceraldehyde-3-phosphate dehydrogenase (GAPDH, EC 1.2.1.12) mediates the sixth step in glycolysis by converting glyceraldehyde-3-phosphate

## 2.4. The role of glyceraldehyde-3-phosphate dehydrogenase

(GAP), inorganic phosphate ( $P_i$ ) and  $NAD^+$  to 1,3-bisphosphoglycerate (1,3 BPG) and NADH [45–47] (Figure 2.4).

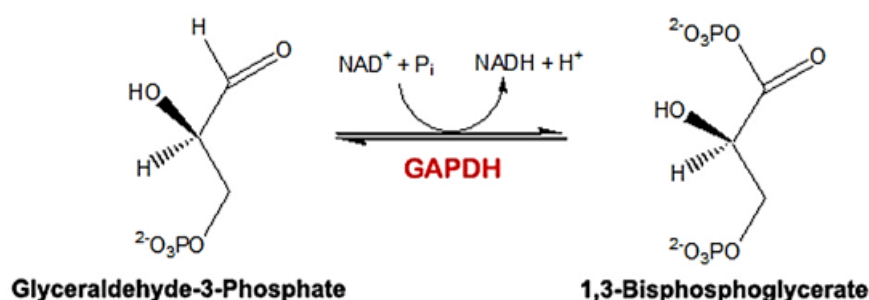


Figure 2.4: The glyceraldehyde-3-phosphate dehydrogenase (GAPDH) catalysed reaction [48].

GAPDH is the only enzyme that produces NADH in the glycolytic pathway and catalyses a phosphorylation step that is essential for the net ATP production in the pathway. In addition, many nonglycolytic functions are also performed by GAPDH, linking it to DNA repair, cytoskeleton regulation, RNA transcription, membrane fusion, cell death, post-translational modification, and calcium flux [49, 50]. It has also been recognized as a biomarker for cellular stress and is able to facilitate the recovery from stressors (internal and external as well as reactive oxygen species (ROS)) or initiate apoptotic signalling [50]. Composed of four identical subunits, this tetrameric enzyme isoform contains one cysteine residue in each subunit [46, 49–52], making GAPDH highly reactive. In cancer cells, GAPDH expression is upregulated and has a strong correlation to tumorigenesis [53]. In addition, GAPDH also interacts with the proteins,  $\beta$  amyloid precursor protein and huntingtin, which cause neurodegenerative diseases such as Alzheimers and Huntington’s disease [50, 53, 54].

When considering GAPDH as a potential drug target in *P. falciparum*, identity between host and parasite GAPDH needs to be considered in an effort to provide minimal disruption to the host. PfGAPDH (GAPDH from *P. falciparum*) was shown to share a sequence identity of 63.5% [33, 55] with the human erythrocytic GAPDH [33, 55, 56] (<https://www.uniprot.org/uniprot/Q8IKK7>). In *L. lactis*, this 36.6kDa protein has 44.4% identity with the human homolog (<https://www.uniprot.org/uniprot/A2RP55>).

Another factor to consider would be the enzyme’s ability to be altered by inhibition with small molecules. Finally, the degree of flux control that an enzyme has, needs to be

## 2.4. The role of glyceraldehyde-3-phosphate dehydrogenase

---

known, as enzymes with high flux control can be regarded as having a greater potential as drug targets [57].

Enzyme inhibitors are drugs or compounds that bind to enzymes to hamper their activity. Obstructing enzyme activity, ultimately hinders the pathway the enzymes are active in. In the instance of *P. falciparum*, if we were to inhibit any of the glycolytic enzymes, glycolysis would be impeded, the production of ATP would be decreased, and the growth of the parasite slowed down. Thus, this form of inhibition would serve as a feasible treatment option.

However, not all enzymes require the same degree of inhibition and/or the same type of inhibition (irreversible, reversible, allosteric, competitive, noncompetitive, uncompetitive). An illustration depicting enzyme inhibition is shown in Figure 2.5. Competitive inhibition is when an inhibitor and a substrate compete for the same active site of a free enzyme, while maintaining the maximal rate ( $V_{max}$ ) of catalysis. Allosteric inhibition happens when a compound binds to an additional site other than the catalytic site on the enzyme to inhibit enzyme activity. During noncompetitive inhibition, the inhibitor has the ability to bind to the enzyme regardless of whether it is already bound to the substrate however, for uncompetitive inhibition the inhibitor binds to the enzyme substrate (ES) complex. Irreversible inhibition is a form of inhibition that occurs when an inhibitor binds covalently with a functional group in the enzyme catalytic site (Figure 2.5) [58, 59]. Additionally, the effects of irreversible inhibition cannot be reversed by the removal of the inhibitor by dilution or dialysis.

In general, an enzyme can be bound to a substrate as well as an inhibitor, leading to the production of an enzyme-substrate complex as well as an enzyme-inhibitor complex. The moment an inhibitor binds to the enzyme, all subsequent processes (or pathways) requiring the enzyme to be catalytically active will be inhibited.

As an inhibitor of a specific enzyme is titrated in, we expect the activity of the enzyme to decline. When this occurs, the flux control coefficient will increase, causing a redistribution of control within the pathway.

In a more general approach, enzyme inhibitors can be used in experimental studies to



## 2.4. The role of glyceraldehyde-3-phosphate dehydrogenase

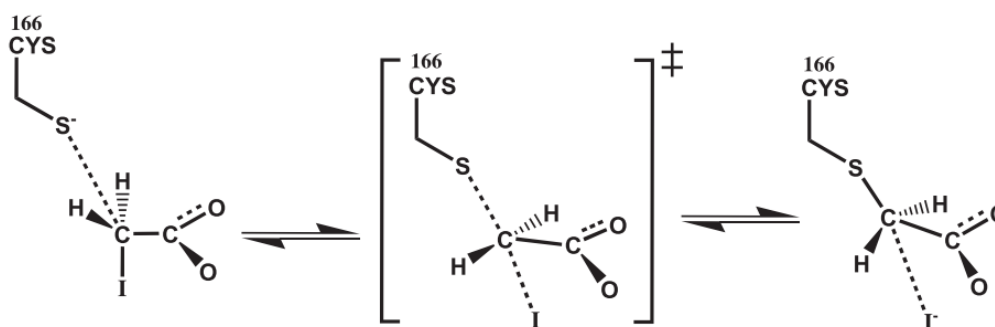


**Figure 2.6: The proposed mechanism of *Trypanosoma cruzi* GAPDH inactivation through IAA.** This illustration by Carneiro *et al.* [59] describes the formation of a S-carboxymethyl covalent complex, which inhibits the formation of GAPDH- $NAD^+$  complex during dehydrogenation as well as the transfer of hydride from Cys<sup>166</sup> of the thioester to  $NAD^+$ .

The covalent attachment of the inhibitor to the enzyme catalytic site suppresses GAPDH- $NAD^+$  complex formation as well as the hydride transfer from the catalytic cysteine of the thioester to  $NAD^+$  [22, 24, 59, 61]. The mechanism of GAPDH inactivation through IAA within *Trypanosoma cruzi* has been proposed by Carneiro *et al.* [59] (Figure 2.6), and describes IAA action when the S-carboxymethyl covalent complex is formed within the molecular mechanism of action of GAPDH. Although no mechanism has been proposed in both *P. falciparum* and *L. lactis* for IAA inhibition, we assume similar effects would be induced based on the molecular mechanism of action in these organisms. This inhibitor has been measured as having an effect on GAPDH activity and lactate production at low concentration levels below 100  $\mu\text{M}$  in cultured astrocytes [22, 24, 60] as opposed to iodoacetamide (IAM) that requires a ten times larger concentration to inhibit 50% of lactate produced in the same cells. IAA was also shown to affect the glutathione metabolism within brain cells minimally as opposed to IAM that has a stronger effect, while affecting glycolysis marginally. Thus, IAM is not the best choice to inhibit GAPDH if the aim is to inhibit glycolysis.

Other GAPDH inhibitors include 3-bromopyruvate (3-BP,  $\text{C}_3\text{H}_2\text{BrO}_3$ ,  $M_r = 164.92$  g/mol), koningic acid (KA,  $\text{C}_{15}\text{H}_{20}\text{O}_5$ ,  $M_r = 280.3$  g/mol), and ornidazole (ORN,  $\text{C}_7\text{H}_{10}\text{ClN}_3\text{O}_3$ ,  $M_r = 219.63$  g/mol) (Table 2.1). 3-BP is a pyruvate analog with alkylating properties and a half-life of 77 minutes known to inhibit hexokinase, however, recent studies have shown that it binds more strongly to GAPDH [45]. This instability questions the integrity of 3-BP as a potential inhibitor. Koningic acid (or heptelidic acid) on the other hand, attacks the thiol groups of GAPDH in a similar manner to IAA [62, 63]. This

## 2.5. Modelling the glycolytic pathway

---

selective inhibitor has antibiotic properties against anaerobic bacteria and also inhibits DNA polymerase [64]. Ornidazole is an antibiotic used for the treatment of protozoan infections and targets both GAPDH and TPI [65, 66], and hence its binding is nonspecific. These GAPDH inhibitors (in contrast to IAA) are not very useful for the current study as they all have detrimental effects or are not very stable and specific to the enzyme to which they bind. Additionally, the irreversible nature of IAA binding makes it possible to incubate IAA and the enzyme for a certain time period before the inhibitors is washed away, and the flux and enzyme activity are measured in the same cells. Examples of other glycolytic enzymes as drug targets can be seen in the appendix.

## 2.5 Modelling the glycolytic pathway

To model the glycolytic pathway in various organisms, a systems biology approach has been followed. Systems biology combines computational techniques and mathematical models to examine the interaction between the biological system components and the behaviour of the system [70]. This approach is used to understand the bigger picture and determine how all the metabolic components and their interactions are integrated within an organism. Systems biology can be subdivided into two approaches, namely top-down and bottom-up. Top-down approaches give information addressing the overall correlations, while bottom-up approaches provide a more mechanistic characterisation of the molecular components [71, 72]. The models used in this study were constructed using bottom-up approaches, with ordinary differential equations (ODEs) describing the time-dependent changes in metabolite concentrations as a function of enzyme mechanistic rate equations.

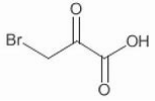
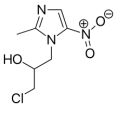
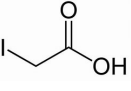
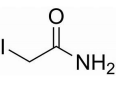
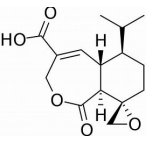
### 2.5.1 Metabolic Control Analysis

Sensitivity analysis can be applied to mathematical models to ascertain the processes responsible for producing the desired outcome and to unravel the uncertainty in the model predictions [73].

Metabolic control analysis (MCA) is a version of sensitivity analysis developed by Heinrich and Rapoport [74], and Kacser and Burns [75]. It quantifies the effect of small local perturbations on the steady-state behaviour in biological systems. MCA quantitatively

## 2.5. Modelling the glycolytic pathway

**Table 2.1: GAPDH inhibitors as potential therapeutics in *P. falciparum*.**

Compound	Compound role	Enzyme target	% identity <sup>a</sup>
 3-bromopyruvate	abolishes ATP production, alkylating agent, inhibits hexokinase II, thermodynamically unstable cytotoxic activity against cancer cells	HK [67] GAPDH[45]	15.76% <sup>1</sup> 63.7% <sup>2</sup>
 ornidazole	an antibiotic used to treat protozoan infections. is converted to chlorolactate instead of producing lactate.	TPI[65, 66] GAPDH[65, 66]	19.61% <sup>3</sup> 63.7% <sup>2</sup>
 iodoacetic acid	reacts with the sulfhydryl (-SH) group of the cysteine residue at the active site of the enzyme to prevent the forma- tion of thiohemiacetal modify thiol groups in proteins by S-carboxymethylation	GAPDH [60, 68]	63.7% <sup>2</sup>
 iodoacetamide	reacts with the sulfhydryl (-SH) group of the cysteine residue at the active site modify thiol groups in proteins by S-carboxyamidomethylation	GAPDH [60]	63.7% <sup>2</sup>
 koniginic acid	covalently binds to catalytic cysteine of GAPDH	GAPDH [60, 69]	63.7% <sup>2</sup>

<sup>a</sup> refers to the enzyme % identity of the target enzyme relative to the human homolog<sup>1</sup> <https://www.uniprot.org/align/A202112094ABAA9BC7178C81CEBC9459510EDDEA300EB68A><sup>2</sup> <https://www.uniprot.org/uniprot/Q8IKK7><sup>3</sup> <https://www.uniprot.org/align/A202112094ABAA9BC7178C81CEBC9459510EDDEA300EB67L>

## 2.5. Modelling the glycolytic pathway

determines the amount of enzyme activity inhibition necessary to alter the overall flux of a pathway [6, 76]. MCA also determines the relationship between the parameters of a model and the steady-state properties to calculate how sensitive the system will be to a change in a specific parameter at a steady state. If we consider the responses of individual enzymes to alterations in concentrations of their substrates and other metabolites [77], we define an elasticity coefficient ( $\epsilon_p^v$ ) to be:

$$\epsilon_p^v = \frac{\partial \ln v}{\partial \ln p} \quad (2.5.1)$$

where  $v$  represents the enzyme reaction rate and  $p$ , the system parameter or metabolite concentration. This coefficient reports how the enzyme activity changes when making a perturbation (by 1%) in a parameter [57].

Control coefficients measure the degree of control a local property, a rate, has on the steady-state concentration of a metabolite ( $C_v^X$ ) or flux ( $C_v^J$ ).

$$C_v^J = \frac{\partial \ln J}{\partial \ln v} \quad C_v^X = \frac{\partial \ln X}{\partial \ln v} \quad (2.5.2)$$

where  $J$  represents the reaction flux,  $X$  is the steady-state metabolite concentration, and  $v$  is the reaction rate. If perturbations, such as inhibitor action, were presented to a pathway and a change in an enzyme activity and a system property quantified, these control coefficients would reveal how much this perturbation (by 1%) in a rate affects the steady-state concentration of a metabolite or a reaction flux, e.g.

$$C_v^J = \frac{\partial J}{J} \times \frac{v}{\partial v} \approx \frac{\Delta J}{\Delta v} \times \frac{v}{J} \quad (2.5.3)$$

Metabolic control analysis provides a solid theoretical foundation for the classical ideas of metabolic regulation because it nullifies any assumption that metabolic systems must be studied with regulatory enzymes whose properties determine the behaviour of the whole system. Instead of assuming the existence of "key enzymes" or rate-limiting steps, metabolic control analysis allows the contribution of each enzyme to be quantified within a pathway.

## 2.5. Modelling the glycolytic pathway

For years, many believed that only one enzyme controls the flux of the pathway, but studies conducted by Groen *et al.* [78] and later by Joy *et al.* [79] have shown the contrary, i. e. multiple enzymes may control the flux and activity of the pathway [80]. According to MCA, this control pattern obeys the summation theorem that states that the sum of the flux control coefficients equates to 1 [81] as shown in equation 2.5.4.

$$C_{v_1}^J + C_{v_2}^J + \dots = 1 \quad (2.5.4)$$

The effect of a local parameter on the steady states of a system is quantified by a response coefficient. Elasticity and control coefficients can be used to calculate the response coefficient as shown in equation 2.5.5 where the sum is over all of the reactions  $v$  affected by the parameter  $p$ :

$$R_p^X = \sum C_v^X \cdot \epsilon_p^v \quad R_p^J = \sum C_v^J \cdot \epsilon_p^v \quad (2.5.5)$$

If the parameter is a rate multiplier such as an enzyme concentration, the elasticity coefficient would equal 1 resulting in the response coefficient and the control coefficient to be equal to each other [82]. In the case of an inhibitor, the system response is dependent on how strong the inhibitor acts on the enzyme  $\epsilon_p^v$  and the control of the enzyme on the system property  $C_v^J$ .

### 2.5.2 Existing models of glycolysis

A systems biology approach has been used by many researchers to describe glycolysis in different microorganisms. Glycolytic models within *Saccharomyces cerevisiae* (yeast) have been established [10] and have laid the foundation for predicting glycolytic flux and metabolite concentrations in different organisms *in vivo* from *in vitro* enzyme kinetic data [10, 83].

Another such example is the trypanosome model constructed by Bakker *et al.* [84] that investigated the control of the glucose transporter. In this study, they showed experimentally that the flux control exerted by the glucose transporter was not absolute, resulting in shared control with other enzymes. Moreover, similar behaviour was seen by the

## 2.5. Modelling the glycolytic pathway

---

model and it was found that glycosomal compartmentation had protection properties in trypanosome glycolysis.

Maria *et al.* propounded a reduced glycolytic model in *Escherichia coli* that was able to reproduce the behaviour of glycolysis under transient, steady-state and oscillatory conditions [11]. Lambeth and Kushmerick [12] constructed a model of glycogenolysis in fast twitch muscle fibers. Mulquiney *et al.* developed a model that investigated 2,3-bisphosphoglycerate metabolism in red blood cells [85]. Researchers such as Mulquiney and Penkler [4, 85] have provided meaningful research on the erythrocyte, and the intraerythrocytic stage (trophozoite) of the plasmodium life cycle. Penkler *et al.* [4] developed a model of the entire glycolytic pathway within the intraerythrocytic stage of *P. falciparum* 3D10 trophozoites. Hoefnagel *et al.* [8] conducted similar experiments to uncover the flux control distribution in *L. lactis*, and constructed a detailed kinetic model of glycolysis and the pyruvate branches within *L. lactis* [8].

### 2.5.3 Modelling glycolysis in *L. lactis* and *P. falciparum*

The glycolytic pathways of *P. falciparum* and *L. lactis* have been studied extensively over the past few years *in vitro* and *in vivo*. However, very few studies have included the effect glycolytic inhibitors have on the carbon metabolism of the parasite and bacterium. Adapting well-known models to include the addition of glycolytic inhibitors, could help us understand how these drugs may act within these species apart from what is proposed in literature.

#### 2.5.3.1 Modelling glycolysis in *L. lactis*

A detailed kinetic model of *L. lactis* glycolysis, constructed by Hoefnagel *et al.*, investigated the dynamics of glycolytic intermediate during glucose run-out experiments [7, 8]. The kinetic model consists of 15 ordinary differential equations (ODEs), 29 rate equations and 34 metabolites that describe glycolysis, polysaccharide and pyruvate branches. Previously, this lactic acid bacterium (LAB) has been investigated in various studies [7, 15, 23, 24] to identify the important mechanisms involved in the regulatory switch between fermentation modes (mixed acid, homolactic) in *L. lactis*. Some studies also investigated the regulation of the LAB sugar metabolism by-products [15, 86, 87].

Poolman *et al.* investigated how GAPDH could control the glycolytic flux in non-growing

*L. lactis* Wg2 cells when exposed to iodoacetic acid (IAA) [88]. They found that GAPDH has absolute control over the glycolytic flux. However, another study conducted by Solem *et al.* [15] found that GAPDH has no control over the glycolytic flux in both growing and non-growing *L. lactis* Mg1363 cells (also using IAA). This discrepancy in the control of *L. lactis* may suggest that the flux control may be species or strain-specific. MCA has also indicated that the glucose transporter, PFK, and GAPDH have significant flux control on the glycolytic pathway [88–91].

### 2.5.3.2 Modelling the glycolytic pathway of *P. falciparum*

A quantitative enzyme kinetic model of glucose metabolism in the trophozoite form of *P. falciparum* was developed by Penkler *et al.* [4]. The Penkler model used a bottom-up systems biology approach to investigate how well the *in vitro* enzyme kinetics can predict and explain the *in vivo* steady-state behaviour. The model comprised of 17 rate equations as well as 15 ordinary differential equations (ODEs) to describe and predict the flux through glycolysis, as well as metabolite concentrations at steady-states and after perturbations [92].

A study by van Niekerk *et al.* investigated the flux control of the glucose transporter upon inhibition with cytochalasin B in *P. falciparum* 3D10 trophozoites [6]. In a model analysis, they also found that a significant amount of glycolytic flux control by GAPDH was present.

## 2.6 Concluding remarks

The glycolytic pathway is an essential source of ATP in the malaria parasite, and the pathway could be a potential drug target to combat malaria through the inhibition of an enzyme such as GAPDH. For *L. lactis*, it is unclear how much control GAPDH has on the glycolytic flux. This study therefore aims to quantify the control that GAPDH has in both organisms experimentally and in models of glycolysis using the known inhibitor of GAPDH, IAA.

## Chapter 3

# Materials and Methods

To quantify the flux control of GAPDH via an IAA titration in both *L. lactis* and *P. falciparum*, a combination of experimental and computational methods were used to determine glucose uptake, lactate production, and enzyme activities. Measurements were conducted in technical replicates within two independent biological repeats for *L. lactis* and one independent experiment for *P. falciparum*. Model analysis was performed using Wolfram Mathematica 12.0 (Wolfram Research, Inc., Champaign, IL, USA).

### 3.1 Research Design

This study was designed as follows: two microorganisms, *Lactococcus lactis* and *Plasmodium falciparum* were cultured, harvested and preincubated with iodoacetic acid. These microorganisms were then lysed using glass bead extraction or freeze-thaw cycles, respectively. The flux for lactate production and glucose consumption from *P. falciparum* 3D7 (refer to section 4.2) and *L. lactis* MG1363 strains exposed to iodoacetic acid was determined by measuring lactate and glucose concentrations in supernatant. To determine the GAPDH enzyme activities within these two micro-organisms, a reverse direction assay of the enzyme was conducted (i.e. the coupling of PGK to GAPDH for the conversion of 3-PGA, ATP and NADH to GAP, ADP and NAD). Spectrophotometric methods were used to quantify metabolites in the supernatant for flux determination and activity assays. An existing mathematical model of *L. lactis* glycolysis and a model of *P. falciparum* glycolysis that was constructed earlier in our group, were adapted to describe the IAA inhibition effect on GAPDH activity. Experimentally determined enzyme kinetic parameters were inserted into these models and they were simulated using Wolfram Mathematica 12.0.

This research was performed in accordance with the ethical standards stated in Helsinki Declaration and all protocols and procedures were approved by the Stellenbosch University Human Research Ethics Committee (X20/02/006) prior to the study.

## 3.2 Raw Materials and Chemicals

All general reagents (salts and buffers) and enzymes used in the study were of analytical grade. *P. falciparum* (3D7) was obtained from the de Villiers laboratory (Department of Biochemistry, Stellenbosch University) and maintained in continuous culture with packed human A<sup>+</sup> or O<sup>+</sup> erythrocytes within EDTA filled BD Vacutainer<sup>®</sup> lavender blood collection tubes (BD Biosciences, South Africa). Bovine serum albumin (BSA), gentamycin sulfate (#G3632), 4-(2-hydroxyethyl)-1-piperazineethanesulfonic acid (HEPES), de Man, Rogosa, and Sharpe (MRS) broth, MES hydrate, RPMI 1640 powder, glucose powder, sodium bicarbonate, acid-washed glass beads (425-600  $\mu\text{m}$ ), sorbitol, and all enzymes were purchased and obtained from Sigma-Aldrich. Albumax and RPMI 1640 GlutaMAX<sup>™</sup> enriched liquid media (#61870036) was obtained from Thermo Fisher Scientific and hypoxanthine from Alfa Aesar.

## 3.3 Preparation of Reagents, Media and Buffers

All enzyme stocks were prepared fresh on the day of use to avoid degradation of the enzyme's activity. Metabolites were prepared in a larger volume, aliquoted and stored at -20°C for use when needed.

### 3.3.1 Reagents

#### 3.3.1.1 ADP stock (20 mM and 50 mM)

To prepare a 20 mM and 50 mM ADP stock solutions, 85.4 mg and 0.0214 g of ADP ( $M_r = 427.201$  g/mol) was weighed out and volume was adjusted to 10 mL and 1 mL with the appropriate buffer for the different micro-organisms (MES buffer for *L. lactis* (section 3.3.3.1) and modified ringers buffer (without glucose) for *P. falciparum* (section 3.3.3.2)), respectively. Aliquots (2 mL) were made and stored in the -20°C freezer.

### 3.3. Preparation of Reagents, Media and Buffers

---

#### 3.3.1.2 ATP stock (40 mM)

A 40 mM ATP stock was prepared using 0.305 g of ATP. Mg<sup>2+</sup> salt powder ( $M_r = 507,18$  g/mol) and adjusting it to 15 mL with the appropriate buffer for the different micro-organisms. Aliquots of 2 mL were prepared, stored at -20°C until needed, but used within two weeks to avoid degradation of the metabolite.

#### 3.3.1.3 F6P disodium salt stock (50 mM)

To prepare a 1 mL 50 mM F6P stock solution, 0.0152 grams of F6P ( $M_r = 304.1$  g/mol) was weighed out and volume adjusted to 1 mL with the appropriate buffer.

#### 3.3.1.4 G6PDH stock (50 U/mL)

To make up a 1 mL 50 U/mL G6PDH stock solution, 12.5  $\mu$ L of G6PDH from *Leuconostoc mesenteroides* is added to 987.5  $\mu$ L of the appropriate buffer.

#### 3.3.1.5 GAPDH stock (50 U/mL)

To make up a 1 mL 50 U/mL GAPDH stock solution, 0.49 mg of GAPDH from rabbit muscle was added to 1 mL of the appropriate buffer.

#### 3.3.1.6 Glucose stock (100 mM)

To prepare a 100 mM glucose stock solution, 0.27 grams of D-glucose ( $M_r = 180.16$  g/mol) was weighed out and the volume was adjusted to 15 mL with the appropriate buffer for the different micro-organisms. This solution was stored at 4°C.

#### 3.3.1.7 Iodoacetic acid stock (100 mM)

All iodoacetic acid stock solutions were made up fresh directly before use to prevent alkylation that will modify tyrosine residues within the sample. A 1 mL 100 mM stock solution was made up by weighing out 18.6 mg of IAA ( $M_r = 185,96$  g/mol) and combining it with the appropriate buffer needed for the different micro-organisms.

#### 3.3.1.8 LDH stock (50 U/mL)

LDH stock solutions were made up fresh directly before use to prevent degradation of its enzyme activity. A 2 mL 50 U/mL stock solution was made up by adding 13.74  $\mu$ L

### 3.3. Preparation of Reagents, Media and Buffers

---

of LDH from bovine heart ( $M_r = 140$  kDa) and combining it with the appropriate buffer needed for the different micro-organisms.

#### 3.3.1.9 NAD<sup>+</sup> stock (8 mM)

A 10 mL of an 8 mM NAD<sup>+</sup> stock was made with 53 mg of NAD<sup>+</sup> powder ( $M_r = 663.43$  g/mol) for the different micro-organisms. The stock solution was divided into 2 mL aliquots and stored at -20°C until it was needed.

#### 3.3.1.10 NADH stock (8 mM)

To prepare a 10 mL of an 8 mM NADH stock solution, 0.059 g of NADH powder ( $M_r = 741.62$  g/mol) were weighed out and volume adjusted to 10 mL with the appropriate buffer needed for the different micro-organisms.

#### 3.3.1.11 NADP<sup>+</sup> stock (8 mM)

A 4 mL of an 8 mM NADP<sup>+</sup> stock was made with 24.48 mg of powder ( $M_r = 765.39$  g/mol) for the different micro-organisms.

#### 3.3.1.12 PEP stock (50 mM)

To prepare a 1 mL 50 mM PEP stock, 9.5 mg of PEP ( $M_r = 190.02$  g/mol) was weighed out and volume adjusted to 1 mL with the appropriate buffer required.

#### 3.3.1.13 2-PGA stock (100 mM and 200 mM)

To prepare a 1 mL 100 mM and 200 mM 3PGA stock, 0.032 g and 0.064 g of 3PGA ( $M_r = 321.37$  g/mol) was weighed out and volume adjusted to 1 mL with the appropriate buffer required.

#### 3.3.1.14 3-PGA stock (20 mM and 100 mM)

To prepare a 2 mL 20 mM and 5 mL 100 mM 3PGA stock, 0.023 g and 0.115 g of 3PGA ( $M_r = 230.02$  g/mol) was weighed out and volume adjusted to 10 mL with the appropriate buffer required, respectively.

### 3.3. Preparation of Reagents, Media and Buffers

---

#### 3.3.1.15 PGK stock (50 U/mL)

A 1 mL 50 U/mL PGK stock solution was prepared by combining 7  $\mu$ L PGK with 993  $\mu$ L of the appropriate buffer (Mes buffer or assay buffer).

#### 3.3.2 Media

##### 3.3.2.1 *L. lactis*

###### *MRS broth*

MRS broth is preferred for culturing *Lactobacilli* from various strains. Fifty one grams (51 g) of MRS broth powder (containing 20 g/L glucose, 10 g/L peptone, 8 g/L meat extract, 4 g/L yeast extract, 0.2 g/L magnesium sulfate heptahydrate, 0.05 g/L manganous sulfate tetrahydrate, 5 g/L sodium acetate trihydrate, and 2 g/L triammonium citrate) was weighed out and combined with one liter deionized water that has been supplemented with 1 mL/L Tween 80. The pH was adjusted to 6.2 to match the pH of MES buffer. The mixture was autoclaved at 121°C for 15 minutes.

##### 3.3.2.2 *P. falciparum*

###### *RPMI 1640 Culture Medium (CM)*

RPMI 1640 GlutaMax supplemented medium (#61870036) obtained from Thermofischer Scientific was used for the study. Five hundred millilitres of this medium was prepared by combining 25 ml media to 1 g glucose, 2.98 g hepes, and 25 mg gentamycin sulfate and filter-sterilized (0.2  $\mu$ m pore filter, Pall Corporation, South Africa) back into the original medium bottle. It was further supplemented with a sterile 10 mL of a 25% (w/v) albumax solution followed by 1.25 mL hypoxanthine solution (13.75 mg in 1.25 ml 0.5 M NaOH solution).

###### *Glycerolyte Medium*

Glycerolyte medium facilitates the cryopreservative processing of *P. falciparum* young cells (rings) at -80°C. The medium contained 1.6 g sodium lactate, 30 mg potassium chloride, 1.38 g sodium dihydrogen phosphate, and 45.3 mL glycerol (which contains 57 g of glycerol). The pH and volume were adjusted to 6.8 using NaOH base and 100 mL Sabax pour water, respectively.

### 3.3. Preparation of Reagents, Media and Buffers

---

#### 3.3.3 Buffers and Solutions

##### 3.3.3.1 *L. lactis* Buffers

###### *MES buffer (0.5 M)*

A 500 mL of a 0.5 M solution of MES buffer was prepared by combining 48.8 g MES hydrate (Sigma-Aldrich) to 500 mL distilled water. The pH of the solution was adjusted to 6.2 to match the pH of the culture media. The solution was then filtered through a 0.2  $\mu\text{m}$  filter and its container was wrapped in foil as MES hydrate is light sensitive in solution.

##### 3.3.3.2 *P. falciparum* Buffers

###### *HEPES/MgSO<sub>4</sub> Buffer (pH 7.6)*

A 250 mL solution of HEPES/MgSO<sub>4</sub> buffer is made by combining 8.939 g 4-(2-hydroxyethyl)-1-piperazineethanesulfonic acid (HEPES), 0.924 g magnesium sulfate (MgSO<sub>4</sub>), and Sabax pour water to a 250 mL media bottle. The pH of the mixture was adjusted to 7.6, accounting for physiological conditions.

###### *Phosphate Buffered Saline (PBS; 10X)*

A 10X solution of PBS is made by combining 4 g sodium chloride (NaCl), 0.1 g potassium chloride (KCl), 0.575 g disodium phosphate (Na<sub>2</sub>HPO<sub>4</sub>), 0.1 g monopotassium phosphate (KH<sub>2</sub>PO<sub>4</sub>) and Sabax Pour water to a 50 mL conical tube. The pH of the mixture was set to 7.2, accounting for physiological conditions.

###### *Modified Ringer Buffer (pH 7.1)*

Two different ringer buffers were prepared with and without 5 mM glucose. The differentiation between glucose addition and absence was used as a means to prevent lactate production during flux inhibition. 45 mg 5 mM Glucose, 595.8 mg 50 mM hepes, 10.2 mg 1 mM magnesium chloride, 37.3 mg 10 mM potassium chloride and 350.6 mg 120 mM sodium chloride were weighed out and combined in Sabax Pour water. Modified ringer solution maintains red blood cell osmolarity, preventing cell death.

### **Wash Buffer**

2.979 g HEPES (50 mM) and 2.6 g RPMI (10 g/L) are combined with 250 mL Sabax Pour water to form the wash buffer. The pH of the buffer is adjusted to 7.1 and filter sterilized (0.45  $\mu\text{m}$ ; Pall Corporation). The wash buffer removes any parasite debris that may remain on the surface of red blood cells upon trophozoite isolation.

### **Enzyme Assay Buffer (pH 7.17)**

A 500 mL assay buffer was prepared using 2.383 g 20 mM HEPES, 0.952 g 20 mM  $\text{MgCl}_2$ , 0.373 g 10 mM KCl, and 0.584 g 20 mM NaCl combined with 500 mL Sabax Pour water (Adcock Ingram). The pH was adjusted using 1 M NaOH to 7.17.

### **Giemsa Stain**

Five millilitres (5 mL) filtered Giemsa and 5 mL filtered PBS were combined with 40 mL milli-Q water. This mixture was then filtered through a 0.45  $\mu\text{m}$  pore filter to remove any residual impurities that may have formed as a result of mixing.

## **3.4 Methodology**

### **3.4.1 *L. lactis***

Methods pertaining to *L. lactis* are from Hoefnagel *et al.* [7, 8] and Jordaan [93].

#### **3.4.1.1 Bacterial strains, growth medium and conditions**

One representative strain belonging to lactic acid bacteria (LAB) genera was selected: *Lactococcus lactis cremoris* MG1363. MRS agar plates were streaked with *L. lactis* obtained from glycerol freezer stocks that were stored at  $-80^\circ\text{C}$ . These plates were grown for 3 to 5 days at  $37^\circ\text{C}$  before cell colonies became visible on the surface of the agar plate. From these colonies, a single cell colony was used to inoculate a 20 mL starter culture (containing MRS broth), which was grown overnight in an orbital shaker (180 rpm) at  $37^\circ\text{C}$ . After 2-3 days, the starter culture reached an  $\text{OD}_{600}$  that was high enough for it to be able to inoculate a 60x volume larger than the starter culture. *L. lactis cremoris* MG1363 strains were grown at  $37^\circ\text{C}$  under anaerobic conditions for 48 hours while agitated at 180 rotations per minute (rpm) (LM-575D orbital shaking incubator, Labec) in de Man,

Rogosa, and Sharpe (MRS) broth mentioned above. Inoculation was at 1.66% (v/v) and initiated with cells from precultures grown in the same MRS broth.

#### 3.4.1.2 Growth curve

Bacterial growth, in terms of optical density, was monitored spectrophotometrically at 600 nm every hour during the lag phase and upon commencement of the exponential phase, measurements were taken every 30 minutes.

#### 3.4.1.3 Harvesting of Cells

Cultures were grown to an OD<sub>600</sub> of approximately 1.0 and harvested in the exponential growth phase. Cultures were harvested by centrifugation at 3000 xg for 10 minutes at 4°C and washed twice with 1 mL deionized water. Cells were either stored at -20°C or resuspended in 1 mL 0.5 M MES buffer before further experiments.

### 3.4.2 *P. falciparum*

Methods pertaining to *P. falciparum* can be found in Penkler *et al.* [4, 56].

#### 3.4.2.1 Red Blood Cell (RBC) Preparation

A<sup>+</sup> and/or O<sup>+</sup> Blood, not older than 14 days, was used as culture medium in addition to Roswell Park Memorial Institute (RPMI) 1640 supplemented medium. The human blood was washed with culture media and centrifuged (Eppendorf 5804) thrice at 1300 xg for 3 minutes to remove leukocytes, nutrients, and metabolites. The buffy coat from the blood was removed to ensure that only erythrocytes were present and suspended at 50% vol/vol hematocrit<sup>1</sup> with complete CM.

#### 3.4.2.2 Thawing Freezer Stocks

Glycerol frozen *P. falciparum* 3D7 infected erythrocytes (iRBCs) were thawed in a 37°C water bath. The iRBCs were transferred to a 50 mL falcon tube where decreasing sodium chloride concentrations: 12%, 1.8%, and 0.9%, were applied to it, respectively. The tube contents were centrifuged for 5 minutes at 400 xg after 1.8% and 0.9% sodium chloride solution, and 20mL culture medium addition. Culture medium (50 mL) and blood (enough

---

<sup>1</sup>Hematocrit: the percentage volume of erythrocytes in blood

for a 2% hematocrit) were then added to the tube. The tube contents were inverted to allow for the incorporation of infected erythrocytes with the culture medium. The contents were transferred to a sterile 250 mL Greiner Bio-one culture flask (Lasec, SA; T75 culture flask) and incubated at 37°C with a tri-gas mixture containing 3% oxygen, 4% carbon dioxide, and 91% nitrogen in an incubator to facilitate growth. Every 24 hours, the infected red blood cells (iRBCs) were refreshed with warm (37°C), fresh culture medium and gassed to facilitate the parasite growth.

#### 3.4.2.3 Making Freezer Stocks

iRBCs were harvested to make freezer stocks when they were predominately rings and a  $\pm 10\%$  parasitemia level reached. Freezer stocks were made with these ring-stage parasites using glycerolyte media (section 3.3.2.2) dropwise and stored at -80°C.

#### 3.4.2.4 Parasitemia Determination

Parasitemia<sup>2</sup> was determined in thin blood smears using two different staining techniques: Giemsa staining and Rapidiff stain set, observed under 100X oil-immersion objective on an UB200i series biological microscope (Ziotech lab, Spain).

##### Giemsa Staining

A thin blood smear consisting of a drop of infected blood on a microscope slide and spread across the surface of the slide in a back-and-forth motion was prepared. Once dry, the slide was submerged in methanol for  $\pm 30$  seconds allowing the cells to be fixed to the slide. The slide was dried and the Giemsa stain was transferred onto the slide cell surface for  $\pm 10$  minutes. Giemsa stain was removed from the slide, the remaining stain rinsed with distilled water and the slide dried. The Giemsa stain allowed for the presence of parasites to be observable as dark blue and erythrocytes pale pink under an oil-immersion microscope objective lens.

##### Rapidiff Stain Set Staining

The Rapidiff stain set was utilized and adapted to suit the staining requirements suited for staining erythrocytes. The package protocol was adapted from using five subsequent

---

<sup>2</sup>Parasitemia: the percentage parasitized erythrocytes.

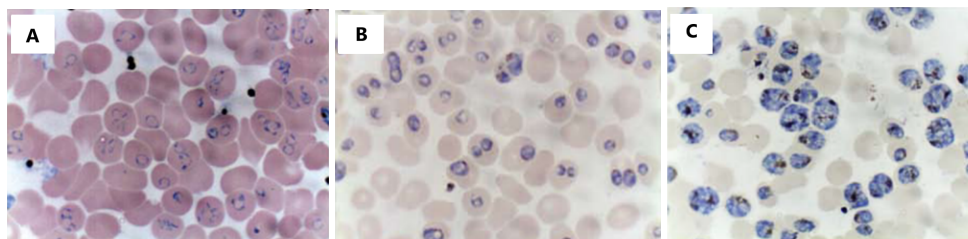


**Figure 3.1:** Example of growth of *P. falciparum* 3D7 at 37°C. Cultures were refreshed every 24 hours with RPMI 1640 supplemented media to supply sufficient amounts of nutrients to the culture and avoid acidification of culture media. Slides were prepared and stained with either Wright's in (A) or 10% Giemsa (B-C) staining procedures. Growth was monitored daily under 100X oil-immersion objective lens and different stages of the parasite life cycle was visible: rings at 45% parasitemia (A), trophozoites (B), and schizonts (C). Figures were obtained from: Radfar, A., Méndez, D., Moneriz, C., Linares, M., Marín-García, P., Puyet, A., Diez, A. & Bautista, J.M.: Synchronous culture of *Plasmodium falciparum* at high parasitemia levels. *Nature Protocols*, vol. 4, no.12, pp.1899-1915, 2009. [94]

dips of Rapidiff fixative, Rapidiff I, and Rapidiff II to using three dips of Rapidiff fixative, and one 30 second dip of Rapidiff II respectively. A thin blood smear, prepared as mentioned above, was submerged into the Rapidiff reagents respectively. After the last dip in Rapidiff II, the slide was rinsed using distilled water, dried and observed under 100X oil-immersion objective lens.

#### 3.4.2.5 Synchronization of *P. falciparum* cultures

Synchronisation was used to ensure that parasites were grown in the same phase. When this was performed, trophozoites were removed so it is best to synchronize when the culture is predominately rings. Synchronization of the cultures was achieved by the use of a 5% *m/v* sorbitol solution and tri-gas mixture (93% nitrogen, 3% oxygen, 4% carbon dioxide).

#### 3.4.2.6 Trophozoite Isolation

Trophozoite isolation was used to separate the metabolically active trophozoite from the erythrocyte and other parasite life forms. Firstly, cells were harvested by centrifugation for 3 min at 750xg and supernatant aspirated. Four cultures, containing 2mL blood blood each, were combined with 40 mL culture medium in a 50 mL falcon cap tube. Trophozoite isolation was achieved by the addition of 5% saponin (110  $\mu$ l 5% saponin per 1 mL blood) to the blood mixture and inverted until the mixture was dark red in colour. Trophozoites were then separated from the mixture by centrifugation for 7 min at 1800 xg and the supernatant aspirated. A wash step was then performed by resuspending the tropho-

zoites in 40 mL wash buffer, followed by centrifugation at 1800 xg for 7 min. Thereafter, trophozoites were resuspended in 2 mL wash buffer and transferred to a 2 mL eppendorf microtube. A fourth centrifugation step was performed at 13000 xg for 5 min and repeated following a final wash step with 2 mL wash buffer.

### 3.4.3 Inhibition Assays

*L. lactis* cell suspension was divided into 11x50 mL conical tubes unlike the *P. falciparum* trophozoite suspension that was divided into 7x1.5 mL microfuge tubes that was necessary for the 11 and 7 inhibitor concentrations needed to be tested. The iodoacetic acid concentrations were 0, 0.7, 1.56, 3.13, 6.25, 12.5, 25, 50, 100, 200 and 400  $\mu$ M for *L. lactis*, and 0, 0.7, 1.56, 3.13, 6.25, 12.5 and 25  $\mu$ M for *P. falciparum*. The pre-incubation time for inhibition was 30 minutes. All inhibitions were carried out at 37°C in MES buffer (0.5 M, pH 6.2) and modified Ringer's buffer (without glucose, pH 7.1) containing the relevant IAA concentration for *L. lactis* and *P. falciparum*, respectively. After the relevant pre-incubation time, IAA was washed off and cells were resuspended in 1 mL of the relevant buffer.

### 3.4.4 Flux Incubation

The *L. lactis* cell pellets stored at -20°C were resuspended in 1 mL fresh MES buffer (0.5 M, pH 6.2) and centrifuged (Eppendorf Centrifuge 5804R) at 3000 xg for 10 minutes. The supernatant was discarded and a 10 mL aliquot of MES buffer (0.5 M, pH 6.2) were then incubated for 15 minutes at 37°C to bring the cell suspension to the required temperature. Thereafter, the cells were resuspended in 1 mL fresh MES buffer containing 200  $\mu$ L 40 mM glucose. This time point was regarded as time = 0 minutes. Thereafter, samples were taken every 15 minutes for a total of 90 minutes and centrifuged at 3000 xg for 10 minutes at 4°C after each sample was taken. *P. falciparum* trophozoite pellets were resuspended in pre-warmed (37°C) modified ringers buffer (containing 5 mM glucose, pH 7.1) and time 0 minute samples were immediately taken. Cells were then incubated for 60 minutes where samples were taken every 15 minutes and spun down (Benchtop microfuge, StarLab). The supernatant was separated from the cell pellet, stored at -20°C (for both *L. lactis* and *P. falciparum*), and utilized for lactate and glucose determinations. The pellet was stored at -20°C (for *L. lactis*) and -80°C (for *P. falciparum*) before cell lysis for enzyme activity determinations.

### 3.4.5 Enzyme Activity Determinations

Activities of all glycolytic enzymes were tested initially to determine the effect of 100  $\mu\text{M}$  IAA on glycolytic enzyme activities at 37°C. Enzyme assays were based on the coupling of enzyme activity to the consumption and production of NADH, monitored at a wavelength of 340 nm in a SpectroStar<sup>®</sup> nano microplate reader (BMG labtech) or PowerWave 340 microtitre plate reader (BioTek Instruments Inc., Winooski, VT, USA),  $\epsilon = 6.22 \times 10^3 \text{ M}^{-1} \cdot \text{cm}^{-1}$ . Enzyme activity was determined from crude cell lysates and measured in units of micromole per minute per milligram of protein ( $\mu\text{mol} \cdot \text{min}^{-1} \cdot \text{mg prot}^{-1}$ ). Enzyme activity assays were then expanded to include varying concentrations of IAA on glyceraldehyde 3-phosphate dehydrogenase (GAPDH) activity in both *L. lactis* and *P. falciparum* at a pH of 6.2 and 7.2 immediately after cell disruption to match the pH of the bacteria and parasite, respectively.

The enzymes were assayed as follows:

*Hexokinase* (HK, EC 2.7.1.1) activity was determined by coupling the HK reaction to glucose-6-phosphate dehydrogenase under the following conditions: 4 mM ATP, 0.8 mM NADP<sup>+</sup>, 10 mM GLC, 5 U/ml G6PDH from baker's yeast (*S. cerevisiae*), and 0.5 M MES buffer (pH 6.2, for *L. lactis*) or enzyme assay buffer (pH 7.17, *P. falciparum*) at 37°C. The reaction was initiated by the addition of 90  $\mu\text{L}$  assay cocktail to 10  $\mu\text{L}$  crude cell lysate in 96-well flat bottomed microtiter plates (Greiner Bio-One GmbH, Frickhouse, Germany) in the forward direction.

*Phosphoglucoisomerase* (PGI, EC 5.3.1.9) activity was determined by coupling the PGI reaction to glucose-6-phosphate dehydrogenase under certain conditions: 5 mM F6P, 0.8 mM NADP<sup>+</sup>, 5 U/ml G6PDH from baker's yeast (*S. cerevisiae*), and 0.5 M MES buffer (pH 6.2, for *L. lactis*) or enzyme assay buffer (pH 7.17, *P. falciparum*) at 37°C. The reaction was initiated by the addition of 90  $\mu\text{L}$  assay cocktail to 10  $\mu\text{L}$  crude cell lysate in 96-well flat bottomed microtiter plates (Greiner Bio-One GmbH, Frickhouse, Germany) in the reverse direction.

*Phosphofructokinase* (PFK, EC 2.7.1.11) activity was determined by coupling the PFK reaction to aldolase, triosephosphate isomerase and glycerol-3-phosphate dehydrogenase under the following conditions in the forward direction: 4 mM ATP, 0.8 mM NADH, 5

U/ml ALD, 5 U/ml G3PDH and 5 U/ml TPI from rabbit muscle, 30 mM F6P, and 0.5 M MES buffer (pH 6.2, for *L. lactis*) or enzyme assay buffer (pH 7.17, *P. falciparum*) at 37°C. The reaction was initiated by the addition of 90  $\mu$ L assay cocktail to 10  $\mu$ L crude cell lysate in 96-well flat bottomed microtiter plates (Greiner Bio-One GmbH, Frickhouse, Germany).

*Aldolase* (ALD, EC 4.1.2.13) activity was determined by coupling the ALD reaction to triosephosphate isomerase under the following conditions in the forward direction: 0.8 mM F16BP, 0.8 mM NADH, 5 U/ml G3PDH and 5 U/ml TPI from rabbit muscle, and 0.5 M MES buffer (pH 6.2, for *L. lactis*) or enzyme assay buffer (pH 7.17, *P. falciparum*) at 37°C. The reaction was initiated by the addition of 90  $\mu$ L assay cocktail to 10  $\mu$ L crude cell lysate in 96-well flat bottomed microtiter plates (Greiner Bio-One GmbH, Frickhouse, Germany).

*Glycerol-3-phosphate dehydrogenase* (G3PDH, EC 1.1.1.8) activity was determined in the forward direction: 5 mM DHAP, 0.8 mM NADH, and 0.5 M MES buffer (pH 6.2, for *L. lactis*) or enzyme assay buffer (pH 7.17, *P. falciparum*) at 37°C. The reaction was initiated by the addition of 90  $\mu$ L assay cocktail to 10  $\mu$ L crude cell lysate in 96-well flat bottomed microtiter plates (Greiner Bio-One GmbH, Frickhouse, Germany).

*Glyceraldehyde-3-phosphate dehydrogenase* (GAPDH, EC 1.2.1.12) activity was determined by coupling the GAPDH reaction to phosphoglycerate kinase under the following conditions in the reverse direction: 4 mM ATP, 0.8 mM NADH, 5 U/ml PGK from baker's yeast (*S. cerevisiae*), 2 mM 3PGA and 0.5 M MES buffer (pH 6.2, for *L. lactis*) or enzyme assay buffer (pH 7.17, *P. falciparum*) at 37°C. The reaction was initiated by the addition of 90  $\mu$ L assay cocktail to 10  $\mu$ L crude cell lysate in 96-well flat bottomed microtiter plates (Greiner Bio-One GmbH, Frickhouse, Germany).

*Phosphoglycerate kinase* (PGK, EC 2.7.2.3) activity was determined by coupling the PGK reaction to GAPDH under the following conditions in the reverse direction: 4 mM ATP, 0.8 mM NADH, 5 U/ml GAPDH from rabbit muscle, 10 mM 3PGA and 0.5 M MES buffer (pH 6.2, for *L. lactis*) or enzyme assay buffer (pH 7.17, *P. falciparum*) at 37°C. The reaction was initiated by the addition of 90  $\mu$ L assay cocktail to 10  $\mu$ L crude cell lysate in

96-well microtiter plates flat bottomed microtiter plates (Greiner Bio-One GmbH, Frickhouse, Germany).

*Phosphoglycerate mutase* (PGM, EC 5.4.2.1) activity was determined by coupling the PGM reaction to GAPDH and PGK under the following conditions in the reverse direction: 2 mM ATP, 0.8 mM NADH, 5 U/ml PGK from baker's yeast (*S. cerevisiae*), 5 U/ml GAPDH from rabbit muscle, 20 mM 2PGA and 0.5 M MES buffer (pH 6.2, for *L. lactis*) or enzyme assay buffer (pH 7.17, *P. falciparum*) at 37°C. The reaction was initiated by the addition of 90  $\mu$ L assay cocktail to 10  $\mu$ L crude cell lysate in 96-well flat bottomed microtiter plates (Greiner Bio-One GmbH, Frickhouse, Germany).

*Enolase* (ENO, EC 4.2.1.11) activity was determined by coupling the ENO reaction to pyruvate kinase and lactate dehydrogenase under the following conditions in the forward direction: 2 mM ADP, 0.8 mM NADH, 5 U/ml PK from rabbit muscle, 10 mM 2PGA, 5 U/ml L-LDH from bovine heart and 0.5 M MES buffer (pH 6.2, for *L. lactis*) or enzyme assay buffer (pH 7.17, *P. falciparum*) at 37°C. The reaction was initiated by the addition of 90  $\mu$ L assay cocktail to 10  $\mu$ L crude cell lysate in 96-well flat bottomed microtiter plates (Greiner Bio-One GmbH, Frickhouse, Germany).

*Pyruvate kinase* (PK, EC 2.7.1.40) activity was determined by coupling the PK reaction to lactate dehydrogenase under the following conditions in the forward direction: 5 mM ADP, 0.8 mM NADH, 5 mM PEP, 5 U/ml L-LDH from bovine heart, and 0.5 M MES buffer (pH 6.2, for *L. lactis*) or enzyme assay buffer (pH 7.17, *P. falciparum*) at 37°C. The reaction was initiated by the addition of 90  $\mu$ L assay cocktail to 10  $\mu$ L crude cell lysate in 96-well flat bottomed microtiter plates (Greiner Bio-One GmbH, Frickhouse, Germany).

*Lactate dehydrogenase* (LDH, EC 1.1.1.27) activity was determined under the following conditions in the forward direction: 2 mM Pyruvate, 0.8 mM NADH, and 0.5 M MES buffer (pH 6.2, for *L. lactis*) or enzyme assay buffer (pH 7.17, for *P. falciparum*) at 37°C. The reaction was initiated by the addition of 90  $\mu$ L assay cocktail to 10  $\mu$ L crude cell lysate in 96-well flat bottomed microtiter plates (Greiner Bio-One GmbH, Frickhouse, Germany).

#### ***Preparation of crude lysate for enzyme activity determination***

Harvested *L. lactis* cell pellets were taken from the -20°C freezer and washed twice with

200  $\mu\text{L}$  (a volume) of MES buffer (at pH 6.2) (corresponding to the volume of the cell pellet) and centrifuged for 10 minutes at 3000  $\times g$  at 4°C. Cell pellets were resuspended with 0.5 M MES buffer and disrupted by glass beads (425 to 600  $\mu\text{m}$  in diameter; Sigma-Aldrich, St Louis, MO, USA). Cell disruption by glass beads consisted of 3 vortex (Vortex-Genie 2, Scientific Industries, Bohemia, NY, USA) cycles of 3 minutes interspaced by 3 minutes on ice. After cell disruption, the cell suspension was immediately centrifuged at 4000  $\times g$  for 20 minutes at 4°C. Thereafter, the supernatant was aspirated, stored at -80°C, and utilized for enzyme activity determination using a SPECTROstar® nano microtiter plate reader (BMG labtech) or BioTek microplate reader, which monitored the concentration of NADH over time at 340 nm ( $A_{340}$ ) in Greiner flat-bottom polystyrene 96-well microplates.

Isolated trophozoites from *P. falciparum* were taken from the -80°C freezer, washed twice with modified Ringer buffer (pH 7.1, without glucose) (corresponding to the volume of the cell pellet) and centrifuged for 5 minutes at 13000  $\times g$  at 4°C. Cell pellets were combined with equal quantities of enzyme assay buffer (pH 7.17) before undergoing three freeze-thaw cycles. These cycles consisted of 30 seconds in liquid nitrogen followed by 30 seconds in a 37°C water bath for a total of three cycles and immediately centrifuged at 13000  $\times g$  for 5 minutes at 4°C. Thereafter, the supernatant was collected, stored at -80°C, and utilized for enzyme determination using a SPECTROstar® nano microtiter plate reader (BMG labtech), which monitored the formation and degradation of NADH at 340 nm.

#### *Determination of the protein concentration from crude lysates*

Protein concentrations of crude cell lysates were determined using the method developed by Bradford [95], where bovine serum albumin (BSA) was used as a standard. A standard curve representing the ratio of absorbance measured at 450 nm and 590 nm (i.e.  $A_{590}/A_{450}$ ) as a function of protein concentration of BSA after the blank (i.e. distilled water or relevant buffer) has been deducted were produced. The straight-line deduced from the most linear section of the data points was used to generate a linear equation that describes the relation that is seen between the BSA protein concentration and the absorbance and can be used to estimate the amount of protein in a sample (crude lysate). Dilutions of the lysate were made to ensure that sample readings were within the linear

range.

### 3.4.6 Metabolic flux Determination Assays

Metabolic flux was measured by following the conversion of extracellular glucose to lactate.

#### Glucose Determination Assay

The consumption of glucose was measured by coupling hexokinase activity to the G6PDH enzyme. The reaction mixture was made up of 0.5 M MES buffer (for *L. lactis*) or HEPES/MgSO<sub>4</sub> buffer (pH 7.6, for *P. falciparum*) and contained 4 mM NAD<sup>+</sup>, 2 mM ATP:Mg<sup>2+</sup>, 0.05 U·100 μL<sup>-1</sup> G6PDH from *L. mesenteroides*, and 0.10895 U·μL<sup>-1</sup> HK from *S. cerevisiae*. Glucose standards (0 mM to 100 mM) were used to produce a glucose standard curve.

#### Lactate Determination Assay

The production of lactate was measured using an LDH-NAD<sup>+</sup>-linked assay. This assay measures L-lactate in terms of nicotinamide (NADH) at 340 nm. The reaction mixture was made up of 0.5 M MES buffer or HEPES/MgSO<sub>4</sub> buffer (pH 7.6, for *P. falciparum*) and contained 4 mM NAD<sup>+</sup>, 4 U/ml LDH, and 320 mM hydrazine. Lactate standards (0 mM to 40 mM) were used to produce a lactate standard curve.

### 3.4.7 Data and model Analysis

All analyses and model simulations were performed in Microsoft Office Excel 2016 and Wolfram Mathematica v12.0 (Wolfram Research, Inc., Champaign, IL, USA). Statistical analysis was performed using a two-sample Student's t-test or analysis of variance (ANOVA).

For modelling analysis, the published mathematical models constructed by Hoefnagel *et al.* [7] and Penkler *et al.* [4] were obtained from JWS Online (available at <https://jjj.biochem.sun.ac.za/models/hoefnagel2/> and <https://jjj.biochem.sun.ac.za/models/penkler2/>) and adapted to include the inhibition by IAA. Control coefficients were determined through metabolic control analysis in the model, and a curve fitting procedures on the data (described below).

### 3.4.7.1 Curve fitting and control coefficients determination

Both the Hoefnagel and Penkler models do not account for the addition of glycolytic inhibitors into their rate equations. Therefore, to estimate the control of GAPDH over the glycolytic flux, we first fitted an exponential decay function (shown in equation 3.4.1) on the experimental GAPDH specific activities (in either *L. lactis* or *P. falciparum*). The relevant exponential decay function was inserted as a multiplier into the kinetic rate equation of GAPDH in both the Hoefnagel model and Penkler models for 30-minute inhibition to account for the experimental data obtained:

$$v = v_0 \cdot e^{-k_i \cdot IAA} \quad (3.4.1)$$

where IAA represents the iodoacetic acid concentration,  $k_i$  the inhibition constant (unit =  $\mu\text{M}^{-1}$ ) after a fixed pre-incubation time,  $v$  the reaction rate and  $v_0$  the uninhibited rate. Note that in this formalism, a compound with a low  $k_i$  functions as a weak inhibitor.

To determine the control coefficients within the model, perturbation control analysis is used. To determine the experimental control coefficient, two different methods were used namely, **Method 1** which consisted of taking the slope of the curve at the 100% flux vs IAA concentration and dividing it by the derivative of the exponential decay activity function at IAA = 0.

$$C_{v_{GAPDH}}^J \approx \frac{\frac{\% \text{ change in flux}}{\text{change in IAA}}}{\frac{\% \text{ change in activity}}{\text{change in IAA}}} \quad (3.4.2)$$

and **Method 2** consisted of fitting a curve to the scaled % flux vs % activity data and taking the slope of the curve at the 100% activity and 100% flux point.

### 3.4.8 Ethical Exemption

Ethical exemption was obtained from the Health Research Ethics Committee of Stellenbosch University for the handling and use of erythrocytes for parasite culture and experiments performed in the study (X20/02/006). For culturing the parasites *in vitro*, blood

### 3.4. Methodology

---

was obtained from the Western Cape Blood Services and, if necessary, from informed and consenting volunteers.

# Chapter 4

## Results

This chapter presents the experimental and model analysis results for the two microorganisms, *L. lactis* and *P. falciparum*.

### 4.1 Growth of *L. lactis*

Growth experiments for *Lactococcus lactis cremoris* MG1363 were performed in MRS broth supplemented with 1mL/L Tween 80 as detailed in Chapter 3. Bacterial growth was monitored in two independent experiments in terms of optical density (OD) at 600nm over time. For all experiments, bacteria were harvested in the exponential (log) phase. Slow growth was observed for *L. lactis*, with growth rates of  $0.070 h^{-1}$  and  $0.065 h^{-1}$  for the two cultures in contrast to the rates of  $0.58 h^{-1}$  determined by Garrigues and colleagues [24] and  $0.55 h^{-1}$  determined by Even *et al.* [96] for cultures grown on MS10 medium and a simplified synthetic medium, MS10R, respectively. This growth limitation may be attributed to the different buffering system and culture medium used, the strength and quality of the starter culture, as well as the different pH and temperature used [97]. Specific growth rates and doubling times for the two cultures are shown in Table 4.1.

**Table 4.1: Growth of *Lactococcus lactis* MG1363 cremoris on MRS broth.**

Biological repeat	Specific growth rate, $\mu (h^{-1})$	Doubling time (min)
1	0.065	641.7
2	0.070	594.9

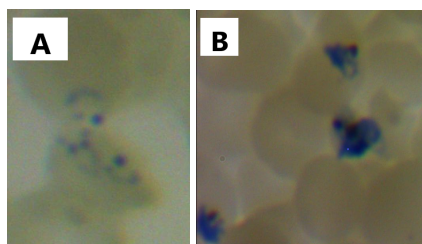


**Figure 4.1: Growth of *P. falciparum* 3D7 at 37°C.** Cultures were refreshed every 24 hours with RPMI 1640 GlutaMAX<sup>TM</sup> enriched medium to supply sufficient amounts of nutrients to the culture and avoid acidification of culture medium. Slides were prepared and stained with Rapidiff Stain Set<sup>TM</sup>. Growth was monitored daily under 100X oil-immersion objective lens and different stages of the parasite life cycle was visible: rings (A), and trophozoites (B).

## 4.2 Growth of *P. falciparum*

*P. falciparum* 3D10 was utilised for the construction of the Penkler model, however, due to the difficulty in getting freezer stocks of this strain to proliferate, a chloroquine-sensitive, metabolically similar strain, *P. falciparum* 3D7, was used. To ensure that the parasite was in the correct stage for further experiments, the intraerythrocytic stage of the parasite life cycle was monitored daily under 100X oil-immersion objective lens. Figure 4.1 illustrates the stages of parasite growth during continuous culture under a microscope. It distinguishes between rings (Fig. 4.1 A), and trophozoites (Fig. 4.1 B). A parasitemia greater than 10% consisting of synchronized trophozoites was used for isolation after approximately two to three weeks of continuous culture.

## 4.3 Effect of IAA on Enzyme Activity

All enzymes in the glycolytic pathway of *L. lactis* were assayed in the absence and presence of 100  $\mu$ M IAA, to determine if any enzyme other than the specific enzyme target, glyceraldehyde-3-phosphate dehydrogenase, was affected (Figure 4.2). A significant and substantial reduction of the GAPDH activity was seen with IAA. Other dehydrogenase enzymes with reactive SH groups, which are potential targets for IAA, did not show a similar reduction in activity.

Note that for the dehydrogenases shown in Figure 4.2, only GAPDH was affected by iodoacetic acid to a large extent, resulting in a statistically significant activity reduction at 100  $\mu$ M IAA compared to the GAPDH control. Thus, IAA did not affect LDH and G3PDH activity significantly at 100  $\mu$ M. The apparent reduction of ENO and PK activities by IAA in Figure 4.2 were not statistically significant. Note that outliers in the data were excluded

## 4.3. Effect of IAA on Enzyme Activity

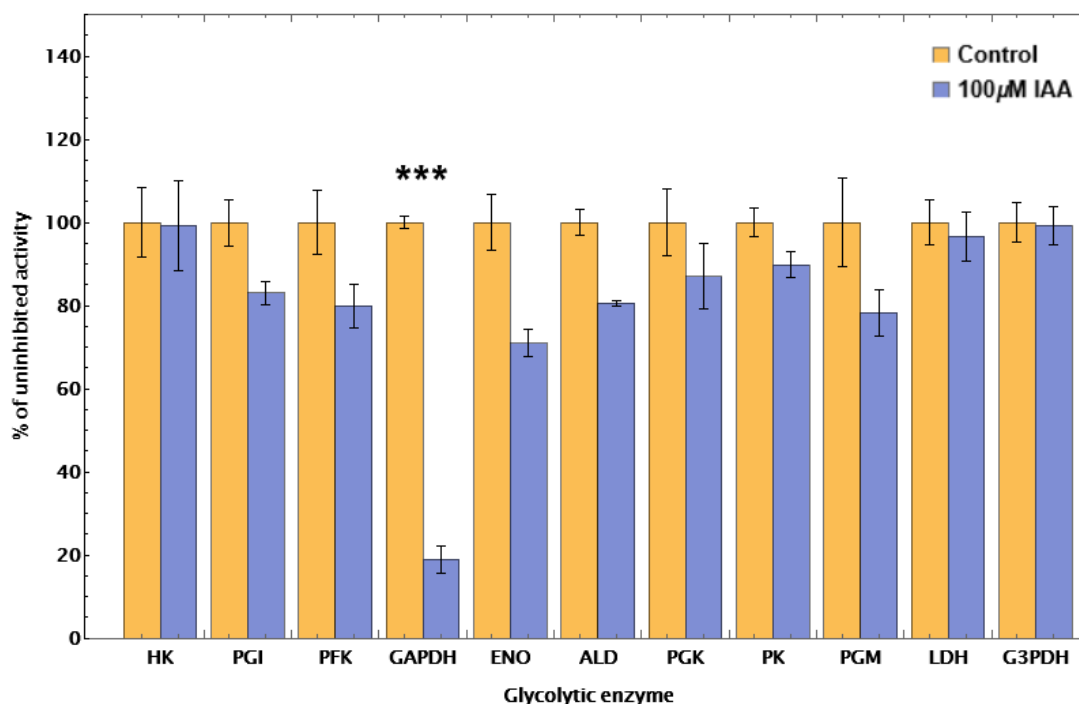


**Figure 4.2: Enzyme specificity of IAA.** A graphical depiction of the effect iodoacetic acid has on the enzyme activity of glycolytic enzymes in *L. lactis*. Crude lysate samples in the absence and presence of 100  $\mu\text{M}$  iodoacetic acid before lysis were assayed for 10-minutes spectrophotometrically at 340 nm. Samples were exposed to iodoacetic acid for a period of 30-minutes before being washed. The results represent the mean  $\pm$  SEM of the specific activity data as a percentage of the uninhibited activity obtained from two (PGI, ENO, ALD, PGK, PGM, PK, and G3PDH) or three (HK, PFK, TPI, GAPDH, and LDH) independent experiments. Statistical significance (\*\*\*) =  $p < 0.0001$ ) of data indicated as determined by Student's t-tests and ANOVA at  $\alpha=0.05$ .

from Figure 4.2. A complete figure including all outliers is shown in the appendix, Figure D.1. This experiment was not repeated on *P. falciparum* due to scarcity of biomass (for the current project it was assumed that IAA displays a similar specificity for GAPDH in *P. falciparum*).

#### 4.3.1 Effect of IAA on Glyceraldehyde-3-Phosphate Dehydrogenase Activity

To study the effect of IAA on GAPDH activity in *L. lactis* and *P. falciparum*, GAPDH was assayed at varying IAA concentrations.

*L. lactis* and *P. falciparum* cells were first pre-incubated with IAA for 30 minutes, washed, and then incubated with glucose for flux determination. Thereafter the same cells were lysed and GAPDH activity was determined. The activity versus IAA profiles for glyceraldehyde-3-phosphate dehydrogenase from *L. lactis* and *P. falciparum* are shown in Figure 4.3. It displayed the percentage specific GAPDH activity as a function of varying IAA concentrations (0-25  $\mu\text{M}$ ). We saw that IAA inhibited GAPDH activity in both species,

## 4.3. Effect of IAA on Enzyme Activity

and that this inhibition appeared to be almost linear between 0 and 3.13  $\mu\text{M}$ . It became evident in Figure 4.3 A that the GAPDH activity of *L. lactis* was almost completely inhibited at approximately 25  $\mu\text{M}$  IAA. However, at the same concentration of IAA, approximately 20% of the GAPDH activity remained active in *P. falciparum* (Figure 4.3 B). This demonstrated that with increasing IAA concentrations, the activity of GAPDH was inhibited slightly more strongly in *L. lactis* than in *P. falciparum*.

Strelow explained that irreversible inhibition kinetics was best described using exponential decay functions [58]. Thus, exponential decay functions were fitted to the data of both organisms to determine the inhibition constants ( $k_i$ , the exponent within the function). It is evident that *P. falciparum* has a lower  $k_i$  ( $1.56 \pm 0.017 \mu\text{M}^{-1}$ ) than *L. lactis* ( $2.63 \pm 0.018 \mu\text{M}^{-1}$ ).

The half-maximal activity for a fixed 30-minute preincubation time gave an  $\text{IC}_{50}$  value of 2.64  $\mu\text{M}$  for *L. lactis* and 4.43  $\mu\text{M}$  for *P. falciparum* (Table 4.2 and Figure 4.3), which supports what was seen in Figure 4.3.

**Table 4.2: Inhibition parameters of GAPDH in *L. lactis* and *P. falciparum***

Parameters	Experimental value	Literature value
$k_{i_{Ll}}$ <sup>b</sup>	$0.263 \pm 0.018 \mu\text{M}^{-1}$	-
$k_{i_{Pf}}$ <sup>b</sup>	$0.156 \pm 0.017 \mu\text{M}^{-1}$	-
$\text{IC}_{50_{Ll}}$ <sup>a</sup>	2.64 $\mu\text{M}$	2.5 $\mu\text{M}$ [62]
$\text{IC}_{50_{Pf}}$ <sup>a</sup>	4.43 $\mu\text{M}$	-

**Abbreviations:** *Ll*, *Lactococcus lactis*; *Pf*, *Plasmodium falciparum*

<sup>a</sup> refers to an  $\text{IC}_{50}$  value for a preincubation time of 30 minutes

<sup>b</sup>  $k_i$  refers to the exponent of the fitted exponential function in Figure 4.3.

## 4.3. Effect of IAA on Enzyme Activity

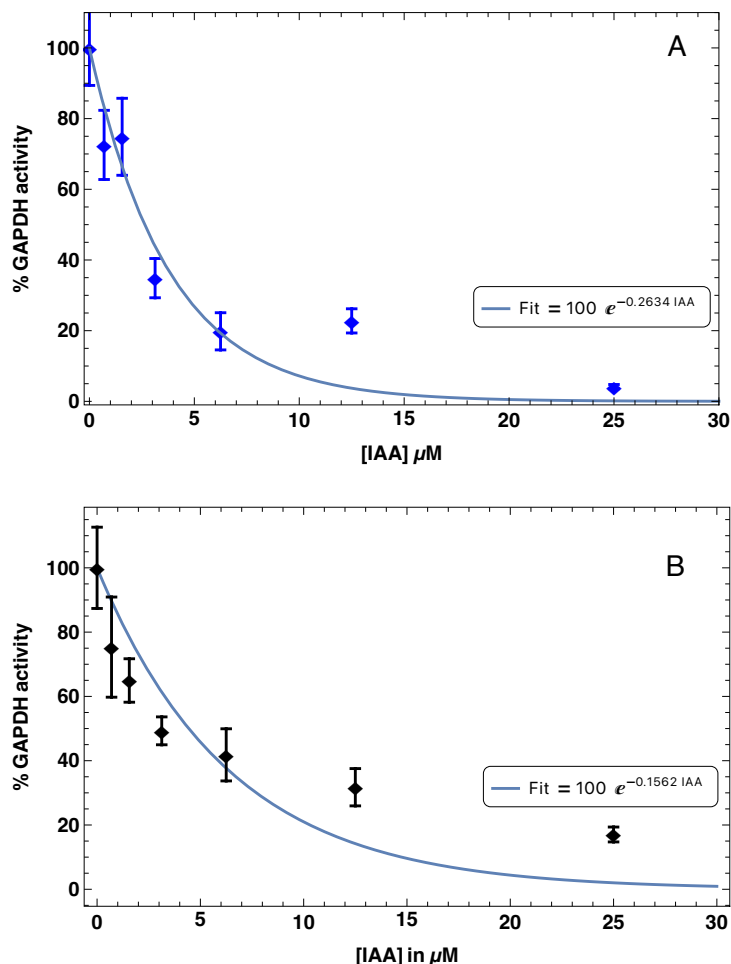


**Figure 4.3: Inhibition of GAPDH activity by IAA in *L. lactis* and *P. falciparum*.** Cells were pre-treated with IAA at the indicated concentrations (0-25  $\mu\text{M}$ ) for 30 minutes, collected and lysed. GAPDH activity in the cell lysate was measured, as described in Materials and Methods. The specific activity of GAPDH from both (A) *L. lactis* (●) and (B) *P. falciparum* (●) were expressed as a percentage of the reference (uninhibited rate) and is plotted as a function of increasing iodoacetic acid (IAA) concentration. Exponential functions, shown in equation 3.4.1 (see Materials and Methods), were fitted to the data. Exponential constants of  $0.263 \pm 0.018 \mu\text{M}^{-1}$  and  $0.156 \pm 0.017 \mu\text{M}^{-1}$  were obtained for IAA inhibition in *L. lactis* and *P. falciparum*, respectively. The data shown in A represent the mean  $\pm$  standard error of the mean (SEM) of two independent experiments with three technical repeats prepared each. The data shown in B represent the mean  $\pm$  standard deviation (SD) of data obtained from one independent experiment with three technical repeats each. The solid curves show the exponential functions that were fitted to the GAPDH enzyme activity data. IAA, iodoacetic acid; GAPDH, glyceraldehyde-3-phosphate dehydrogenase.

## 4.4 Effect of IAA on the Glycolytic flux

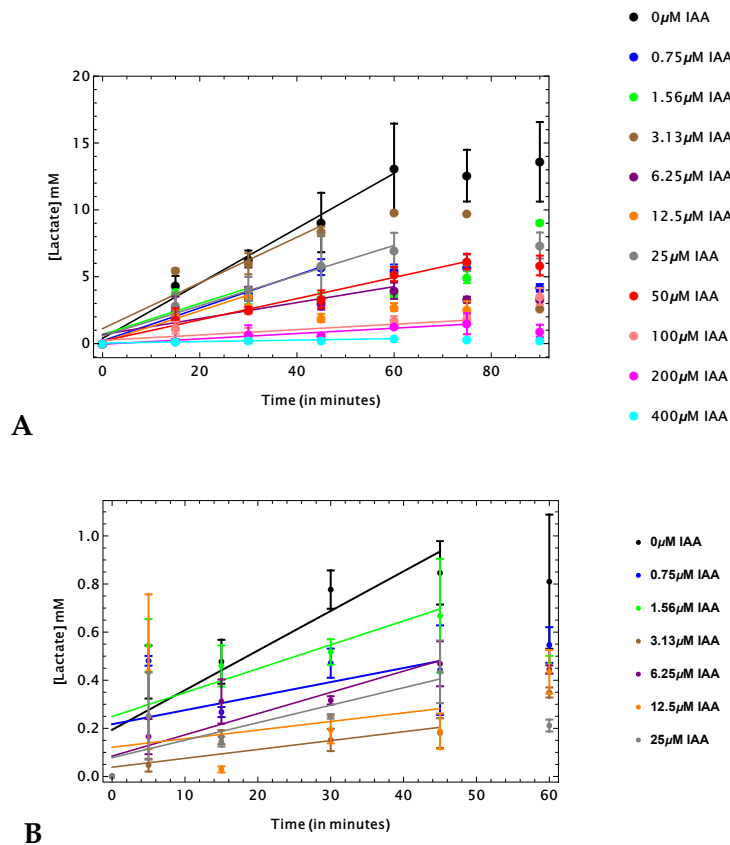
Glycolytic flux, in terms of lactate production and glucose consumption rates, were measured and are displayed graphically as functions of time and IAA concentrations in Figures 4.4 and 4.6, and Figures 4.5 and 4.7, respectively. The lactate and glucose concentrations in the supernatant were monitored as an indication of glycolytic activity. These concentrations were obtained spectrophotometrically using glucose and lactate calibration curves (see Appendix) constructed for both organisms.

### 4.4.1 Effect of IAA on lactate production

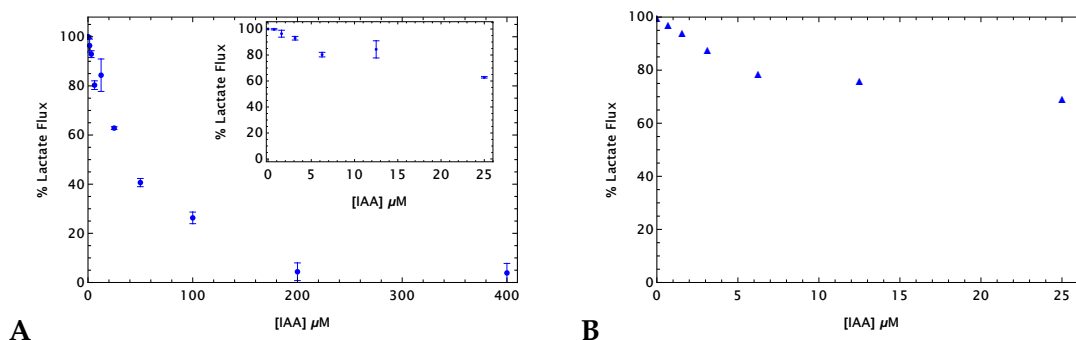
To study the effect of IAA on lactate production rates (i.e. lactate flux), the production of lactate was monitored for various concentrations of IAA after a 30-minute preincubation. The rate of change in lactate was determined from the initial linear portion of the curve. We observed that similar relationships are seen between lactate production in *L. lactis* and *P. falciparum* as a function of time (Figure 4.4). However, the absolute lactate production rate was greater in *L. lactis* ( $0.915 \mu\text{mol}/\text{min}/\text{mg}$  protein) opposed to *P. falciparum* ( $0.097 \mu\text{mol}/\text{min}/\text{mg}$  protein). In *L. lactis*, concentrations from 0 to  $200 \mu\text{M}$  IAA resulted in lactate production for 60 minutes at different rates, and at  $400 \mu\text{M}$  IAA lactate production was completely inhibited (Figure 4.4 A). The lactate production in *P. falciparum* was followed for 45 - 60 minutes with IAA concentrations ranging from 0 to  $25 \mu\text{M}$  (Figure 4.4 B).

Figure 4.5 showed the lactate production flux inhibition as a function of increasing IAA concentrations. It can be seen that with increasing IAA concentrations, the lactate production fluxes decreased in both species. Note that Figure 4.5 B has a different set of axes compared to Figure 4.5 A to account for the different IAA concentrations range used (an inset was included in Figure 4.5 A to allow the direct comparison to Figure 4.5 B). Although the lactate fluxes in *P. falciparum* trophozoites appeared to be lower than those in *L. lactis*, we observed that in both species similar trends, in terms of the manner in which they decreased, were seen for the same IAA concentration range used namely, 0- $25 \mu\text{M}$ .

## 4.4. Effect of IAA on the Glycolytic flux



**Figure 4.4: Lactate production curves as a function of time.** The lactate production curves of samples exposed to 30-minute incubation with iodoacetic acid. Lactate production was monitored in terms of lactate concentration. Technical triplicates of two independent experiments are expressed per time point and the data points and error bars represent the mean  $\pm$  standard error of the mean (SEM) in (A) *L. lactis*. In (B), technical triplicates of one independent experiment are shown per time point and the data points and error bars represent the mean  $\pm$  standard deviation (SD) for *P. falciparum*. The lines reflect the fits to the most linear initial portions of the curves and their gradients were used to determine the lactate fluxes at the specified IAA concentrations (Figure 4.5).



**Figure 4.5: Lactate production flux inhibition by IAA.** Lactate production rates as a function of increasing IAA concentrations for (A) *L. lactis* (0-400  $\mu\text{M}$ ) and (B) *P. falciparum* (0-25  $\mu\text{M}$ ). An inset in (A) shows an enlarged section of the lactate flux at 0-25  $\mu\text{M}$  IAA concentration range in *L. lactis*. Two independent experiments are shown per concentration and data points and error bars represent the mean  $\pm$  SEM in (A) *L. lactis*. The data in (B) represent the mean of one independent experiment consisting of three technical repeats.

## 4.4. Effect of IAA on the Glycolytic flux

## 4.4.2 Effect of IAA on glucose consumption

40 mM and 5 mM glucose were used as a carbon source for the bacterium and parasite, respectively. Glucose consumption was measured as the reduction of glucose concentration over time (Figure 4.6). We observed a better distinction in glucose consumption between the different IAA treated samples in *P. falciparum* (Figure 4.6 B) than in *L. lactis* (Figure 4.6 A), likely due to the fact that *L. lactis* consumed glucose much faster than *P. falciparum* between 0 and 15 minutes. This suggested that the experimental glucose determination did not work as well for *L. lactis* (Figure 4.6 A) as it did for *P. falciparum* (Figure 4.6 B).

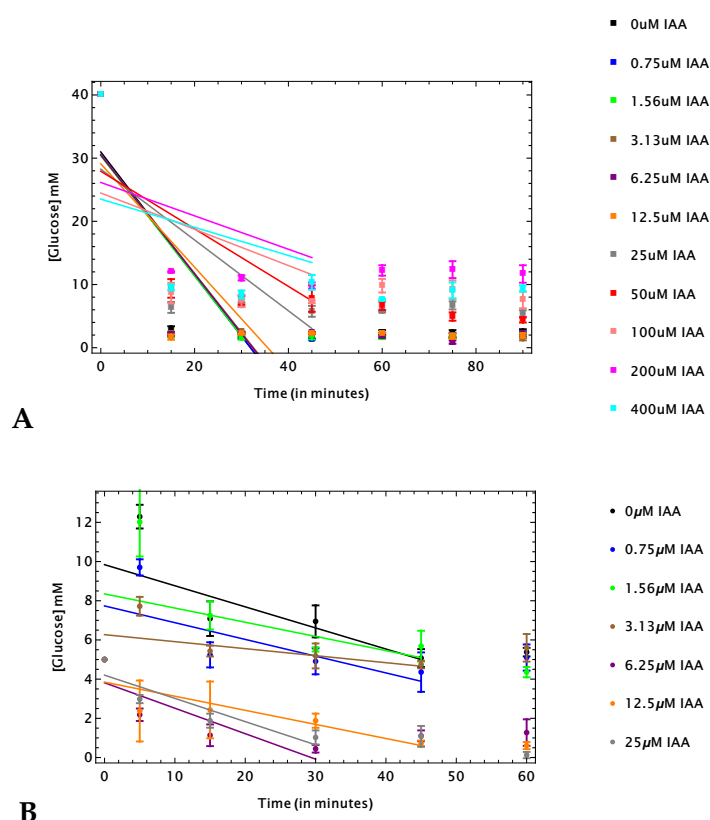


**Figure 4.6: Glucose consumption curves as a function of time.** Glucose consumption curves of samples exposed to 30-minute preincubation with iodoacetic acid (IAA). Glucose consumption was monitored in terms of glucose concentration, and plotted as a function of time for the different IAA concentrations for both (A) *L. lactis* and (B) *P. falciparum*. The results are shown as the mean  $\pm$  SEM of two independent experiments in (A) and the mean  $\pm$  SD of one independent experiment in (B). The lines reflect the fits to the most linear initial portions of the curves and their gradients were used to determine the glucose fluxes at the specified IAA concentrations (Figure 4.7).

## 4.4. Effect of IAA on the Glycolytic flux

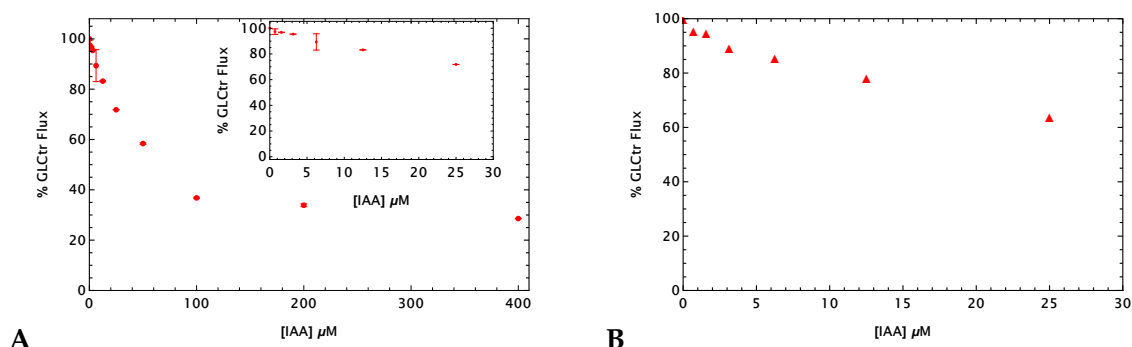


**Figure 4.7: Glucose flux as a function of varying iodoacetic acid concentrations.** Glucose consumption was measured as end-point values after incubation for 90 minutes with Hexokinase-G6PDH coupled assay reagent at 340 nm spectrophotometrically and the slopes of the most linear portion of the curve were taken for each concentration to derive the rates for both **(A)** *L. lactis* and **(B)** *P. falciparum*. An inset in **(A)** shows an enlarged section of the glucose flux at 0-25 μM IAA concentration range in *L. lactis*. The data in **(A)** *L. lactis* represents the mean±SEM of two independent experiments consisting of three technical repeats each, while the data in **(B)** *P. falciparum* represents the mean of one independent experiment consisting of three technical repeats.

Glucose consumption flux inhibition as a function of varying iodoacetic acid concentrations can be observed for both organisms (Figure 4.7). It is evident from Figure 4.7 that with increasing IAA concentrations, the glucose consumption flux in both species decreased. At lower IAA concentrations, i.e. 25 μM, depicted in the inset in Figure 4.7 A and in Figure 4.7 B, we saw that IAA has a stronger effect on the glucose flux in *P. falciparum* than *L. lactis*.

#### 4.4.3 Experimental summary

Table 4.3 provides a summary of the experimental results showing the effect of IAA on the GAPDH activity and glycolytic flux in the two organisms.

**Table 4.3: Effect of a 30-minute IAA inhibition within *L. lactis* and *P. falciparum*.**

IAA ( $\mu\text{M}$ )	0	0.7	1.5	3.13	6.25	12.5	25	50	100	200	400
<b><i>L. lactis</i></b>											
<i>30-minutes</i> *											
% Activity	100	70.85	76.03	33.03	19.80	23.01	2.98	3.83	1.81	1.29	1.84
% Lactate Flux	100	99.32	99.05	91.53	81.74	77.75	62.27	38.99	28.65	6.50	2.08
% Glucose Flux	100	99.48	96.60	95.23	95.70	83	71.77	58.08	36.50	33.32	28.47
<i>30-minutes</i> **											
% Activity	100	74.27	73.68	36.69	19.84	22.53	5.34	3.16	1.75	1.22	1.82
% Lactate Flux	100	95.08	95.70	92.64	92.79	89.88	63.39	42.33	23.93	7.83	7.76
% Glucose Flux	100	95.22	96.98	95.56	83.02	83.40	71.87	58.68	37.08	34.43	28.68
<b><i>P. falciparum</i></b>											
<i>30-minutes</i> *											
% Activity	100	75.33	64.96	49.29	41.82	31.75	17.05				
% Lactate Flux	100	97.30	94.16	84.74	78.81	63.96	60.40				
% Glucose Flux	100	95.76	94.71	89.33	85.73	78.43	63.91				

\* biological repeat 1, \*\* biological repeat 2

## 4.5 Model Analysis

To incorporate the effect of iodoacetic acid on GAPDH activity we adapted the models by Hoefnagel and Penkler to include an irreversible inhibition on GAPDH activity. Equations describing the IAA effect on GAPDH kinetics were adapted in a similar manner (see Materials and Methods) to Odendaal [98] who studied the inhibition of yeast GAPDH. An exponential function was fitted on the activity versus IAA concentration data (Figure 4.3) and inserted into the rate equations in the models of Hoefnagel *et al.* [8] and Penkler *et al.* [4]. These rate equations describe the effect of IAA on the GAPDH activity and when the models for the glycolytic pathway are simulated, the effect of such an inhibition is propagated to the concentrations and fluxes in the glycolytic network. The modified equations are:

$$v_{GAPDH_{Hoefnagel}} = \frac{e^{-k_{iL1} \cdot IAA} \cdot V_{max} \cdot G3P \cdot NAD \cdot Phos \cdot \left(1 - \frac{DPG \cdot NADH}{K_{eq} \cdot G3P \cdot NAD \cdot Phos}\right)}{km_{G3P} \cdot km_{NAD} \cdot km_P \left(1 + \frac{DPG}{km_{DPG}} + \frac{G3P}{km_{G3P}}\right) \left(1 + \frac{NAD}{km_{NAD}} + \frac{NADH}{km_{NADH}}\right) \left(1 + \frac{Phos}{km_P}\right)} \quad (4.5.1)$$

$$v_{GAPDH_{Penkler}} = e^{-k_{iPf} \cdot IAA} \cdot \frac{\left(Vf_{GAPDH} \cdot \frac{gap \cdot nad}{K_{GAP} \cdot K_{NAD} \cdot V_{pf}} - V_{rGAPDH} \cdot \frac{nadh \cdot b13pg}{K_{NADH} \cdot K_{B13PG} \cdot V_{pf}}\right)}{\left(1 + \frac{nad}{K_{NAD} \cdot V_{pf}} + \frac{nadh}{K_{NADH} \cdot V_{pf}}\right) \left(1 + \frac{gap}{K_{GAP} \cdot V_{pf}} + \frac{b13pg}{K_{B13PG} \cdot V_{pf}}\right)} \quad (4.5.2)$$

As shown, the rate equations are multiplied by the exponential decay functions (see Materials and Methods) describing iodoacetic acid (IAA) effect at varying concentrations with a relevant inhibition constant ( $k_i$ ) as determined in Section 4.3.1.

## 4.6 Glycolytic flux control

To determine the control coefficients within the model, perturbation control analysis was used. To determine the experimental control coefficient, two different  $V_{pf}$  methods were used namely, Method 1 which consisted of taking the slope of the curve at the 100% flux vs IAA concentration and dividing it by the derivative of the exponential decay activity function and Method 2 consisted of taking the slope of the % flux vs % activity at the 100% activity and 100% flux point.

#### 4.6. Glycolytic flux control

---

The determination of control coefficients via Method 1 (as described in Chapter 3) can be seen in Figure 4.8. The percentage normalized enzymatic activity and percentage normalized pathway flux for i) lactate and ii) glucose, were plotted as a function of varying iodoacetic acid concentrations. Here it is evident that the slope of the activity curve (determined from the derivative of the exponential function) of GAPDH is steeper at low IAA concentrations (0-10  $\mu\text{M}$ ) in *L. lactis* compared to *P. falciparum*, which is also reflected in the  $\text{IC}_{50}$  value determined earlier ( $\text{IC}_{50}$ , Table 4.2). Similarly, the slope of the flux curves (determined from the gradient of the linear regression) for both lactate and glucose as a function of IAA concentrations are steeper in *L. lactis* than in *P. falciparum*. The quotients of the slopes of the flux and the activity were used in the calculation of the experimental control coefficients for Method 1. In *L. lactis*, the experimental control coefficient for lactate and glucose flux equated to 0.09 and 0.0761 respectively. For *P. falciparum* these values were 0.125 and 0.139.

For Method 2 the experimental % flux versus % activity values were plotted (Fig. 4.9). Lines (not shown) were fitted to the four right-most activity data points approaching the 100% activity and 100% flux point in each figure, and the gradients of these lines were directly interpretable as the control coefficients. This resulted in experimental lactate and glucose flux control coefficients of 0.0549 and 0.1 for *L. lactis*, and 0.156 and 0.155 for *P. falciparum*.

The curves in Fig. 4.9 are the results of model predictions obtained by varying the IAA concentration in the GAPDH rate equations (equations 4.5.1 and 4.5.2) and determining the corresponding GAPDH activity and flux values. The model lactate and glucose flux control coefficients, as determined using MCA, were 0.0261 and 0.0257 for *L. lactis*, and 0.104 and 0.0882 for *P. falciparum*.

The experimental and model flux control coefficients are summarised in Figure 4.9 and Table 4.4.

When comparing the experimental and model results it can be seen that there is good agreement between them. Note that the model parameters were not altered, and that the only alteration made to the models was the inclusion of the IAA effect in the GAPDH reaction. Flux control coefficients for *L. lactis*, were similar between the model and the experimental results, and indicate that GAPDH has low control on the glycolytic flux

## 4.6. Glycolytic flux control

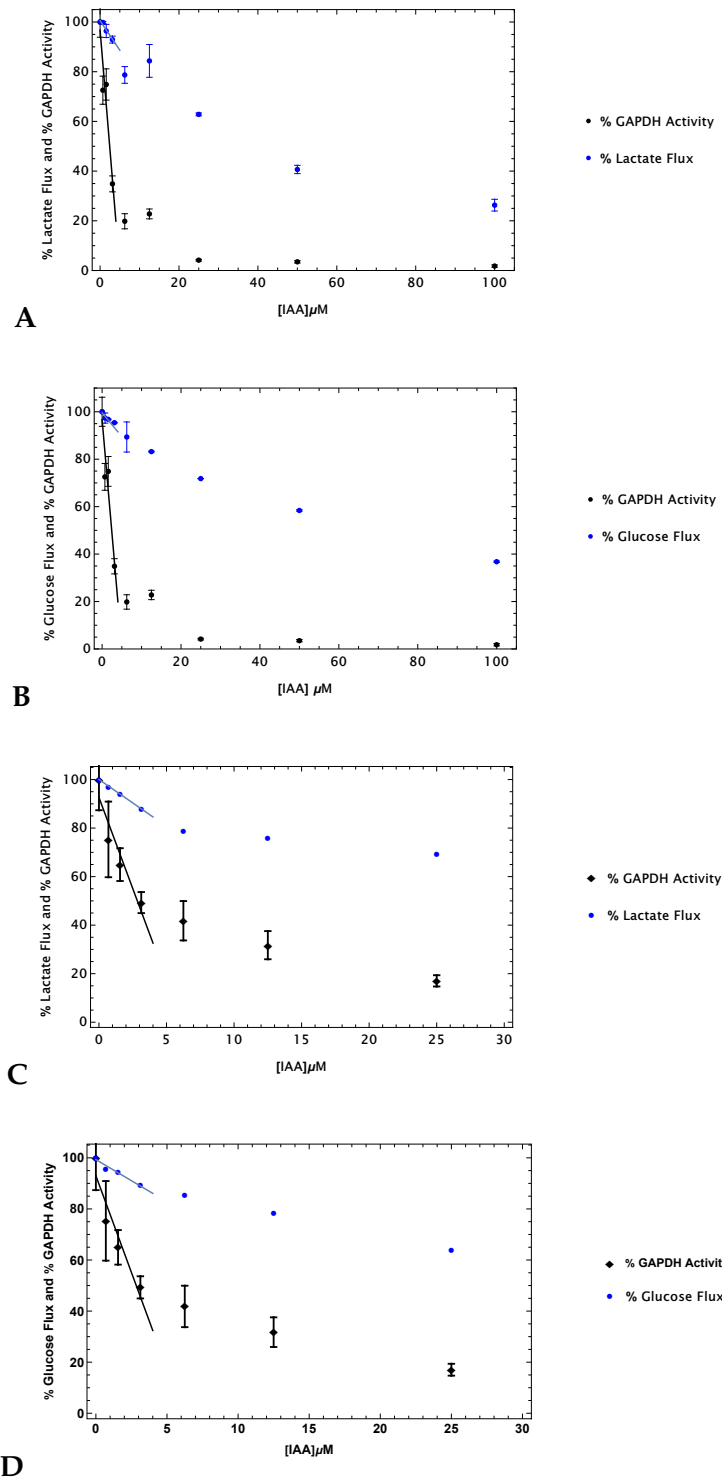


**Figure 4.8: Determination of experimental control coefficients.** This method (Method 1 as described in Chapter 3) consisted of taking the slope of the curve at the 100% flux versus IAA concentration (represented in blue) and dividing it by the derivative of the exponential decay function (represented in black). **(A-B)** represents the percentage lactate and glucose flux in combination with GAPDH activity as a function IAA concentration in *L. lactis* respectively, whereas **(C-D)** represents the percentage lactate and glucose flux in combination with GAPDH activity as a function IAA concentration in *P. falciparum*. The blue lines are the linear fits to the flux data at low IAA. Black lines show the gradients in the activity data obtained from the fitted exponential functions at IAA = 0. For *L. lactis* **(A-B)**, data is shown as the mean $\pm$ SEM of two independent experiments (n=2), whereas for *P. falciparum* **(C-D)** the data show the mean $\pm$ SD of technical triplicates from one independent experiment (n=1).

## 4.6. Glycolytic flux control

and lactate production at the wild-type level. For *P. falciparum* the model and the experimental control coefficients were in better agreement with one another than in *L. lactis* and indicated that GAPDH (when treated with IAA) had higher control on both glucose consumption and lactate production in *P. falciparum* compared to *L. lactis*.

Overall, the low control coefficients indicate that altering levels of GAPDH would have a relatively small effect on the glycolytic flux of the system, i.e. the glucose metabolism of both species. The curves in Fig. 4.9, however, indicate that in both species the flux control of GAPDH increases dramatically when the enzyme activity is decreased to below 20% of the wild-type activity.

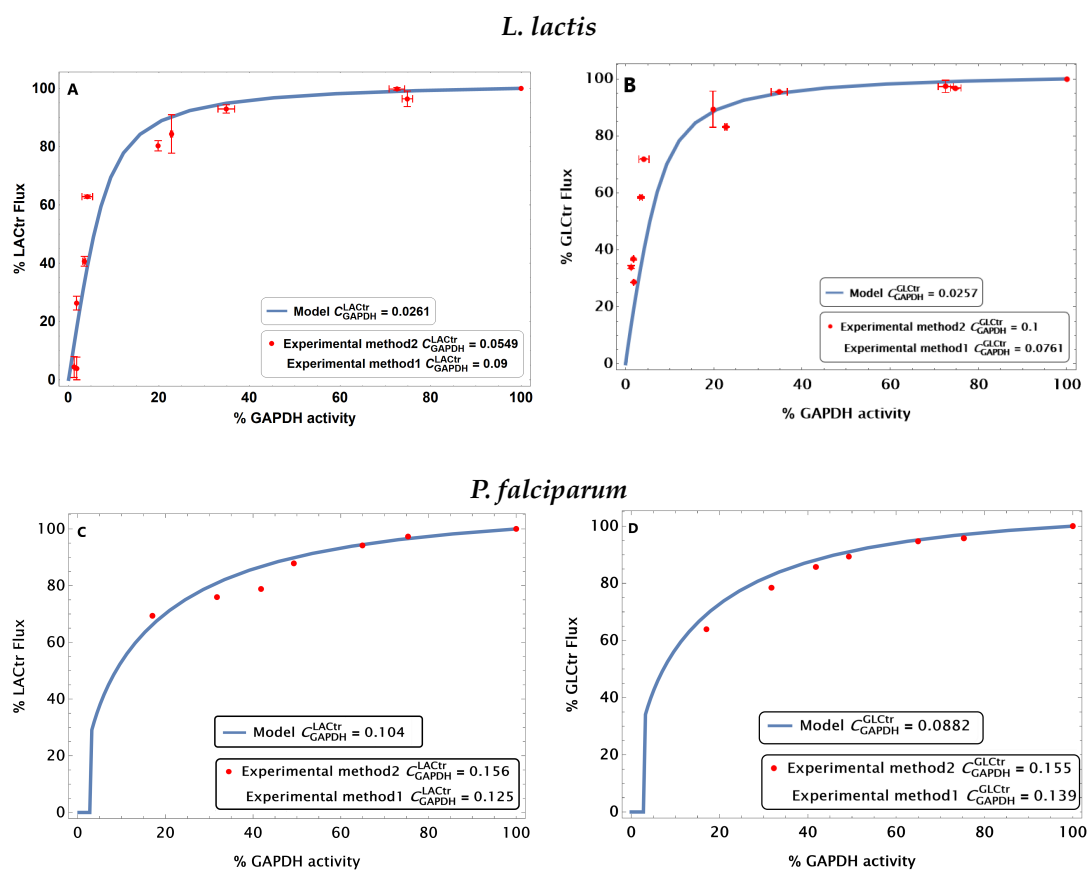


**Figure 4.9: Glycolytic flux control of GAPDH.** Glycolytic flux, in terms of lactate flux and glucose flux, were plotted as a function of GAPDH activity for iodoacetic acid inhibition. The glycolytic models (Hoefnagel and Penkler models) in the respective organisms (*L. lactis* and *P. falciparum*) were used to simulate the glycolytic flux as a function of GAPDH activity. For Method 2, independent fits were made to the glycolytic flux and enzyme activity data at 100% IAA activity to derive the glycolytic flux control coefficients of glyceraldehyde-3-phosphate dehydrogenase (lines not shown here). **A-B** and **C-D** show the data for lactate and glucose flux against GAPDH activity for *L. lactis* and for *P. falciparum* trophozoites, respectively. Data points (●) represent the mean of two biological repeats and error bars the SEM in *L. lactis*. For *P. falciparum* the data points represent the mean of one biological repeat. The solid curves (—) show the model predictions.

**Table 4.4: Flux control coefficients.** A comparison between the control coefficients of *L. lactis* and *P. falciparum* trophozoites using two different MCA calculation methods.

Control coefficient	Model	Experimental average*
<i>L. lactis</i>		
$C_{v_{GAPDH}}^{J_{LAC}}$	0.0261	0.0725
$C_{v_{GAPDH}}^{J_{GLC}}$	0.0257	0.0881
<i>P. falciparum</i>		
$C_{v_{GAPDH}}^{J_{LAC}}$	0.104	0.141
$C_{v_{GAPDH}}^{J_{GLC}}$	0.0882	0.147

\* is the average of the control coefficients calculated using two different MCA methods.

## Chapter 5

# Discussion and Conclusions

In this study the glycolytic flux control of GAPDH was quantified in *P. falciparum* and *L. lactis*. *P. falciparum* malaria is a major health burden that has devastating consequences on the lives of individuals residing in the subtropics. The glycolytic flux control of GAPDH was investigated in an attempt to identify drug-targets in *P. falciparum*. *L. lactis* is both an organism of industrial importance as well as a model organism used to study the glycolytic pathway. Previous studies have resulted in contradictory results regarding the glycolytic flux control of GAPDH in *L. lactis*, which we aimed to resolve in this study.

Glycolysis is an important source of energy for both organisms, and its enzymes are therefore attractive targets for the manipulation of glycolytic flux and energy supply. In the case of *P. falciparum*, glycolysis is required for the development of the parasite life forms (merozoites, rings, trophozoites, and schizonts), specifically the metabolically active trophozoite, within the erythrocyte. In the case of *L. lactis*, glycolysis is mainly used to drive the production of lactate that could be used in industrial applications.

Glyceraldehyde-3-phosphate dehydrogenase (GAPDH) has emerged as an enzyme of interest as it may contribute significantly to the control of the glycolytic flux in *P. falciparum* and in *L. lactis*. Additionally, GAPDH is not only a glycolytic enzyme that generates reducing equivalents (NADH), but it provides moonlighting functions that extend to other processes (see section 2.4, [49, 50]) as well. In this study, we investigated to what extent GAPDH inhibition by iodoacetic acid affects the glycolytic flux in *L. lactis* and *P. falciparum*, and we simulated the experiments with two relevant models, to determine if GAPDH is a feasible drug target for malaria studies and to settle the dispute in *L. lactis* flux control.

To evaluate the flux control of GAPDH, we performed a titration study with IAA, an

## 5.1. IAA attenuates GAPDH activity in both microorganisms

---

inhibitor of the enzyme. Iodoacetic acid (IAA) functions as an alkylating agent that irreversibly binds to the thiol groups of the catalytic cysteine by the formation of an S-carboxymethylation covalent complex (Figure 2.6).

This study was divided into two main aims. Firstly, the flux control of GAPDH in *L. lactis* had to be determined. This was done experimentally and computationally by characterizing the effect IAA titrations have on the glycolytic flux, measuring the enzyme activity of GAPDH in cell lysates at varying IAA concentrations, and by analyzing the IAA effect on the Hoefnagel model [7]. Secondly, the flux control of GAPDH in *P. falciparum* had to be determined. Similar objectives to aim 1 were used to determine the flux control of GAPDH in *P. falciparum*, where the Penkler model was used for the model simulations.

In the following sections, a discussion and interpretation of the results are presented first, followed by a summary of the results of this study. The limitations of the study are then highlighted followed by the recommendations for future research.

### 5.1 IAA attenuates GAPDH activity in both microorganisms

*L. lactis* and *P. falciparum* were preincubated with varying IAA concentrations for 30 minutes. Firstly, the enzyme specificity of IAA in *L. lactis* was determined. This was followed by the determination of GAPDH activity in cell lysates.

#### 5.1.1 Enzyme specificity of IAA

Enzymes of the glycolytic pathway of *L. lactis* were assayed to determine which were affected during IAA exposure, other than the specific enzyme target glyceraldehyde-3-phosphate dehydrogenase. When examining whether iodoacetic acid (IAA) inhibits activity of glycolytic enzymes (Figure 4.2), it was observed that only GAPDH inhibition was statistically significant in *L. lactis* whether outliers were excluded (Figure 4.2) or included (see appendix, Figure D.1). Despite theories that hypothesize that IAA can irreversibly inhibit all enzymes containing catalytic cysteine residues [99, 100], we saw that neither dehydrogenase enzymes (LDH and G3PDH) nor pyruvate kinase or enolase were affected when exposed to 100  $\mu$ M. This implies that although dehydrogenase enzymes may have similar roles as oxidoreductases, their thiol modification by IAA at the catalytic cysteine residues may differ due to differences in enzyme structure.

## 5.2. IAA inhibits the glycolytic flux in both microorganisms

---

### 5.1.2 GAPDH activity inhibition

To study the effect of IAA on GAPDH activity in *L. lactis*, GAPDH was assayed using a PGK enzyme coupled assay in cell lysates at varying IAA concentrations.

As expected GAPDH activity decreased with increasing IAA concentrations. When exponential decay functions were fitted on the data shown in Figure 4.3, the exponential constant  $k_i$  of *L. lactis* ( $k_{i_{Ll}}$ ) was greater than that of *P. falciparum* ( $k_{i_{Pf}}$ ). This means that the IAA effect is stronger in *L. lactis* and that you would require a smaller concentration of IAA to inhibit GAPDH in *L. lactis*. The work by Sabri and Ochs [101] suggested that a concentration of 2.5 mM was able to completely inhibit the GAPDH enzyme activity in cat sciatic nerves after 10 minutes of IAA exposure and that this inhibition was irreversible for 3 hours after IAA was washed out. In this study, we found that a concentration of 2.64  $\mu$ M reduced activity by half and a concentration as low as 25  $\mu$ M could completely inhibit GAPDH activity in *L. lactis*. For *P. falciparum* this concentration is estimated to be in excess of 100  $\mu$ M.

## 5.2 IAA inhibits the glycolytic flux in both microorganisms

Samples of *L. lactis* and *P. falciparum* preincubated with varying IAA concentrations for 30 minutes, were used for glucose incubation assays. Glucose consumption and lactate production fluxes were determined by monitoring glucose and lactate concentrations in the supernatant.

As expected the inhibition of GAPDH by IAA concomitantly reduced the glycolytic flux, in terms of lactate production and glucose consumption, in *L. lactis*. Figure 4.4 A showed that with increasing time, lactate was produced, while a concurrent reduction in the initial glucose concentration (Figure 4.6) was shown. The initial consumption of glucose between 0 and 15 minutes may suggest that glucose is consumed at a very fast rate. However, if one omits the initial point from the curve, the rates become dramatically lower (data not shown), which may suggest that the glucose determination assay was faulty. Due to time constraints repeats could not be included. Comparable effects in glucose and lactate fluxes, however, place a measure of confidence in these results.

Figure 4.7 A shows the percentage glucose consumption flux as a function of increasing

### 5.3. Low flux control is observed experimentally and within models in both *L. lactis* and *P. falciparum*

IAA concentrations. It is evident that the glucose flux decreased with increasing IAA concentration. Additionally, the lactate flux also decreased with increasing IAA concentrations (Figure 4.5). This illustrated that IAA has an effect on the glycolytic flux through inhibition of GAPDH. The extent of this effect is quantified in the subsequent control coefficient calculation.

Figure 4.5 B shows the percentage lactate flux as a function of IAA concentrations. It is evident that the lactate flux decreases with increasing IAA concentrations. The glucose flux also declines with increasing IAA concentrations. The glucose determination assay seems to have worked to a better extent in *P. falciparum*. Thus, IAA inhibition by GAPDH reduced the glycolytic flux of both organisms.

### 5.3 Low flux control is observed experimentally and within models in both *L. lactis* and *P. falciparum*

Two different MCA methods (as described in Materials and Methods, Chapter 3) were used to determine the experimental control coefficients. Published models of glycolysis in the two organisms were adapted using an exponential decay function, fitted to the activity inhibition data, to describe the effect of IAA inhibition on GAPDH activity. GAPDH activity and glycolytic flux could then be determined for different IAA concentrations, and the model GAPDH flux control coefficients could be determined using MCA.

#### 5.3.1 Flux control in *L. lactis*

For *L. lactis* we found that the Hoefnagel model accurately predicts the experimental data, with minimal deviation in the control coefficients. Lower IAA concentrations (between 0.7 and 12.5  $\mu\text{M}$ ) did not appear to have large effects on the glycolytic flux and the GAPDH activity. Concentrations ranging between 25 and 400  $\mu\text{M}$  resulted in greater reduction in both properties. Low control by GAPDH on the glycolytic flux was observed (Figure 4.9 A-B) in both experimental and model determinations. These results build on existing evidence depicted by Solem *et al.* [15] who found GAPDH to have no flux control in *L. lactis*, but contradicts the data obtained by Poolman and colleagues [88], who found GAPDH to have absolute control over the glycolytic flux in *L. lactis* Wg2 [15, 88].

### 5.3. Low flux control is observed experimentally and within models in both *L. lactis* and *P. falciparum*

The degree of inhibition by IAA has been linked to the time interval that a sample has been exposed to it and is corroborated with studies by Schroeder et al. [102]. Poolman et al. [88] showed that inhibition by IAA for 15 minutes at 30°C and after subsequent washes with buffer similar to our protocol, resulted in a significant GAPDH control coefficient of 0.9 in the *L. lactis* Wg2 strain. In the current study, when inhibition time was increased to 30 minutes in *L. lactis* MG 1363 at 37°C, mean control coefficients of 0.0725 and 0.0881 were obtained for lactate and glucose fluxes, respectively (Table 4.4).

Model control coefficients of 0.0261 and 0.0257 were observed for lactate and glucose fluxes, respectively. We see that both the model and the experimentally determined control coefficients were in good agreement. The control coefficients determined in the current study, the Hoefnagel model [7, 8] and the data in the Solem et al. publication [15] are in good agreement, which suggests that the Poolman et al. [88] study may be an outlier.

#### 5.3.2 Flux control in *P. falciparum*

We found that the Penkler model has strong predictive power in determining the control coefficients with slight differences when compared to the experimental control coefficients. In *P. falciparum* 3D7, mean control coefficients of 0.141 and 0.147 were observed for lactate and glucose fluxes, respectively (Table 4.4) compared with the model control coefficients of 0.104 and 0.0882, respectively. GAPDH has low control on the glycolytic flux and lactate production at the wild-type level.

#### 5.3.3 Comparison of flux control in both *L. lactis* and *P. falciparum*

For both organisms we found that the prediction of the models for the effect of GAPDH activity inhibition on flux was in excellent agreement with experimental results. In addition, we found that GAPDH in *Lactococcus lactis* subspecies cremoris MG1363 and *Plasmodium falciparum* 3D7 had low control on the glycolytic flux (Figure 4.9). Mean control coefficients of 0.0725 and 0.0881 were obtained for lactate and glucose fluxes in *L. lactis*, respectively and in *P. falciparum* 3D7, mean control coefficients of 0.141 and 0.147 were observed for lactate and glucose fluxes, respectively (Table 4.4).

The low flux control of GAPDH suggests that the control resides in other enzymes in glycolysis, the glucose transporter [90] or ATP-consuming pathways. Overall, we found

### 5.3. Low flux control is observed experimentally and within models in both *L. lactis* and *P. falciparum*

that the enzyme GAPDH had low control over the glycolytic flux (Table 4.4 and Figure 4.9) and that IAA acts weakly on GAPDH as shown by the  $k_i$  values (Table 4.2) in both species. It is evident that IAA had a slightly larger effect on the GAPDH activity in *L. lactis* compared to *P. falciparum* (Figure 5.1), and that both the model and experimental control coefficient for lactate and glucose are lower in *L. lactis* than *P. falciparum* (Table 4.4, Figure 4.9).

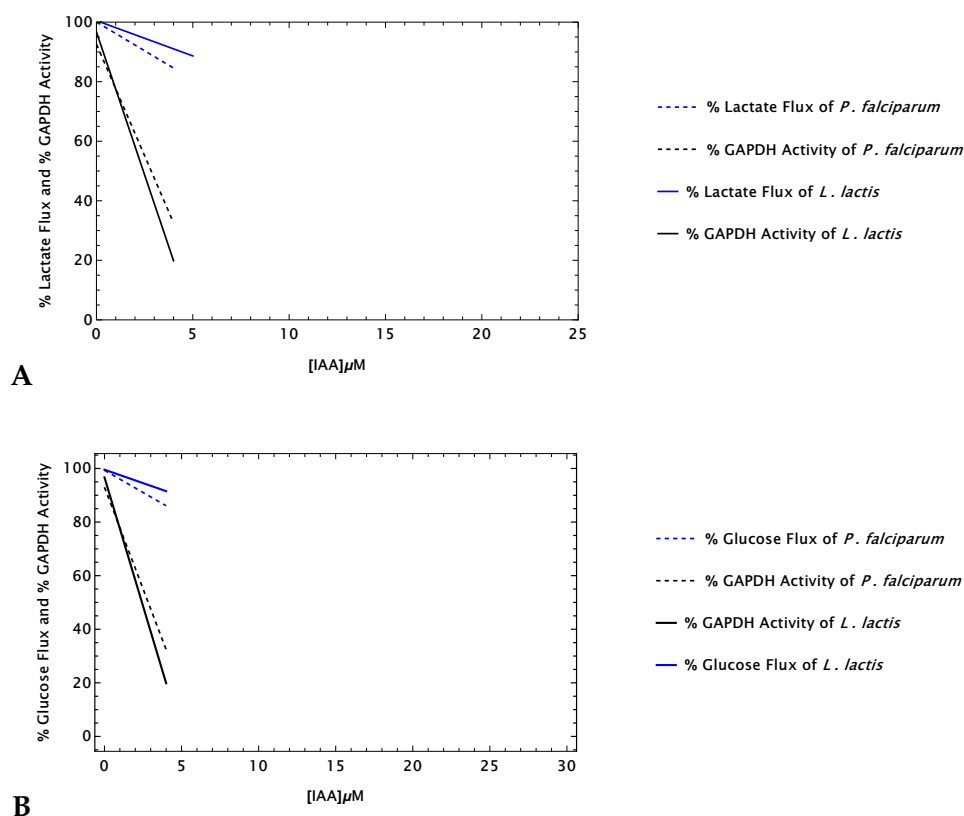


**Figure 5.1: Elasticities of the experimental control coefficients as described in Figure 4.8 for both *L. lactis* and *P. falciparum*.** The gradients of the solid blue (—) and black lines (—) represent the change in the percentage flux for lactate (**A**) and glucose (**B**), and the change in the percentage GAPDH activity of *L. lactis*, respectively. The gradients of the blue (··) and black dashed lines (··) represent the change in the percentage flux for lactate (**A**) and glucose (**B**), and the change in the percentage GAPDH activity of *P. falciparum*, respectively. The slopes in *L. lactis* samples come from data describing the mean±SEM of two independent experiments (n=2), whereas the slopes in *P. falciparum* samples come from the data describing the mean±SD in technical triplicates of one independent experiment (n=1).

When considering the role of control in the response coefficient ( $R_p^J$ ) as described in equation 2.5.5, it becomes clear that in the presence of an inhibitor, the system's response is dependent on how strong the inhibitor acts on the enzyme and the control of the enzyme on the system property. Fig. 5.1 again shows the results we obtained for relative changes

### 5.3. Low flux control is observed experimentally and within models in both *L. lactis* and *P. falciparum*

in flux and activity in both organisms as a function of IAA concentration, reproduced from Fig. 4.8. Although the gradients of these lines are not numerically equal to the response coefficients (blue lines) or the elasticity coefficients (black lines) due to the IAA concentration not being expressed as a fraction or percentage, they do behave similarly and the differences between organisms can be compared. As is evident here, the response coefficients in *P. falciparum* are larger than in *L. lactis*, as seen in the steeper gradients of the dashed blue lines compared to the solid blue lines. The gradients of the black lines, however, show that the elasticity of GAPDH for IAA is larger in *L. lactis*. The larger response in *P. falciparum* is therefore brought about by the larger control that GAPDH has on the flux in this organism. MCA performed on the modified Hoefnagel and Penkler models showed a similar pattern. Response, control and elasticity coefficients were calculated independently of one another at low IAA concentration (0.001  $\mu\text{M}$ ) (and checked for consistency using the partitioned response equation 2.5.5). The results showed that the response coefficients  $R_{IAA}^{J_{GLC}}$  and  $R_{IAA}^{J_{LAC}}$  are larger in *P. falciparum*, the elasticity  $\epsilon_{IAA}^{v_{GAPDH}}$  is larger in *L. lactis*, and the control coefficients  $C_{v_{GAPDH}}^{J_{GLC}}$  and  $C_{v_{GAPDH}}^{J_{LAC}}$  are larger in *P. falciparum*<sup>1,2</sup>.

Overall, it was found that IAA influences the steady states of the glycolytic flux in both species weakly, suggesting that the effect at low IAA concentrations were not large enough to induce a change in the wild type steady state. This also deduced that GAPDH may not be controlling the flux, and that other glycolytic enzymes and pathways should be explored. Since the control coefficients are calculated at the wildtype level (i.e.  $[\text{IAA}] \approx 0$ ), however, the effect of higher IAA concentrations ( $\geq 25 \mu\text{M}$ ) are not accounted for by MCA at the wildtype level. One can, however, observe the effect of higher IAA concentrations in Figure 4.9. Here it is evident that a sufficiently high concentration of IAA is able to significantly affect the enzyme activity and the flux. What is also remarkable is that the model results across the range of enzyme activities, are in such good agreement with the experimental results.

---

<sup>1</sup>*L. lactis*:  $R_{IAA}^{J_{GLC}} = -6.76 \times 10^{-6}$ ,  $R_{IAA}^{J_{LAC}} = -6.90 \times 10^{-6}$ ,  
 $C_{v_{GAPDH}}^{J_{GLC}} = 0.0257$ ,  $C_{v_{GAPDH}}^{J_{LAC}} = 0.0261$ ,  $\epsilon_{IAA}^{v_{GAPDH}} = -2.63 \times 10^{-4}$   
<sup>2</sup>*P. falciparum*:  $R_{IAA}^{J_{GLC}} = -1.38 \times 10^{-5}$ ,  $R_{IAA}^{J_{LAC}} = -1.63 \times 10^{-5}$ ,  
 $C_{v_{GAPDH}}^{J_{GLC}} = 0.0882$ ,  $C_{v_{GAPDH}}^{J_{LAC}} = 0.104$ ,  $\epsilon_{IAA}^{v_{GAPDH}} = -1.56 \times 10^{-4}$

## 5.4 Findings summary

Glycolysis plays an important role in energy production in both *L. lactis* and *P. falciparum* and is arguably the most studied metabolic pathway. This study contributed meaningful information to the identification of drug targets in the malaria parasite, *P. falciparum*, showing that GAPDH is not an ideal target if low inhibitor concentrations are required, due to its low flux control. To accomplish this, the following objectives were achieved:

1. The GAPDH activity and glycolytic flux in *P. falciparum* were successfully measured in the presence and absence of IAA.
2. An exponential decay function was derived from the GAPDH activity versus IAA concentration curves and the exponential inhibition constant,  $k_{i_{Pf}}$ , was successfully determined in *P. falciparum* for one independent experiment.
3. The Penkler model was successfully adapted with an exponential decay function to include IAA's effect on the GAPDH rate equations.
4. Flux control coefficients were determined *in silico* (with the model) and *in vitro* (experimentally) using two different methods (mentioned in Materials and Methods). These methods were successful in determining flux control coefficients for both glucose and lactate flux. Model and experimental results were in good agreement.

This study also contributes flux control information for the bacterium, *L. lactis*, showing that GAPDH has low flux control. To accomplish this, the following objectives were achieved:

1. The GAPDH activity and glycolytic flux in *L. lactis* were successfully measured in the presence and absence of IAA.
2. An exponential decay function was derived from the GAPDH activity versus IAA concentration curves and the exponential inhibition constant,  $k_{i_{Ll}}$ , was successfully determined in *L. lactis* for two independent experiments.

## 5.5. Limitations, recommendations and future studies

---

3. The glycolytic flux, in terms of glucose consumption and lactate production rates, was only successfully characterized for lactate production at various IAA concentrations. The glucose determination assay for glucose consumption, was not correct as it had some initial error that was the same throughout this assay in *L. lactis*.
4. The Hoefnagel model was successfully modified with the exponential decay function to include IAA's effect on the GAPDH rate equations.
5. Flux control coefficients were determined *in silico* (with the model) and *in vitro* (experimentally) using two different methods (mentioned in Materials and Methodologies). These methods were successful in determining flux control coefficients for both glucose and lactate flux. Model and experimental results were in good agreement.

### 5.5 Limitations, recommendations and future studies

This section describes the limitations, recommendations and future studies that may be needed to improve the quality of the results.

#### 5.5.1 Effect of IAA on GAPDH activity

A possible limitation that affected this study was that only the reverse direction of GAPDH activity was assayed using a coupled assay with PGK due to low detectable GAPDH activity obtained in the forward direction. Validations for these results could be performed using forward direction assays containing the larger amounts of lysate necessary and to conduct similar studies using either HPLC or NMR spectroscopy. A possible way to overcome this limitation is to optimize the assay so that it is possible to perform similar experimentation for the forward direction by increasing the concentrations of metabolites to reach saturating conditions in both organisms.

#### 5.5.2 Effect of IAA on glycolytic flux

The glucose determination assay for glucose consumption should be repeated, as there are some indications of a consistent error throughout this assay in *L. lactis*. The glucose determination assay in *L. lactis* shows that glucose is being consumed at a much faster rate than in *P. falciparum* and that a higher sampling rate might be required in the first

## 5.5. Limitations, recommendations and future studies

---

few minutes or a lower biomass should be used. It could also be the case that the glucose determination assay did not work correctly. However, if we omit the first data point in the line fitting for rate determination (Figure 4.6), the gradient seems to be much lower and it appears that this initial point may be decisive in determining the obtained flux values. However, due to time constraints we proceeded with these results. Thus, repeats are necessary to verify what is seen in the glucose consumption flux.

### 5.5.3 Glycolytic flux control

In this study only GAPDH control coefficients were determined in both species. Although there was good agreement between model and experimental results, similar work will need to be done for other enzymes in the pathway. Future studies should therefore include the determination of control coefficients for all glycolytic enzymes including the branched pathways to get a better representation of the flux control distribution of the entire glycolytic pathway. This will assist us in identifying which enzyme contributes a significant amount of flux control within the pathway.

It might be the case that flux control may be strain specific and repetitions would need to be conducted in different strains of the two microorganisms used in the study. Nevertheless, we found that the experimental results for the 3D7 strain of *P. falciparum* did agree very well with the results from the model constructed using the 3D10 strain.

In future, the sample size of *P. falciparum* culture should be increased to include the results of multiple biological repeats. For the study of possible drug targets, the model should be extended to the entire plasmodium life cycle in an attempt to uncover the dynamics in gametocyte metabolism as well.

This research will contribute to the understanding of *in vivo* disease dynamics of *P. falciparum* and could lead to drug-target identification. This approach could be used to identify other enzymatic drug targets and the quantification of drug effects on the metabolism of pathogens.

## 5.6 Conclusion

The experimental and theoretical evaluations of both *L. lactis* and *P. falciparum* GAPDH inhibition was achieved through inhibition of GAPDH activity by IAA. We saw that no other enzymes within glycolysis were significantly affected by IAA. The methods used were successful in determining the GAPDH flux control. Overall, models of the glycolytic pathways were in excellent agreement with experimental results and very small disparities between the model and the experimental flux data could be improved by additional experimentation or minor model refinement. Although a reliable determination of control coefficients was seen using two different determination methods in both organisms, repetitions would need to be conducted specifically within *P. falciparum* since this is the first characterisation of GAPDH inhibition using IAA as inhibitor.

## Appendix A

# Other glycolytic enzymes as targets

**Could other glycolytic enzymes be targeted for therapeutic development?** According to prior research, enzymes that have high control over the glycolytic flux may be potential drug targets for therapeutic relief [6, 103] and these enzymes have to be different enough in structure from the human counterpart. Such enzymes: Hexokinase (HK), pyruvate kinase (PK), lactate dehydrogenase (LDH), phosphofructokinase (PFK), and triose-phosphate isomerase (TPI) including the glucose transporter and lactate transporter, have also been identified as potential drug targets. Other studies have identified that most of the enzymes found in upper glycolysis may be suitable targets [104]. However, contrasting studies suggest that if enzymes that occur in lower glycolysis were to be inhibited, it would lead to the accumulation of metabolic intermediates upstream of the enzyme reaction, inevitably blocking glycolysis either way.

### A.1 Role of Hexokinase

Hexokinase (HK, EC 2.7.1.1) phosphorylates glucose by taking a  $\gamma$ -phosphoryl group from adenosine triphosphate (ATP) and adding it to glucose producing glucose-6-phosphate (G6P) and adenosine diphosphate (ADP) [105]. The 55.3 kDa hexokinase of *P. falciparum* (PfHK) shares similar biochemical processes with mammalian HKs, however differs largely in primary structure with 26% amino acid identity to the human HKs [21, 105] as opposed to *L. lactis* HK (LIHK) with an amino acid identity of 7.2% with the human homolog. This suggests that the high variability in amino acid identity in both species could be used as targets within HK. The drugs specifically targeting HK may be developed.

### A.1.1 Hexokinase Inhibitors: Approaches for Discovery

Lonidamine (LND; 1-(2,4-dichlorobenzyl)-1, H-indazol-3-carboxylic acid), an anticancer drug, has been subjected to human clinical trials for many years for the inhibition of human HK but was found to inhibit recombinant *Trypanosoma brucei* HKs as well [28]. HK inhibition by lonidamine depletes and prevents ATP reserves and production, respectively [28, 106]. Additionally, it dissociates hexokinase from the mitochondrion, in other words, it removes hexokinase from the mitochondrion preventing the pentose phosphate pathway from occurring. Meanwhile, 2-deoxy-D-glucose (2-DG) is a glucose analog that prevents the phosphorylated form of 2-DG, i.e. 2DG-P, from becoming metabolized by PGI [107]. This leads to the accumulation of 2DG-P and the exhaustion of ATP and thus prevents the maximal effect expressed by the glycolytic pathway. Rego et al. [108] claimed that a 10-20% reduction in the HK enzyme activity was prevalent when exposed to 2DG. 3-Bromopyruvate (3-BP;  $C_3H_3BrO_3$ ), an anticancer drug acting as an alkylating agent, has been subjected to research within the cancer metabolism that targets energy metabolism [109]. This alkylating agent is known for its properties in reducing the hexokinase II activity of cancer cells. Fundamentally, it works by covalently blocking the cysteine residues with bromide on the enzyme. In turn, it abolishes ATP production. Although it may be a potential inhibitor, it has unstable thermodynamic properties that make it difficult to act on every HK [109].

## A.2 Role of Lactate dehydrogenase

Lactate dehydrogenase recycles  $NAD^+$  to NADH by reducing the keto group on pyruvate to form a hydroxyl group on lactate. This tetrameric enzyme has five isoenzymes and LDH-A is responsible for the conversion of pyruvate to lactate as compared to LDH-B that catalyzes the reverse reaction (lactate to pyruvate) [5]. High concentrations of pyruvate have been shown not to inhibit the LDH of the parasite [33].

### A.2.1 Lactate Dehydrogenase Inhibitors: Approaches for Discovery

Hakala *et al.* [110] found that LDH inhibition by oxamate (Table A.1) is competitive with pyruvate, while LDH inhibition by oxalate is competitive with lactate. Pelicano *et al.* [67] found oxalate to be a potential inhibitor of LDH, but no confirmation has been established in *P. falciparum*.

### A.3. Role of Triosephosphate isomerase

---

Sodium oxamate (SO;  $C_2H_2NNaO_3$ ), a monoamide of oxalic acid and possible pyruvate analog, is a noncompetitive inhibitor of lactate dehydrogenase capable of preventing lactate production by blocking off the active site when it is added to it.

Oxalate (OXA;  $C_2O_4^{2-}$ ), an *in vitro* competitive inhibitor of lactate dehydrogenase, phosphoglycerate mutase, and pyruvate kinase, was found to have an effect on pyruvate kinase within erythrocytes.

### A.3 Role of Triosephosphate isomerase

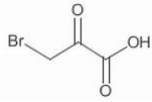
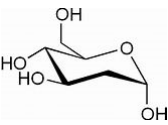
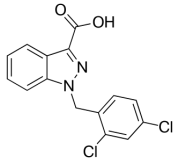
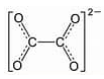
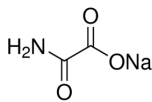
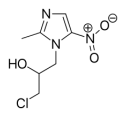
Triose-phosphate isomerase (TPI) catalyzes the interconversion of GAP to dihydroxyacetone phosphate (DHAP) [111, 112], and plays a pivotal role in gluconeogenesis, fatty acid biosynthesis and the hexosemonophosphate shunt [112]. Within *P. falciparum*, TPI is homodimeric containing four cysteine residues, which is replaced with methionine in the human counterpart [111].

#### A.3.1 Triosephosphate Isomerase Inhibitors: Approaches for Discovery

Ornidazole (ORN;  $C_7H_{10}ClN_3O_3$ ) inhibits both GAPDH and TPI [65, 66]. In rats, ornidazole is converted to chlorolactate instead of producing lactate preventing the conversion of pyruvate to lactate [113], which behaves similar to  $\alpha$ -chlorohydrin.  $\alpha$ -Chlorohydrin is a compound known to cause an antifertility effect in sperm due to its affect during energy metabolism [113]. Oberländer *et al.* [66] showed that TPI may become more inhibited by ornidazole than GAPDH. This unspecific nature of ornidazole action makes it an unreliable source for selective inhibition studies.

## A.3. Role of Triosephosphate isomerase

**Table A.1: Potential glycolytic enzymes as targets for therapeutic development in *P. falciparum*.** 3-Bromopyruvate (3-BP), 2-deoxy-D-glucose (2-DG), and lonidamine are known anticancer inhibitors.

Compound	Compound role	Enzyme target	% identity <sup>a</sup>
 3-bromopyruvate	abolishes ATP production, alkylating agent, inhibits hexokinase II, thermodynamically unstable cytotoxic activity against cancer cells	HK [67, 109] GAPDH[45]	15.76% <sup>1</sup> 63.7% <sup>2</sup>
 2-deoxy-D-glucose	glucose analog prevents the phosphorylation of 2DG. exhaustion of ATP	HK [114]	15.66% <sup>1</sup>
 lonidamine	dissociates HK from mitochondria, depletes ATP reserves, prevents ATP production	HK [28]	15.66% <sup>1</sup>
 oxalate	competitive inhibitor of LDH	LDH [110]	23.15% <sup>4</sup>
 sodium oxamate	a structural analogue of pyruvate, monoamide of oxalic acid suppresses cancer cell growth reduces lactate production short-term decrease in ATP	LDH [110, 115, 116]	23.15% <sup>4</sup>
 ornidazole	an antibiotic used to treat protozoan infections. is converted to chlorolactate instead of producing lactate.	TPI[65, 66] GAPDH[65, 66]	19.61% <sup>3</sup> 63.7% <sup>2</sup>

<sup>a</sup> refers to the enzyme % identity relative to the human homolog

<sup>1</sup> <https://www.uniprot.org/align/A202112094ABAA9BC7178C81CEBC9459510EDDEA300EB68A>

<sup>2</sup> <https://www.uniprot.org/uniprot/Q8IKK7>

<sup>3</sup> <https://www.uniprot.org/align/A202112094ABAA9BC7178C81CEBC9459510EDDEA300EB67L>

<sup>4</sup> <https://www.uniprot.org/align/A202112094ABAA9BC7178C81CEBC9459510EDDEA300EB656>

## Appendix B

# Glucose Calibration Curve

A function to convert absorbances at 340 nm to glucose concentrations (mM) was developed, with a linear model fit derived as  $y=0.0625x+0.0087$  and  $y=0.0121x+0.0346$  in *L. lactis* and *P. falciparum*, respectively. Different calibration curves were constructed for these organisms (*L. lactis* and *P. falciparum*) due to different buffers (MES and modified ringer buffer) used.

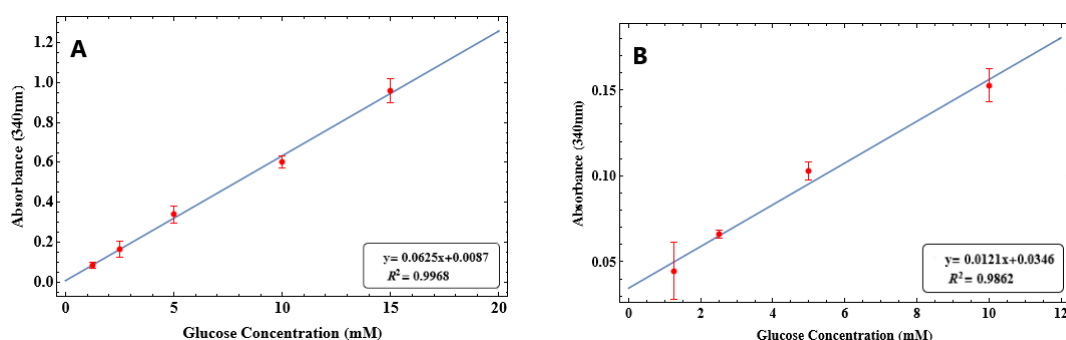


**Figure B.1: Glucose calibration curve.** An illustration of the absorbances measured at 340 nm (after blanks were deducted) as a function of glucose concentration (mM) for **(A)** *L. lactis* and **(B)** *P. falciparum*. The relationship between glucose concentration and the measured absorbance was linear. The solid line in blue represent the mean linear regression line ( $R^2 = 0.9968$  and  $R^2 = 0.9862$ ) of the data points for the respective organisms. The red data points represent the mean  $\pm$  SEM of two independent experiments (conducted in technical triplicates each) in *L. lactis* (A) and the mean  $\pm$  SD of one independent experiment (conducted in technical triplicates) in *P. falciparum* (B). Assay conditions: [glucose], 0 to 15 mM;  $\text{NAD}^+$ , 4 mM; HK, 0.10895 U.  $\mu\text{L}^{-1}$ ;  $\text{ATP.Mg}^{2+}$ , 2 mM; G6PDH, 0.05 U.100  $\mu\text{L}^{-1}$  (n=2 or 1 independent experiments, respectively).

## Appendix C

# Lactate Calibration Curve

A function to convert absorbances at 340 nm to lactate concentrations (mM) was determined, with a linear model fit derived as  $y=0.0456x+0.0417$  and  $y=0.0574x+0.0023$  in *L. lactis* and *P. falciparum*, respectively. Different calibration curves were constructed for these organisms (*L. lactis* and *P. falciparum*) due to different buffers (MES and modified ringer buffer) used.

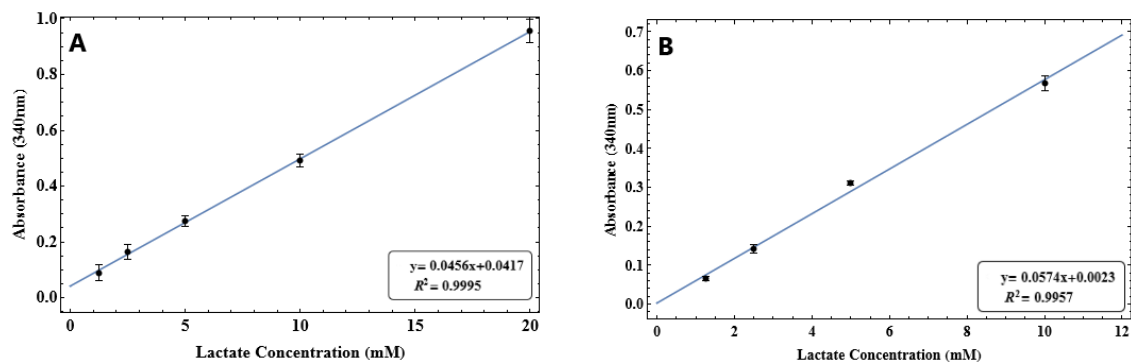


**Figure C.1: Lactate calibration curve.** An illustration of the absorbances measured at 340 nm (after blanks were deducted) as a function of lactate concentration (mM) for **(A)** *L. lactis* and **(B)** *P. falciparum*. The relationship between lactate concentration and the measured absorbance was linear. The solid line in blue represent the mean linear regression line ( $R^2 = 0.9995$  and  $R^2 = 0.9957$ ) of the data points for the respective organisms. The black data points represent the mean  $\pm$  SEM of two independent experiments (conducted in technical triplicates each) in *L. lactis* and the mean  $\pm$  SD of one independent experiment (conducted in technical triplicates) in *P. falciparum*. Assay conditions: [lactate], 0 to 20 mM;  $\text{NAD}^+$ , 4 mM; LDH, 4 U/ml; Hydrazine, 320 mM (n=2 or 1 independent experiments, respectively).

## Appendix D

# Enzyme Specificity

Tests for statistical significance (student t-tests and ANOVA) were performed at  $\alpha=0.05$  on the enzyme specificity data with both the inclusion and exclusion of outliers in the data. No significance changes were seen irrespective of outliers (Figure D.1), however, the errors seen in the data were reduced in outlier absence (Figure 4.2).

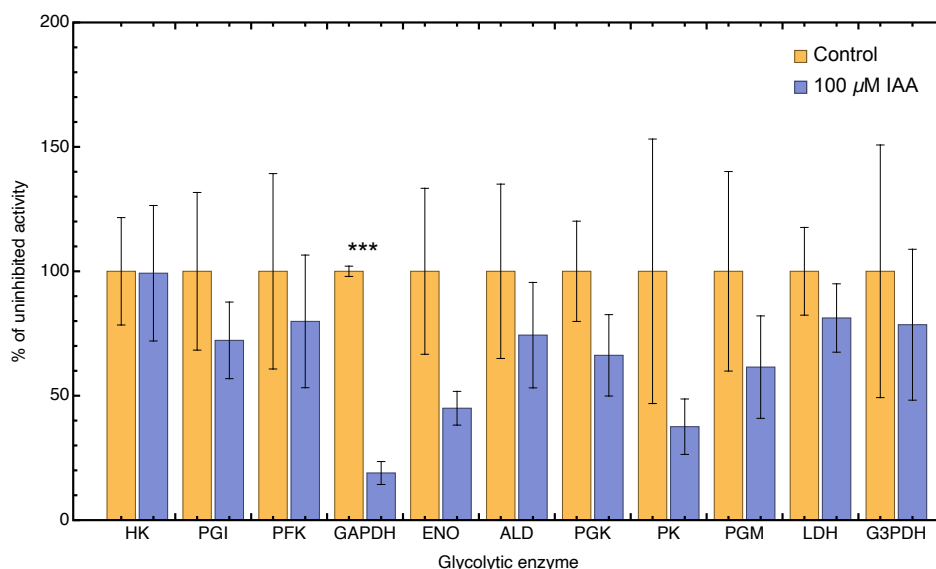


**Figure D.1: Enzyme specificity of IAA.** A graphical depiction of the effect iodoacetic acid has on the enzyme activity of glycolytic enzymes in *L. lactis*. Crude lysate samples in the absence and presence of 100  $\mu$ M iodoacetic acid before lysis were assayed for 10-minutes spectrophotometrically at 340 nm. Samples were exposed to iodoacetic acid for a period of 30-minutes before being washed off. The results represent the mean  $\pm$  SEM of the specific activity data as a percentage of the uninhibited activity obtained from three independent experiments. Statistical significance (\*\*\*) =  $p < 0.0001$ ) of data indicated as determined by Student's t-tests.

# Bibliography

- [1] Organization, W. H. et al. World malaria report 2020: 20 years of global progress and challenges, 2020.
- [2] Batista, F. A., Gyau, B., Vilacha, J. F., Bosch, S. S., Lunev, S., Wrenger, C., and Groves, M. R. New directions in antimalarial target validation. *Expert Opinion on Drug Discovery*, 15(2): 189–202, 2020.
- [3] von Braun, J., Afsana, K., Fresco, L. O., and Hassan, M. Food systems: seven priorities to end hunger and protect the planet. *Nature*, 597(7874):28–30, 2021.
- [4] Penkler, G., Du Toit, F., Adams, W., Rautenbach, M., Palm, D. C., Van Niekerk, D. D., and Snoep, J. L. Construction and validation of a detailed kinetic model of glycolysis in *Plasmodium falciparum*. *The FEBS journal*, 282(8):1481–1511, 2015.
- [5] Possemiers, H., Vandermosten, L., and Van den Steen, P. E. Etiology of lactic acidosis in malaria. *PLoS pathogens*, 17(1):e1009122, 2021.
- [6] Van Niekerk, D. D., Penkler, G. P., du Toit, F., and Snoep, J. L. Targeting glycolysis in the malaria parasite *Plasmodium falciparum*. *The FEBS journal*, 283(4):634–646, 2016.
- [7] Hoefnagel, M. H., Starrenburg, M. J., Martens, D. E., Hugenholtz, J., Kleerebezem, M., Van Swam, I. I., Bongers, R., Westerhoff, H. V., and Snoep, J. L. Metabolic engineering of lactic acid bacteria, the combined approach: kinetic modelling, metabolic control and experimental analysis. *Microbiology*, 148(4):1003–1013, 2002.
- [8] Hoefnagel, M., Van Der Burgt, A., Martens, D., Hugenholtz, J., and Snoep, J. Time dependent responses of glycolytic intermediates in a detailed glycolytic model of *Lactococcus lactis* during glucose run-out experiments. *Molecular biology reports*, 29(1):157–161, 2002.
- [9] Bakker, B. M., Michels, P. A., Opperdoes, F. R., and Westerhoff, H. V. What controls glycolysis in bloodstream form *Trypanosoma brucei*? *Journal of Biological Chemistry*, 274(21): 14551–14559, 1999.
- [10] Teusink, B., Passarge, J., Reijenga, C. A., Esgalhado, E., Van der Weijden, C. C., Schepper, M., Walsh, M. C., Bakker, B. M., Van Dam, K., Westerhoff, H. V., et al. Can yeast glycolysis

- be understood in terms of in vitro kinetics of the constituent enzymes? testing biochemistry. *European Journal of Biochemistry*, 267(17):5313–5329, 2000.
- [11] Maria, G., Mihalachi, M., and Luminita Gijiu, C. Model-based identification of some conditions leading to glycolytic oscillations in *E. coli* cells. *Chemical and Biochemical Engineering Quarterly*, 32(4):523–533, 2018.
- [12] Lambeth, M. J. and Kushmerick, M. J. A computational model for glycogenolysis in skeletal muscle. *Annals of biomedical engineering*, 30(6):808–827, 2002.
- [13] Liu, J., Chan, S. H. J., Chen, J., Solem, C., and Jensen, P. R. Systems biology—a guide for understanding and developing improved strains of lactic acid bacteria. *Frontiers in microbiology*, 10:876, 2019.
- [14] Neves, A. R., Pool, W. A., Kok, J., Kuipers, O. P., and Santos, H. Overview on sugar metabolism and its control in *Lactococcus lactis*—the input from in vivo nmr. *FEMS microbiology reviews*, 29(3):531–554, 2005.
- [15] Solem, C., Koebmann, B. J., and Jensen, P. R. Glyceraldehyde-3-phosphate dehydrogenase has no control over glycolytic flux in *Lactococcus lactis* mg1363. *Journal of Bacteriology*, 185(5):1564–1571, 2003.
- [16] Mauritz, J. M., Esposito, A., Ginsburg, H., Kaminski, C. F., Tiffert, T., and Lew, V. L. The homeostasis of *Plasmodium falciparum*-infected red blood cells. *PLoS Comput Biol*, 5(4): e1000339, 2009.
- [17] Mehta, M., Sonawat, H. M., and Sharma, S. Glycolysis in *Plasmodium falciparum* results in modulation of host enzyme activities. *Journal of vector borne diseases*, 43(3):95, 2006.
- [18] Bruce-Chwatt, L. Chemoprophylaxis of malaria in africa: the spent" magic bullet". *British medical journal (Clinical research ed.)*, 285(6343):674, 1982.
- [19] Krishna, S., Woodrow, C. J., Staines, H. M., Haynes, R. K., and Mercereau-Puijalon, O. Re-evaluation of how artemisinin work in light of emerging evidence of in vitro resistance. *Trends in molecular medicine*, 12(5):200–205, 2006.
- [20] Rautenbach, M., Vlok, N. M., Stander, M., and Hoppe, H. C. Inhibition of malaria parasite blood stages by tyrocidines, membrane-active cyclic peptide antibiotics from *Bacillus brevis*. *Biochimica et Biophysica Acta (BBA)-Biomembranes*, 1768(6):1488–1497, 2007.
- [21] Preuss, J., Jortzik, E., and Becker, K. Glucose-6-phosphate metabolism in *Plasmodium falciparum*. *IUBMB life*, 64(7):603–611, 2012.

- [22] Even, S., Garrigues, C., Loubiere, P., Lindley, N., and Coccagn-Bousquet, M. Pyruvate metabolism in *Lactococcus lactis* is dependent upon glyceraldehyde-3-phosphate dehydrogenase activity. *Metabolic engineering*, 1(3):198–205, 1999.
- [23] Coccagn-Bousquet, M., Even, S., Lindley, N. D., and Loubière, P. Anaerobic sugar catabolism in *Lactococcus lactis*: genetic regulation and enzyme control over pathway flux. *Applied microbiology and biotechnology*, 60(1):24–32, 2002.
- [24] Garrigues, C., Loubiere, P., Lindley, N. D., and Coccagn-Bousquet, M. Control of the shift from homolactic acid to mixed-acid fermentation in *Lactococcus lactis*: predominant role of the nadh/nad<sup>+</sup> ratio. *Journal of Bacteriology*, 179(17):5282–5287, 1997.
- [25] Bahey-El-Din, M. and Gahan, C. G. *Lactococcus lactis*: from the dairy industry to antigen and therapeutic protein delivery. *Discovery medicine*, 9(48):455–461, 2010.
- [26] Song, A. A.-L., In, L. L., Lim, S. H. E., and Rahim, R. A. A review on *Lactococcus lactis*: from food to factory. *Microbial cell factories*, 16(1):1–15, 2017.
- [27] Lee, A. H., Symington, L. S., and Fidock, D. A. Dna repair mechanisms and their biological roles in the malaria parasite *Plasmodium falciparum*. *Microbiology and Molecular Biology Reviews*, 78(3):469–486, 2014.
- [28] Coley, A. F., Dodson, H. C., Morris, M. T., and Morris, J. C. Glycolysis in the african trypanosome: targeting enzymes and their subcellular compartments for therapeutic development. *Molecular biology international*, 2011, 2011.
- [29] Sherman, I. W. Biochemistry of *Plasmodium* (malarial parasites). *Microbiological reviews*, 43(4):453, 1979.
- [30] Goldberg, D. E. and Zimmerberg, J. Hardly vacuuous: The parasitophorous vacuolar membrane of malaria parasites. *Trends in parasitology*, 36(2):138–146, 2020.
- [31] Ginsburg, H. Some reflections concerning host erythrocyte-malarial parasite interrelationships. *Blood cells*, 16(2-3):225–235, 1990.
- [32] Tewari, S. G., Swift, R. P., Reifman, J., Prigge, S. T., and Wallqvist, A. Metabolic alterations in the erythrocyte during blood-stage development of the malaria parasite. *Malaria journal*, 19(1):1–18, 2020.
- [33] Alam, A., Neyaz, M., Ikramul Hasan, S., et al. Exploiting unique structural and functional properties of malarial glycolytic enzymes for antimalarial drug development. *Malaria research and treatment*, 2014, 2014.

- 
- [34] Srivastava, A., Philip, N., Hughes, K. R., Georgiou, K., MacRae, J. I., Barrett, M. P., Creek, D. J., McConville, M. J., and Waters, A. P. Stage-specific changes in *Plasmodium* metabolism required for differentiation and adaptation to different host and vector environments. *PLoS pathogens*, 12(12):e1006094, 2016.
- [35] MacRae, J. I., Dixon, M. W., Dearnley, M. K., Chua, H. H., Chambers, J. M., Kenny, S., Bottova, I., Tilley, L., and McConville, M. J. Mitochondrial metabolism of sexual and asexual blood stages of the malaria parasite *Plasmodium falciparum*. *BMC biology*, 11(1):1–10, 2013.
- [36] Jensen, M. D., Conley, M., and Helstowski, L. D. Culture of *Plasmodium falciparum*: the role of ph, glucose, and lactate. *The Journal of parasitology*, pages 1060–1067, 1983.
- [37] Mehta, M., Sonawat, H. M., and Sharma, S. Malaria parasite-infected erythrocytes inhibit glucose utilization in uninfected red cells. *FEBS letters*, 579(27):6151–6158, 2005.
- [38] Roth, Jr, E. F., Calvin, M.-C., Max-Audit, I., Rosa, J., and Rosa, R. The enzymes of the glycolytic pathway in erythrocytes infected with *Plasmodium falciparum* malaria parasites. *Blood*, 72(6):1922–1925, 1988.
- [39] Zolg, J. W., Macleod, A. J., Scaife, J. G., and Beaudoin, R. L. The accumulation of lactic acid and its influence on the growth of *Plasmodium falciparum* in synchronized cultures. *In vitro*, 20(3):205–215, 1984.
- [40] Olszewski, K. L. and Llinás, M. Central carbon metabolism of *Plasmodium* parasites. *Molecular and biochemical parasitology*, 175(2):95–103, 2011.
- [41] Broadbent, K. M., Park, D., Wolf, A. R., Van Tyne, D., Sims, J. S., Ribacke, U., Volkman, S., Duraisingh, M., Wirth, D., Sabeti, P. C., et al. A global transcriptional analysis of *Plasmodium falciparum* malaria reveals a novel family of telomere-associated lncRNAs. *Genome biology*, 12(6):1–15, 2011.
- [42] Boels, I. C., van Kranenburg, R., Hugenholtz, J., Kleerebezem, M., and De Vos, W. M. Sugar catabolism and its impact on the biosynthesis and engineering of exopolysaccharide production in lactic acid bacteria. *International Dairy Journal*, 11(9):723–732, 2001.
- [43] Chen, J., Shen, J., Hellgren, L. I., Jensen, P. R., and Solem, C. Adaptation of *Lactococcus lactis* to high growth temperature leads to a dramatic increase in acidification rate. *Scientific reports*, 5(1):1–15, 2015.
- [44] Oyelade, J., Isewon, I., Rotimi, S., and Okunoren, I. Modeling of the glycolysis pathway in *Plasmodium falciparum* using petri nets. *Bioinformatics and Biology insights*, 10:BBI–S37296, 2016.

- [45] Fan, T., Sun, G., Sun, X., Zhao, L., Zhong, R., and Peng, Y. Tumor energy metabolism and potential of 3-bromopyruvate as an inhibitor of aerobic glycolysis: implications in tumor treatment. *Cancers*, 11(3):317, 2019.
- [46] Muronetz, V., Melnikova, A., Barinova, K., and Schmalhausen, E. Inhibitors of glyceraldehyde 3-phosphate dehydrogenase and unexpected effects of its reduced activity. *Biochemistry (Moscow)*, 84(11):1268–1279, 2019.
- [47] Karja, N. W. K., Fahrudin, M., and Kikuchi, K. Inhibitory effect of iodoacetate on developmental competence of porcine early stage embryos in vitro. *HAYATI Journal of Biosciences*, 16(1):25–29, 2009.
- [48] Butterfield, D. A., Hardas, S. S., and Lange, M. L. B. Oxidatively modified glyceraldehyde-3-phosphate dehydrogenase (gapdh) and alzheimer’s disease: many pathways to neurodegeneration. *Journal of Alzheimer’s Disease*, 20(2):369–393, 2010.
- [49] Tristan, C., Shahani, N., Sedlak, T. W., and Sawa, A. The diverse functions of GAPDH: views from different subcellular compartments. *Cell. Signal.*, 23(2):317–323, 2011.
- [50] Tristan, C., Shahani, N., Sedlak, T. W., and Sawa, A. The diverse functions of gapdh: views from different subcellular compartments. *Cellular signalling*, 23(2):317–323, 2011.
- [51] Simpson, R. and Davidson, B. Glyceraldehyde-3 phosphate dehydrogenase from the red kangaroo (*Megalelia rufa*): Purification and the amino acid sequence around a reactive cysteine. *Australian journal of biological sciences*, 24(2):263–274, 1971.
- [52] Galbiati, A., Zana, A., and Conti, P. Covalent inhibitors of gapdh: From unspecific warheads to selective compounds. *European Journal of Medicinal Chemistry*, 207:112740, 2020.
- [53] Ramos, D., Pellin-Carcelen, A., Agusti, J., Murgui, A., Jorda, E., Pellin, A., and Monteagudo, C. Deregulation of glyceraldehyde-3-phosphate dehydrogenase expression during tumor progression of human cutaneous melanoma. *Anticancer research*, 35(1):439–444, 2015.
- [54] Nicholls, C., Li, H., and Liu, J.-P. Gapdh: a common enzyme with uncommon functions. *Clinical and Experimental Pharmacology and Physiology*, 39(8):674–679, 2012.
- [55] Daubenberger, C. A., Pörtl-Frank, F., Jiang, G., Lipp, J., Certa, U., and Pluschke, G. Identification and recombinant expression of glyceraldehyde-3-phosphate dehydrogenase of *Plasmodium falciparum*. *Gene*, 246(1-2):255–264, 2000.
- [56] Penkler, G. P. *A kinetic model of glucose catabolism in Plasmodium falciparum*. PhD thesis, Stellenbosch: Stellenbosch University, 2013.

- 
- [57] Cascante, M., Boros, L. G., Comin-Anduix, B., de Atauri, P., Centelles, J. J., and Lee, P. W.-N. Metabolic control analysis in drug discovery and disease. *Nature biotechnology*, 20(3): 243–249, 2002.
- [58] Strelow, J. M. A perspective on the kinetics of covalent and irreversible inhibition. *SLAS DISCOVERY: Advancing Life Sciences R&D*, 22(1):3–20, 2017.
- [59] Carneiro, A. S., Lameira, J., and Alves, C. N. A theoretical study of the molecular mechanism of the gapdh *Trypanosoma cruzi* enzyme involving iodoacetate inhibitor. *Chemical Physics Letters*, 514(4-6):336–340, 2011.
- [60] Schmidt, M. and Dringen, R. Differential effects of iodoacetamide and iodoacetate on glycolysis and glutathione metabolism of cultured astrocytes. *Frontiers in neuroenergetics*, 1:1, 2009.
- [61] Nagradova, N. K., Schmalhausen, E. V., Levashov, P. A., Asryants, R. A., and Muronetz, V. I. D-glyceraldehyde-3-phosphate dehydrogenase. *Applied biochemistry and biotechnology*, 61(1):47–56, 1996.
- [62] Zhu, X., Jin, C., Pan, Q., and Hu, X. Determining the quantitative relationship between glycolysis and gapdh in cancer cells exhibiting the warburg effect. *Journal of Biological Chemistry*, 296, 2021.
- [63] Kato, M., Sakai, K., and Endo, A. Koningic acid (heptelidic acid) inhibition of glyceraldehyde-3-phosphate dehydrogenases from various sources. *Biochimica Et Biophysica Acta (BBA)-Protein Structure and Molecular Enzymology*, 1120(1):113–116, 1992.
- [64] Endo, A., Hasum, K., Hasumi, K., Sakai, K., and Kanbe, T. Specific inhibition of glyceraldehyde-3-phosphate dehydrogenase by koningic acid (heptelidic acid). *The Journal of antibiotics*, 38(7):920–925, 1985.
- [65] Bone, W. and Cooper, T. In vitro inhibition of rat cauda epididymal sperm glycolytic enzymes by ornidazole, alpha-chlorohydrin and 1-chloro-3-hydroxypropanone. *International journal of andrology*, 23(5):284–293, 2000.
- [66] Oberländer, G., Yeung, C., and Cooper, T. Influence of oral administration of ornidazole on capacitation and the activity of some glycolytic enzymes of rat spermatozoa. *Reproduction*, 106(2):231–239, 1996.
- [67] Pelicano, H., Martin, D., Xu, R., and Huang, P. Glycolysis inhibition for anticancer treatment. *Oncogene*, 25(34):4633–4646, 2006.
- [68] Russell, N. Book review: Textbook of biochemistry with clinical correlations, 1989.

- [69] Perie, J., Riviere-Alric, I., Blonski, C., Gefflaut, T., de Viguerie, N. L., Trinquier, M., Willson, M., Opperdoes, F. R., and Callens, M. Inhibition of the glycolytic enzymes in the trypanosome: An approach in the development of new leads in the therapy of parasitic diseases. *Pharmacology and Therapeutics*, 60(2):347–365, 1993.
- [70] Aderem, A. Systems biology: its practice and challenges. *Cell*, 121(4):511–513, 2005.
- [71] Badenhorst, M., Barry, C. J., Swanepoel, C. J., Van Staden, C. T., Wissing, J., and Rohwer, J. M. Workflow for data analysis in experimental and computational systems biology: using python as ‘glue’. *Processes*, 7(7):460, 2019.
- [72] Bruggeman, F. J. and Westerhoff, H. V. The nature of systems biology. *TRENDS in Microbiology*, 15(1):45–50, 2007.
- [73] Saltelli, A. Sensitivity analysis for importance assessment. *Risk analysis*, 22(3):579–590, 2002.
- [74] Heinrich, R. and Rapoport, T. A. A linear steady-state treatment of enzymatic chains: general properties, control and effector strength. *European journal of biochemistry*, 42(1):89–95, 1974.
- [75] Kacser, H. The control of flux. In *Symp. Soc. Exp. Biol.*, volume 27, pages 65–104, 1973.
- [76] Liberti, M. V., Dai, Z., Wardell, S. E., Baccile, J. A., Liu, X., Gao, X., Baldi, R., Mehrmohamadi, M., Johnson, M. O., Madhukar, N. S., Shestov, A. A., Chio, I. I., Elemento, O., Rathmell, J. C., Schroeder, F. C., McDonnell, D. P., and Locasale, J. W. A Predictive Model for Selective Targeting of the Warburg Effect through GAPDH Inhibition with a Natural Product. *Cell Metabolism*, 26(4):648–659.e8, 2017.
- [77] Cornish-Bowden, A. Metabolic control analysis in theory and practice. In *Advances in molecular and cell biology*, volume 11, pages 21–64. Elsevier, 1995.
- [78] Groen, A. K., Wanders, R., Westerhoff, H., Van der Meer, R., and Tager, J. Quantification of the contribution of various steps to the control of mitochondrial respiration. *Journal of Biological Chemistry*, 257(6):2754–2757, 1982.
- [79] Joy, M. P., Elston, T. C., Lane, A. N., Macdonald, J. M., and Cascante, M. Introduction to metabolic control analysis (mca). In *The Handbook of Metabolomics*, pages 279–297. Springer, 2012.
- [80] Albert, M.-A., Haanstra, J. R., Hannaert, V., Van Roy, J., Opperdoes, F. R., Bakker, B. M., and Michels, P. A. Experimental and in silico analyses of glycolytic flux control in bloodstream form *Trypanosoma brucei*. *Journal of Biological Chemistry*, 280(31):28306–28315, 2005.

- 
- [81] Koebmann, B. J., Andersen, H. W., Solem, C., and Jensen, P. R. Experimental determination of control of glycolysis in *Lactococcus lactis*. *Lactic Acid Bacteria: Genetics, Metabolism and Applications*, pages 237–248, 2002.
- [82] Hofmeyr, J.-H. S. Metabolic control analysis in a nutshell. In *Proceedings of the 2nd International conference on systems biology*, pages 291–300. Citeseer, 2001.
- [83] van Eunen, K., Kiewiet, J. A., Westerhoff, H. V., and Bakker, B. M. Testing biochemistry revisited: how in vivo metabolism can be understood from in vitro enzyme kinetics. *PLoS Comput Biol*, 8(4):e1002483, 2012.
- [84] Bakker, B. M., van Eunen, K., Jeneson, J. A., van Riel, N. A., Bruggeman, F. J., and Teusink, B. Systems biology from micro-organisms to human metabolic diseases: the role of detailed kinetic models. *Biochemical Society Transactions*, 38(5):1294–1301, 2010.
- [85] Mulquiney, P. J. and Kuchel, P. W. Model of 2, 3-bisphosphoglycerate metabolism in the human erythrocyte based on detailed enzyme kinetic equations: equations and parameter refinement. *Biochemical Journal*, 342(3):581–596, 1999.
- [86] Cocaign-Bousquet, M., Garrigues, C., Loubiere, P., and Lindley, N. D. Physiology of pyruvate metabolism in *Lactococcus lactis*. *Antonie Van Leeuwenhoek*, 70(2):253–267, 1996.
- [87] Fordyce, A. M., Crow, V., and Thomas, T. D. Regulation of product formation during glucose or lactose limitation in nongrowing cells of *Streptococcus lactis*. *Applied and Environmental Microbiology*, 48(2):332–337, 1984.
- [88] Poolman, B., Bosman, B., Kiers, J., and Konings, W. N. Control of glycolysis by glyceraldehyde-3-phosphate dehydrogenase in *Streptococcus cremoris* and *Streptococcus lactis*. *Journal of Bacteriology*, 169(12):5887–5890, 1987.
- [89] Andersen, H. W., Solem, C., Hammer, K., and Jensen, P. R. Twofold reduction of phosphofructokinase activity in *Lactococcus lactis* results in strong decreases in growth rate and in glycolytic flux. *Journal of Bacteriology*, 183(11):3458–3467, 2001.
- [90] Papagianni, M., Avramidis, N., and Filioysis, G. Glycolysis and the regulation of glucose transport in *Lactococcus lactis* spp. *lactis* in batch and fed-batch culture. *Microbial cell factories*, 6(1):1–13, 2007.
- [91] Moreno-Sánchez, R., Saavedra, E., Rodríguez-Enríquez, S., and Olín-Sandoval, V. Metabolic control analysis: a tool for designing strategies to manipulate metabolic pathways. *Journal of Biomedicine and Biotechnology*, 2008, 2008.

- 
- [92] Bakker, B. M., Krauth-Siegel, R. L., Clayton, C., Matthews, K., Girolami, M., Westerhoff, H. V., Michels, P. A., Breitling, R., and Barrett, M. P. The silicon trypanosome. *Parasitology*, 137(9):1333–1341, 2010.
- [93] Jordaan, S. *Supply-demand analysis of energy metabolism in Lactococcus lactis under anaerobic conditions*. PhD thesis, Stellenbosch: Stellenbosch University, 2011.
- [94] Radfar, A., Méndez, D., Moneriz, C., Linares, M., Marín-García, P., Puyet, A., Diez, A., and Bautista, J. M. Synchronous culture of *Plasmodium falciparum* at high parasitemia levels. *Nature Protocols*, 4(12):1899–1915, 2009.
- [95] Bradford, M. M. A rapid and sensitive method for the quantitation of microgram quantities of protein utilizing the principle of protein-dye binding. *Analytical biochemistry*, 72(1-2): 248–254, 1976.
- [96] Even, S., Lindley, N. D., and Cocaign-Bousquet, M. Molecular physiology of sugar catabolism in *Lactococcus lactis* il1403. *Journal of bacteriology*, 183(13):3817–3824, 2001.
- [97] McSweeney, P., Walsh, E., Fox, P., Cogan, T., Drinan, F., and Castelo-Gonzalez, M. A procedure for the manufacture of cheddar cheese under controlled bacteriological conditions and the effect of adjunct lactobacilli on cheese quality. *Irish journal of agricultural and food research*, pages 183–192, 1994.
- [98] Odendaal, C. Glycolytic flux control of glyceraldehyde 3-phosphate dehydrogenase in yeast. Master's thesis, Stellenbosch: Stellenbosch University, 2019.
- [99] Aitken, A. and Learmonth, M. Carboxymethylation of cysteine using iodoacetamide/iodoacetic acid. In *The protein protocols handbook*, pages 455–456. Springer, 2002.
- [100] Chumsae, C., Gaza-Bulseco, G., and Liu, H. Identification and localization of unpaired cysteine residues in monoclonal antibodies by fluorescence labeling and mass spectrometry. *Analytical chemistry*, 81(15):6449–6457, 2009.
- [101] Sabri, M. and Ochs, S. Inhibition of glyceraldehyde-3-phosphate dehydrogenase in mammalian nerve by iodoacetic acid. *Journal of neurochemistry*, 18(8):1509–1514, 1971.
- [102] Schroeder, E., Woodward, G. E., and Platt, M. E. The effect of amines on yeast poisoned by iodoacetic acid. *Journal of Biological Chemistry*, 100(2):525–535, 1933.
- [103] Saavedra, E., González-Chávez, Z., Moreno-Sánchez, R., and Michels, P. A. Drug target selection for *Trypanosoma cruzi* metabolism by metabolic control analysis and kinetic modeling. *Current medicinal chemistry*, 26(36):6652–6671, 2019.

- 
- [104] Shestov, A. A., Liu, X., Ser, Z., Cluntun, A. A., Hung, Y. P., Huang, L., Kim, D., Le, A., Yellen, G., Albeck, J. G., et al. Quantitative determinants of aerobic glycolysis identify flux through the enzyme gapdh as a limiting step. *elife*, 3:e03342, 2014.
- [105] Davis, M. I., Patrick, S. L., Blanding, W. M., Dwivedi, V., Suryadi, J., Golden, J. E., Coussens, N. P., Lee, O. W., Shen, M., Boxer, M. B., et al. Identification of novel *Plasmodium falciparum* hexokinase inhibitors with antiparasitic activity. *Antimicrobial agents and chemotherapy*, 60(10):6023–6033, 2016.
- [106] Floridi, A., Paggi, M. G., Marcante, M. L., Silvestrini, B., Caputo, A., and de Martino, C. Lonidamine, a selective inhibitor of aerobic glycolysis of murine tumor cells. *Journal of the National Cancer Institute*, 66(3):497–499, 1981.
- [107] Brown, J. et al. Effects of 2-deoxyglucose on carbohydrate metabolism: review of the literature and studies in the rat. *Metabolism*, 11:1098–1112, 1962.
- [108] Rego, A. C., Areias, F. M., Santos, M. S., and Oliveira, C. R. Distinct glycolysis inhibitors determine retinal cell sensitivity to glutamate-mediated injury. *Neurochemical research*, 24(3):351–358, 1999.
- [109] Geschwind, J.-F., Georgiades, C. S., Ko, Y. H., and Pedersen, P. L. Recently elucidated energy catabolism pathways provide opportunities for novel treatments in hepatocellular carcinoma. *Expert review of anticancer therapy*, 4(3):449–457, 2004.
- [110] Hakala, M. T., Glead, A. J., and Schwert, G. W. Lactic dehydrogenase ii. variation of kinetic and equilibrium constants with temperature. *Journal of Biological Chemistry*, 221(1):191–210, 1956.
- [111] Maithal, K., Ravindra, G., Balaram, H., and Balaram, P. Inhibition of *Plasmodium falciparum* triose-phosphate isomerase by chemical modification of an interface cysteine: Electrospray ionization mass spectrometric analysis of differential cysteine reactivities. *Journal of Biological Chemistry*, 277(28):25106–25114, 2002.
- [112] Velanker, S. S., Ray, S. S., Gokhale, R. S., Suma, S., Balaram, H., Balaram, P., and Murthy, M. Triosephosphate isomerase from *Plasmodium falciparum*:. the crystal structure provides insights into antimalarial drug design. *Structure*, 5(6):751–761, 1997.
- [113] Jones, A. and Cooper, T. Metabolism of 36cl-ornidazole after oral application to the male rat in relation to its antifertility activity. *Xenobiotica*, 27(7):711–721, 1997.
- [114] Wick, A. N., Drury, D. R., Nakada, H. I., Wolfe, J. B., et al. Localization of the primary metabolic block produced by 2-deoxyglucose. *Journal of Biological Chemistry*, 224(2):963–969, 1957.

- [115] Papaconstantinou, J. and Colowick, S. P. The role of glycolysis in the growth of tumor cells: I. effects of oxamic acid on the metabolism of ehrlich ascites tumor cells in vitro. *Journal of Biological Chemistry*, 236(2):278–284, 1961.
- [116] Li, X., Lu, W., Hu, Y., Wen, S., Qian, C., Wu, W., and Huang, P. Effective inhibition of nasopharyngeal carcinoma in vitro and in vivo by targeting glycolysis with oxamate. *International journal of oncology*, 43(5):1710–1718, 2013.